From Coal to Negative Emissions:
Modelling the Decarbonisation of Alberta's Power Grid

by
Benjamin Cal Lyseng

B.Sc., University of Alberta, 2007
M.Sc., Telemark University College, 2012

A Dissertation Submitted in Partial Fulfillment of the
Requirements for the Degree of

DOCTOR OF PHILOSOPHY

in the Department of Mechanical Engineering

We acknowledge and respect the Lək̓ʷəŋən (Songhees and Xʷsepsəm/Esquimalt) Peoples on whose territory the university stands, and the Lək̓ʷəŋən and W̱SÁNEĆ Peoples whose historical relationships with the land continue to this day.

From Coal to Negative Emissions:
Modelling the Decarbonisation of Alberta's Power Grid

by
Benjamin Cal Lyseng

B.Sc., University of Alberta, 2007
M.Sc., Telemark University College, 2012

SUPERVISORY COMMITTEE

_____
Dr. Andrew Rowe (Department of Mechanical Engineering)
Co-Supervisor

_____
Dr. Peter Wild (Department of Mechanical Engineering)
Co-Supervisor

_____

Dr. Ralph Evins (Department of Civil Engineering)
Outside Member

ABSTRACT

This dissertation models the decarbonisation of Alberta's power grid, transitioning from primarily coal-fired generation to delivering net-negative emissions. Three key stages of the transition are analysed using optimisation and simulation methods: the transition from coal to natural gas under carbon pricing, integration of 80% variable renewable energy (VRE) using power-to-gas (PtG) for long-duration energy storage, and the operational implications of direct air capture (DAC) for achieving negative emissions.

In the first study, carbon pricing is found to accelerate emissions reductions, especially through coal-to-gas switching. The second study demonstrates that PtG can support an 80% VRE system by reducing VRE capacity and curtailment through long-duration energy storage. In the final study, DAC operation is shown to be closely tied to the marginal low-carbon generator.

Overall, this work provides robust modelling and insights for regional decarbonisation strategies.

CONTENTS

LIST OF FIGURES

LIST OF TABLES

ACKNOWLEDGMENTS

First off, thank you Peter and Andrew for your patience and professionalism. I am grateful for your understanding and continued support. And thank you, Ralph Evins, for stepping in and helping me across the finish line.

Thank you, Sandra Espinola and Sandra Baskett, and all those who wrangled my paperwork.

Thank you, Pacific Institute for Climate Solutions, for your financial and academic support.

Thank you, Institute for Integrated Energy Systems, for teaching me the system perspective.

Thank you, Susan Walton and Pauline Shepherd, for the IESVic family.

Thank you, Lawrence Pitt and Amy Sopinka, for the invaluable experience you brought to our team.

Thank you, 2060 Project colleagues and friends, for making it hurt so good.

Thank you, Sam, for the support, love, and stability that made this possible.

DEDICATION

This dissertation is dedicated to my family.

Brooklyn, Bella, Sarah, Ashley, Jeff, Anne, and Cal.

1 INTRODUCTION

1.1 MOTIVATION

All pathways limiting global warming to 1.5°C published in a recent IPCC special report (1) as well as those in a recent IEA Net Zero study (2) include negative emission technologies (NET). This is despite negligible NET globally, where power generation from coal and natural gas set new annual highs in 2023, combining for 58% of all electricity generation[1]. Identifying transition plans that account for NET maturity and resulting systemic demands is subject to significant uncertainty. Energy planning models can provide insights on technologies and portfolios that enable decarbonisation.

Energy planning studies are typically national or international in scope and hinge on an unprecedented buildout of inter-regional transmission to unlock the benefits of resource and load diversity (2–5). Most pathways in Princeton's Net-Zero America study require high voltage transmission capacity to at least triple in the continental US by 2050. Building new bulk transmission lines, however, is a lengthy and highly uncertain endeavour. Whether due to politics, geography, resources, or something else, it is at the regional level where many successful energy and carbon policies have been implemented, such as Renewable Portfolio Standards (RPS) in multiple US states, and carbon taxes in several Canadian provinces.

Maintaining power system reliability without conventional baseload generation is a major challenge. Without baseload generation from nuclear or carbon capture on fossil fuel generation, long-term storage requirements drive exponential cost increases as variable renewable energy (VRE) penetration approaches 100% (6–8). Multiple modelling approaches are needed to assess the trade-offs between VRE generation capacity, fossil fuel generation, storage, and curtailment. Grid-powered direct air capture (DAC), which extracts carbon dioxide

[1] https://ourworldindata.org/electricity-mix

from the atmosphere, is a potential new demand for power systems in the pursuit of limiting climate change.

By examining an islanded power system with energy models, we can gain a better understanding of the challenges and opportunities of transitioning to a low-carbon energy future.

1.2 Related Work

1.2.1 Canadian energy system modelling

The Canadian energy system modelling community has grown strong over the past decade. Much of this research is conducted as part of the *2060 Project*, a research group hosted at the University of Victoria. The 2060 Project research focuses on decarbonisation in Alberta and British Columbia, applying open-source energy system modelling tools. Other notable energy system research in Canada have come from the Energy Modelling Hub (EMH)(9,10); ΔE+ (Delta-Energy Plus) research group(11–13), and the Canadian Open Energy Model (CANOE), a national, multi-sector energy model[2].

1.2.2 Capacity expansion models for energy planning

Many deep decarbonisation studies consider multiple sectors, fuel switching, and construction of new bulk-transmission (2–4,14,15). The benefits of increased resource and load diversity are highlighted in several multi-region decarbonisation studies (16–19). Diversity that spans multiple sectors or jurisdictions can require ongoing cooperation between multiple entities for it to remain an available resource. Energy plans reliant on these expanding connections have additional sources of uncertainty and analysis can be complemented by simpler, single-region models. By narrowing the focus, the research presented here provides clear insights for tractable energy policy.

[2] https://sustainablesystems.civmin.utoronto.ca/canadian-open-energy-canoe-model/#our-research

1.2.3 Long Duration Energy Storage, VRE penetration, and flexibility

The transition to decarbonised power systems includes increasing shares of variable renewable energy (VRE) resources. Successful integration of VRE requires greater system flexibility to manage the uncertainty and intermittency inherent in these resources.

Flexibility in power systems can cover a range of meanings, technologies, and strategies (20–24). One categorisation for flexibility is by the following needs: energy, power, voltage, and transfer capacity (20,24). Assessing power and voltage flexibility is a stability problem and requires specific models with sub-minute resolution and is not considered in this research. The models presented in this research assume a "copper plate" system without transmission constraints, therefore transfer capacity is out of scope. The research presented here addresses energy flexibility, the balance between supply and demand on the hourly to multi-year timescale. As generation technologies like coal and natural gas plants retire, the amount of fuel storage-based electricity supply decreases, and the challenge to integrate VRE increases.

Multiple studies have concluded that high penetrations of VRE require long-duration energy storage (LDES) (25–28). While storage durations less than 10 hours may be sufficient to integrate 50%-80% of annual energy from wind and solar power, greater penetrations require LDES (25). Research on the design space for LDES by Sepulveda et al. concludes that storage systems with the greatest impact on electricity cost and firm generation have durations exceeding 100 hours (27). Managing seasonal mismatches between VRE and load drives escalating costs and complexity. An extensive literature review on power-to-gas can be found in Appendix B:.

1.2.4 Negative carbon dioxide emissions and energy planning models

The concept of net-negative carbon dioxide emission power systems is emerging as a crucial element in decarbonisation. Despite resource availability and scaling issues associated with Bioenergy with Carbon Capture and Storage (BECCS), it remains the most referenced negative emission technology. A 2025 review of 43 studies contains only 14 models that incorporate Direct Air Capture (DAC), none of which discuss DAC's impact on grid operations(29). The only

energy planning study to examine DAC operation is by Arwa and Schell (30), where the DAC is modelled with process flexibility that provides load-shifting to the power system.

1.3 Objectives and Outline

The research presented in this dissertation models the transition of a coal-based power system to a net-negative power system with the goal of providing insights on pathways to a low-carbon energy future.

This research addresses three stages of grid decarbonisation:

1. switch from coal to natural gas plus VRE growth (Chapter 2)
2. long-duration energy storage in high VRE systems (Chapter 3), and
3. planning and operation of grid-powered direct air capture (Chapter 4).

The stylised emission pathways in Figure 1.1 help illustrate emission reductions achieved by each of these three stages. Understanding the unique challenges of each stage helps focus key questions, improves model representations, and provides correct perspective to interpret results.

Each chapter in this dissertation delves into a different stage of decarbonisation, describing relevant research, applying appropriate modelling, presenting insightful results, and discussing impacts on power systems.

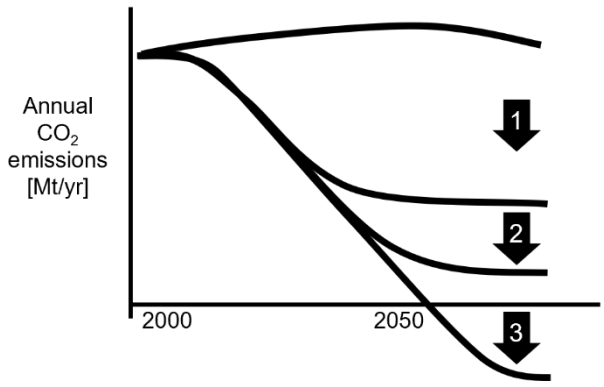

Figure 1.1: Three stages of the transition to negative emissions, and topics of Chapters 2, 3, and 4, respectively.

Chapter 2 introduces the Alberta power system and its representation with the OSeMOSYS optimisation model. In this study, escalating carbon taxes applied over multiple scenarios force the decarbonisation of the coal-based system. Results highlight generation mix changes from 2015 to 2060 with analysis of costs and emission reductions. The study finds that replacing coal-fired generation with natural gas-fired generation provides the most cost-effective emission reductions. Results also show wind and solar generation displace natural gas generation as their capital costs decline. Plants with carbon capture and sequestration (CCS) appear in most generation mixes by the end of the model period, indicating continuing need for baseload generation. Since this study was conducted, Alberta has phased out coal-fired generation and built large amounts of wind and solar power.

Chapter 3 explores how long-duration energy storage (LDES) can substitute for baseload generation on the Alberta grid. In this study, an hourly simulation model is introduced to assess the role of Power-to-Gas (PtG) in reaching 80% VRE penetration. The study examines the balance of VRE generation, storage capacity, and curtailment. Results indicate short storage events are common throughout the year, but most of the energy stored comes from events lasting longer than 10 hours. The study also proposes Alberta's natural gas grid could feasibly manage the amount of hydrogen generated by PtG in the study. This research was published several years ago and does not capture recent developments.

Chapter 4 explores how grid-connected direct air capture (DAC) reshapes capacity planning and operations under net-negative emission constraints in Alberta. Building on the OSeMOSYS model from Chapter 2, DAC is optimised along with the generation mix and compared against a low-carbon reference scenario. DAC operation is evaluated over several timeframes, highlighting daily, seasonal, and annual differences.

Table 1: Chapter topics, objectives, primary modelling method, and associated publications

Chapter	Topic	Objective	Modelling	Publications associated with OSeMOSYS version
2	Decarbonisation of regional power system	Establish model for long-term grid studies	LP optimisation with OSeMOSYS	(17,31–33)
3	Long-duration storage with power-to-gas	Explore LDES in 80% VRE system with PtG	Hourly simulation with MATLAB	(19,34–36)
4	Negative emissions with DAC	Examine potential operation	LP optimisation with OSeMOSYS	(37,38)

1.4 METHODS

Computational energy models are important tools in energy planning research, policy, and investment. Capacity expansion models have been evolving to better represent the increasing portion of unconventional resources (wind, solar, storage, etc.) to provide insights on the future of power systems (39,40). The energy system modelling platform OSeMOSYS is the foundation for the Alberta power system model developed in this research. This model is the primary tool for the research presented in Chapters 2 and 4. Beyond the studies contained in this dissertation, this Alberta power system model is applied in several other decarbonisation studies exploring topics of trade (16,17), biomass (19), and emission risk (33).

While Chapters 2 and 4 are concerned with multi-decade transitions and pathways, Chapter 3 focuses on one year and the interaction of wind, solar, and storage for 80% VRE penetration.

For an investigation of this type, an hourly simulation model is developed in MATLAB to capture the short-term variability and chronology.

1.4.1 Key limitations in research and modelling

This dissertation uses linear optimisation and simulation tools that involve simplifications and assumptions that should be acknowledged.

First, the optimisation model assumes perfect foresight, when real-world decision making happens under uncertainty. With perfect foresight the model is impossibly efficient with resource expansion, avoiding any overbuild. Generation is also perfectly dispatched because the models do not incorporate uncertainty in load, wind, nor solar generation. As a result, the model likely underestimates the operational flexibility and backup requirements to ensure system reliability.

Second, the capacity expansion model captures seasonality and daily dynamics, but does not capture chronological limitations. Behaviour impacted by chronology that is not represented in the capacity expansion model includes: ramping limits, minimum load level, minimum up/down time, charging and discharging of storage, or multi-day events like extended cold spells or wind droughts. Chapter 3 uses an hourly simulation model that is chronological to specifically analyse storage.

Transmission is represented with a copper-plate assumption, meaning power from any generator can serve the load without congestion or regional limitations. This may underestimate the integration costs of some variable resources which are not near the transmission system.

Finally, behavioural dynamics are not represented. Electricity demand is treated as static and price-inelastic. Generation technologies are evaluated solely on costs (including emission costs) drawn from national and international sources; public sentiment or policy favouring or hindering specific technologies are not considered.

These limitations do not undermine the value of the modelling, but constrain the scope of questions the model is suitable to address. The results should be interpreted as insights into

system-level dynamics, where differences between scenario results are likely more informative than the absolute values from one scenario.

2 DECARBONISING THE ALBERTA POWER SYSTEM WITH CARBON PRICING[3]

[3] An earlier version of this chapter was published in (32)

2.1 INTRODUCTION

Although Canada, as a whole, has a low-carbon electricity mix, with nearly 80% of generation provided by hydro and nuclear, generation mixes and carbon intensities vary widely from province to province. The Alberta system is based on abundant coal and natural gas resources and, at the time of writing, the carbon intensity of electricity generated in the province is the highest of any province in Canada, and higher than the global average. For decades power generation in the province has been the principal source of carbon dioxide (CO_2) emissions and was only recently surpassed by oil sands as the highest emitting sector (41).

In Alberta, high load growth and an aging coal fleet are projected to require development of approximately 14 GW of new electricity generating capacity by 2034, nearly doubling the system capacity in 2015 (42). Alberta possesses some of Canada's best wind and solar resources, there is potential for additional hydropower, and there is government support for carbon capture and sequestration (43). As seen in Figure 2.1, many jurisdictions face challenges that mirror the Alberta situation, namely, a fossil fuel dominated generation mix, pending capacity shortage and pressures to reduce carbon emissions. Therefore, the results of this study are of interest to a wide audience.

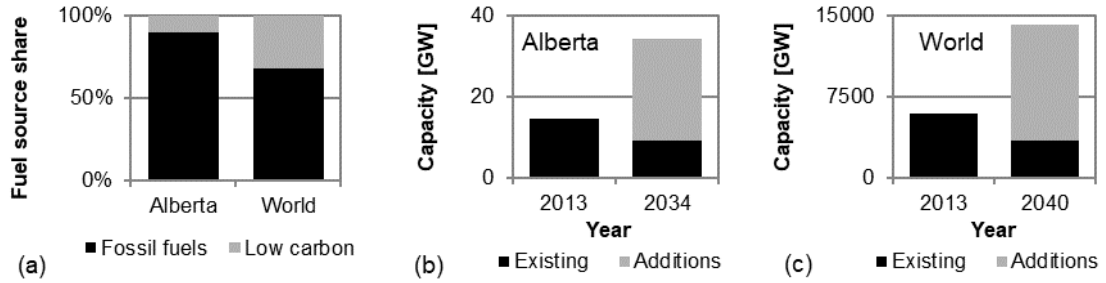

Figure 2.1: (a) Share of annual electricity generation by fuel source (44,45). Expected generation capacity additions for (b) Alberta (42), and (c) World (46).

Carbon taxes have become ubiquitous in discussions of policy mechanisms to drive the decarbonisation of energy systems. First pioneered by Finland in 1990, many nations and regions have implemented carbon taxes under a range of structures that encompass various fuels, sectors, and rates. Analyses of the impacts of these policies over nearly two decades have found mixed results (47,48). For example, despite having one of the highest carbon tax

rates as of 2004, Norway's policy did not reduced *per capita* CO_2 emissions because of exemptions for certain sectors, rapid growth of oil and gas exports, and inelastic demand (49). Successful policies, like that of Finland, were found to cover a greater range of fuels and sectors, with flexibility in the system to shift to lower carbon alternatives (48,49).

Energy models are frequently used to provide insight into how future demands can be met. For example, a partial equilibrium model was used to compare the impacts of carbon taxes and energy taxes on Japan's energy system (50). These researchers found the carbon tax to be an effective option, but details of the system preference for generation technologies to meet the emission target were not reported. More recently, a CA-TIMES (The Integrated MARKAL-EFOM System[4], California system) model was used to study how the California energy system could achieve an 80% reduction in greenhouse gases by 2050 (51). Results indicate that meeting the emission target requires electrification of industry and transportation sectors, enabled by an expansion of wind and solar power after 2030, or carbon capture and sequestration (CCS) and nuclear if permitted. This comprehensive study shows that ambitious emission targets can be met, but the Alberta power system is currently much more carbon intensive than California's and, therefore, requires different policy measures, at least in the near-term. Carbon taxes were applied previously in a basic model of the Alberta power system, indicating that nuclear and large hydro power, if permitted, provide the greatest emission reductions (31).

In this study, potential pathways to a low-carbon power system for Alberta are explored using a long-term, techno-economic, optimisation supply model. Simulations to 2060 are conducted for scenarios based on various carbon tax structures. The resulting energy mixes, system costs, and CO_2 reductions are evaluated, including sensitivity to fuel prices, technology costs, and load growth.

In Section 2, relevant background for the Alberta power system is provided, as well as key model characteristics and a description of the scenarios modelled. Results and discussion (Section 3) are presented in terms of carbon intensity, generation mix, emissions by source and

[4] http://www.iea-etsap.org/web/Times.asp

type, and the impacts of high gas prices. Conclusions and implications of the research are in Section 4.

2.2 METHODS

2.2.1 Background: The Alberta power system

Alberta has a deregulated energy-only electricity market, managed by the Alberta Electric System Operator (AESO), with 16 GW of capacity delivering 75 TWh annually, as of 2015. In mid-2014 there were nearly 100 generators offering into the Alberta market. Small gas-fired units under 100 MW are the most common, but the bulk of capacity is held by large coal-fired plants rated over 400 MW. Coal-fired thermal generation plants have been the system backbone since its inception, but cogeneration units sited for oil sands projects and fuelled by inexpensive natural gas have met most of the load growth since 2000. Over this same time frame, many new wind farms have been commissioned, resulting in a tenfold increase in wind generation between 2002 and 2012. Impressive as this growth is, wind generation met only 3.9% of demand in 2013, while coal and natural gas plants contributed 55% and 35% respectively (52).

Alberta is connected with interties to British Columbia (BC Hydro) at effectively ~700 MW, Saskatchewan (SaskPower) at 153 MW, and Montana (NorthWestern Energy) via a new ~300 MW merchant intertie. In Alberta's deregulated power market, imports may be purchased from external participants that offer in at $0/MWh, the pool price floor. Export bids to send electricity out of the province are set at $999.99/MWh, the pool price ceiling at the time of writing. Both import and export transactions ultimately occur at the final pool price for that trading block, a structure that prevents either imports or exports from controlling the pool price. Demand for power in Alberta has doubled over the last twenty years, and trade has shifted increasingly to imports, especially from hydro-rich BC during peak hours. Net imports in 2014 contributed 2.2% of demand, 62% of which came from BC (52,53).

2.2.2 OSeMOSYS energy model

The research presented here is conducted with the Open Source Energy Modelling System (OSeMOSYS), developed by the Royal Institute of Technology (KTH) in Sweden (54,55). OSeMOSYS is a technology explicit, energy optimisation supply model well suited for analysis and planning purposes. OSeMOSYS is chosen for its open and accessible nature, which, as argued by DeCarolis (56), are extremely valuable when informing public policy by allowing third parties to independently reproduce results.

In OSeMOSYS, a system is represented by technologies and the energy carriers that they use and/or produce. For example, a coal fired power plant (technology) uses coal (energy carrier) to generate electricity (energy carrier) that contributes to meeting a specified electricity demand. The user defines technologies by costs (capital, fixed, and variable), efficiencies, emission rates, existing capacities, production constraints, discount rates, etc. Energy carriers must satisfy the constraint that production must be greater than or equal to the sum of time-specific use and exogenous demand. Figure 2.2 illustrates the Alberta model used in this study, showing technologies and energy carriers.

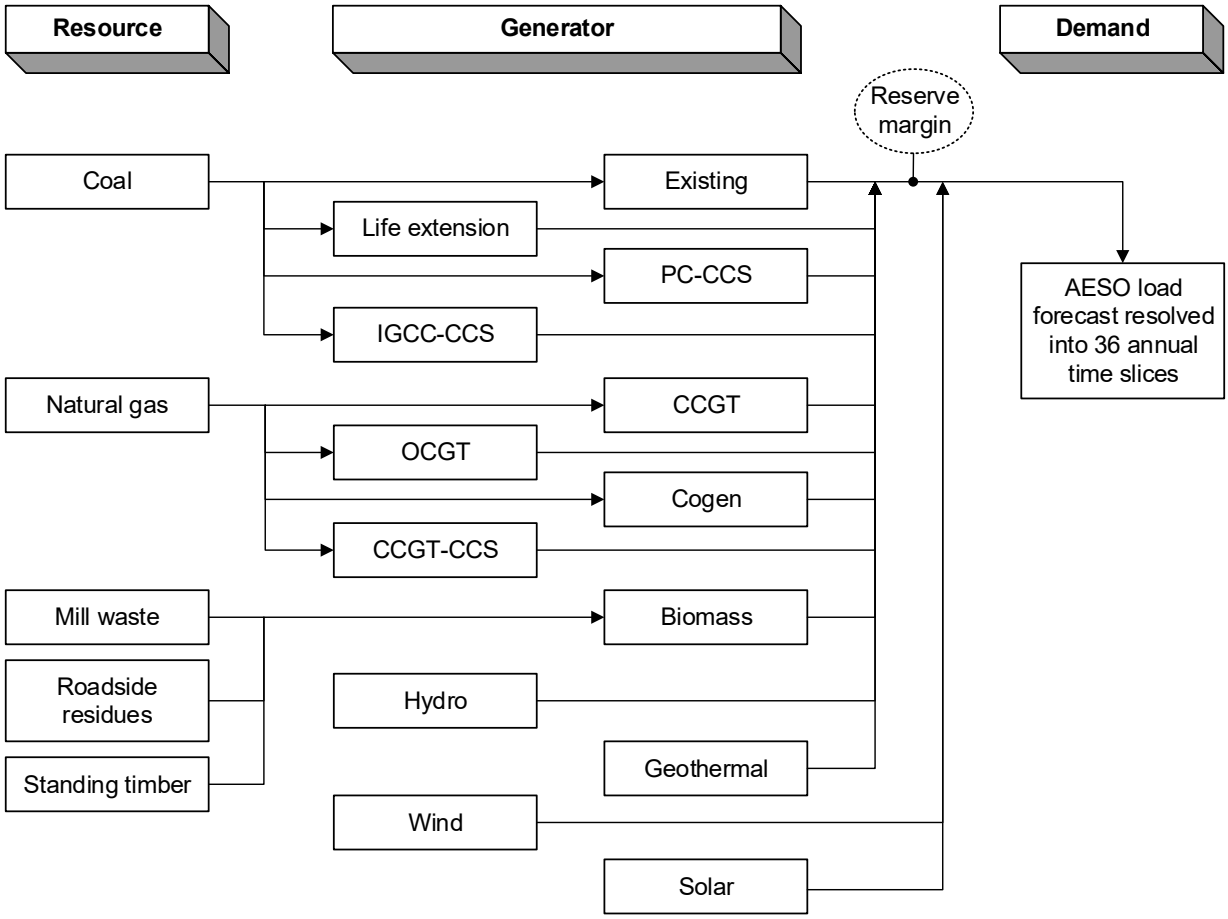

Figure 2.2 Schematic representation of the Alberta power system as modelled in OSeMOSYS. The rectangles are technologies defined by efficiencies, heat rates, costs, etc.; the lines represent the energy carriers. Fuel costs and emission rates are attributed to the resources as applicable; wind and solar capacity do not contribute to the reserve margin. PC: pulverised coal, CCS: carbon capture and sequestration, IGCC: integrated gasification combined cycle, CCGT: combined cycle gas turbine, OCGT: open cycle gas turbine.

2.2.3 Temporal structure

The model optimises over the period 2010 through 2060. The average load growth forecast by AESO for 2024-2034 (1.5% annually) is extrapolated beyond 2034, reaching 190 TWh in 2060. Historical demand data[5] from 2009-2013 are used to create five representative load profiles, which are repeated nine times, in sequence, over the model period. Within each profile,

[5] http://ets.aeso.ca/ets_web/

annual demand is separated into twelve *seasons* (months of the year). Within each season, three daily *time slices* are defined, corresponding to *off-peak*, *mid-peak*, and *on-peak* load periods. This results in a total of 36 time slices per annual profile, which captures the daily and seasonal load variations while permitting reasonable computation times for a model with a 50-year scope.

To capture the annual peak hour that is lost by aggregating load into 36 time slices, AESO annual peak load predictions[6] are combined with the historic reserve margin (18%) to define a *peak factor*. The peak factor is applied in each year of the model to ensure sufficient capacity is installed. Details of determining the time slices and corresponding load can be found in Appendix A.

2.2.4 Generation options

The model has seven technology definitions that represent existing generators: coal, three types for natural gas, hydropower, biomass, and wind (Table 2.1). Initial capacities for these generators are set to match reported assets from 2010-2012, a few years before the time of writing.

[6] The AESO 2014 Long-term Outlook estimates both annual energy (GWh) and system peak load (MW)

Table 2.1: Existing generators at the time of writing.

Fuel	Technology	Abbreviation	Existing capacity (2012) [MW]	Capacity notes[a]
Coal	Existing coal	Existing	6286	Capacity declines with expected retirements
Natural gas	Comb. cycle	CCGT	1064	N/A
Natural gas	Cogeneration	Cogen	3600	7.5 GW max in 2060[b] (5.2 GW max in *Low Growth*)[c]
Natural gas	Open cycle	OCGT	963	N/A
Mixed wood[c]	Biomass	Biomass	404	Fuel limit based on forestry industry[d]
Water	Hydropower	Hydro	894	2.3 GW max in 2034, stepped to 3.3 GW in 2050[e]
Wind	Wind turbine	Wind	1087	8 GW max in 2060[e]

[a] For all technologies, the maximum new capacity that can be installed each year is 5% of the forecasted peak demand

[b] Extrapolated from AESO 2014 LTO - Main Outlook scenario (42)

[c] Extrapolated from AESO 2014 LTO - Low Growth scenario (42)

[d] Mill waste, roadside residues, standing timber. See Supplementary material for references and calculations.

[e] Extrapolated from AESO 2014 LTO - Energy Transformation scenario (42)

2.2.4.1

The capacity of *Existing coal* technology decreases with anticipated retirements over the model period. The efficiency of this coal-fired generation is a weighted average of actual reported plant values which changes over time to reflect the retirement of older, less efficient units.

The model includes three in-use technologies fuelled by natural gas: open cycle gas turbines (OCGT), combined cycle gas turbines (CCGT), and cogeneration units. OCGTs, also known as simple cycle or combustion turbines, are typically smaller and less efficient than the other two varieties and are used primarily for peaking purposes. CCGTs have a steam turbine, which increases investment cost over OCGTs, but the improved efficiency and makes them suitable for baseload operation. In Alberta, cogeneration units currently make up the largest fraction of gas-fired capacity (3.6 out of 5.7 GW), primarily for the steam and power demand in oil sands extraction and upgrading.

Alberta has nine hydropower plants with a combined capacity of 894 MW. Their role in the system as contingency reserve and peaker plants is represented in the model through capacity, fixed and variable costs, and monthly capacity factors based on average historical (1994-2011) generation totalling 1906 GWh/yr (52).

Wind turbines are aggregated into a single technology definition, like the other generation types. Hourly aggregate wind generation in the province from 2009-2013 is used to calculate capacity factors for each of the 36 time slices for each of the five load profiles. Generation from wind farms is highly variable during the annual peak load, with capacity factors varying from 0% in 2010 to 53% in 2013, and averaging 15% over the past five years (53). Two constraints are applied in the model to ensure sufficient dispatchable generating capacity to serve peak demand and meet the reserve margin. First, wind cannot be used to meet load in the peak demand slice and, second, wind cannot be used to meet the reserve margin requirement. These constraints represent the non-dispatchable nature of wind generation and are consistent with AESO metrics (57).

The remaining existing generation capacity, consistent with the data shown in Table 2.1, is specified as biomass, which constitutes 90% of the "other" capacity. There are three biomass fuels included in the model - mill waste, roadside residues, and standing timber - with costs and availability limits based on historic production, as well as BC Hydro's 2013 Resource Options Report (see Appendix A).

Six additional generation technologies are specified that may be chosen in the optimisation to meet future demands: a life extension of existing coal plants, two designs of new coal plants equipped with CCS, a natural gas-fired plant with CCS, geothermal, and solar PV (Table 2.2).

Table 2.2 Additional generators.

Fuel	Technology	Abbreviation	Capacity notes[a]
Coal	Life extension	Coal-LE	Available only in certain years, 4456 MW total
Coal	Pulverised Coal with CCS	PC-CCS	Cannot be installed before 2018
Coal	IGCC[a] with CCS	IGCC-CCS	Cannot be installed before 2018
Natural gas	Combined cycle with CCS	CCGT-CCS	Cannot be installed before 2018
Geothermal	Geothermal	Geothermal	1 GW[b]
Sun	Solar PV	Solar	N/A

[a] For all technologies, the maximum new capacity that can be installed each year is 5% of the forecasted peak demand

[b] Double the 500 MW limit in AESO 2014 LTO (42)

The model includes the option of a year-long refurbishment to extend the life of eligible coal plants by ten years while maintaining compliance with the *Reduction of Carbon Dioxide Emissions from Coal-fired Generation of Electricity Regulations* enacted by the federal government in 2012 (58). Additional detail for expected retirements, efficiencies, and life extensions are given in Appendix A.

The Government of Canada regulates emissions of CO_2 from coal-fired power plants such that any new facilities must emit a maximum of 420 gCO_2/kWh (58). Practically, this means any new coal-fired plants must be equipped with carbon capture and sequestration technology. In 2008, Alberta announced $2 billion in funding for CCS projects and, in their climate change plan, attributed 70% of targeted greenhouse gas emission reductions by 2050 to CCS (59). Two types of coal-fired generation with CCS are specified in the model: pulverised coal (PC-CCS) and integrated gasification combined cycle (IGCC-CCS). PC-CCS plants would consist of an advanced pulverised coal-fired steam-electric generating unit with a post-combustion amine scrubbing system. IGCC-CCS plants create syngas prior to combustion and utilise both gas and steam turbines to achieve higher efficiencies. However, the pre-combustion processing and capture of CO_2 makes IGCC-CCS plants more capital intensive than PC-CCS plants. While no combined cycle gas turbine plants with CCS (CCGT-CCS) currently exist, it is included as a low-carbon

generation option that may prove economic with carbon taxes. All CCS-equipped technologies are assumed to be 85% efficient at capturing CO_2 and are permitted to begin operation in 2018.

Despite the potential of geothermal to provide low-carbon baseload electricity, the technology is disadvantaged by high capital costs combined with high risk of drilling to find adequate reservoirs. The model limits the capacity of geothermal to 1 GW, double the maximum future capacity estimated in AESO's *2014 Long-term Outlook* (42).

There are no transmission connected solar facilities in the province from which to draw historic data. PVWatts[7] by NREL is used for resource availability in determining capacity factors for the 36 annual time slices. Cost and performance are based on a 150 MW single-axis tracking PV facility in southern Alberta (see Appendix A). As described above for the case of wind power, solar power cannot be used to serve peak demand nor meet the reserve margin.

As seen in Table 2.1 and Table 2.2, most generation technologies are given upper capacity limits based on the highest values from AESO's *2014 Long-term Outlook* (42), linearly extrapolated to 2060. Each of the generation technologies is constrained by an upper limit on new annual capacity equal to 5% of forecast annual peak demand, which is the average rate of total annual capacity additions over the last ten years.

Nuclear power is an established generation technology that may have a major role in future low-carbon energy systems (60–62). While eastern Canada is home to 13.5 GW of nuclear power generation, western Canada is without a single plant. Bruce Power applied to build a reactor in Alberta in 2008 but the project was abandoned in 2011, and while Toshiba was reportedly planning a small 10 MW reactor (42), the design requires approval by the Canadian Nuclear Safety Commission prior to application for a generation permit in Alberta. In light of the abandoned Bruce Power initiative and regulatory approvals required for small reactors, nuclear power is not included as a technology option in the model, an assumption consistent with the most recent AESO outlook (42).

[7] http://pvwatts.nrel.gov/index.php

Under current reliability standards, interconnections have limited ability to meet the growing need for capacity in the province ('N-1' redundancy condition) (63). Therefore, interconnections with neighbouring jurisdictions are not included in the model. A forthcoming study explores the effects of expanded interconnections with the province of British Columbia.

2.2.5 Generation performance and costs

Generator performance, overnight capital costs, fixed operations and maintenance (O&M) costs, and variable O&M costs are taken from the U.S. Energy Information Administration (EIA) *Updated Capital Cost Estimates for Utility Scale Electricity Generating Plants* (64). Learning rates are applied to generator technologies according to long-term estimates by the International Energy Agency (IEA) (65). A table of detailed costs used in the model can be found in Appendix A:. Expected lifetimes for generation technologies are taken from the IEA (66).

Cogeneration is the only plant type for which the EIA does not provide characteristics. The model definition of this technology is based on the combined cycle natural gas plant with cost and performance modifications (see Appendix A).

EIA price forecasts for natural gas and coal are used up to 2040 (67), and the average growth rate from 2030-2040 is applied to extrapolate costs of these commodities to 2060. More information on the price forecasts is provided in Section 2.6 and Table 3.

All costs are converted to constant (i.e. inflation-adjusted) US2010$. A discount rate of 6% is assumed in the optimisation when determining lowest net present system cost.

2.2.6 Modelled scenarios

Twelve scenarios are modelled, as shown in Table 2.3, representing a range of carbon taxes, natural gas prices, capital costs, and load growth profiles. The *Reference* scenario assumes a carbon tax consistent with current policy. Facilities in Alberta that emit more than 100,000 tonnes of GHGs annually are subject to the *Specified Gas Emitters Regulation*, which places a price on carbon. Companies must reduce their CO_2 emission intensity per unit of product by 12% from a reference year, or comply in other ways, such as by paying a fee of $15 for every

tonne of CO_2 emitted above the targeted reductions. A recent policy update specifies increases in 2016 to \$20/tCO_2 with a 15% reduction target, and, in 2017, \$30/tCO_2 with a 20% reduction target[8] . This intensity structure is equivalent to carbon taxes of \$1.80/tCO_2[9] in 2010-2015, \$3/tCO_2 in 2016, and \$6/tCO_2, in 2017 through to 2060.

Table 2.3: Modelled scenarios.

Scenario Name	Natural gas price	Carbon tax escalation rate	Max carbon tax	Max tax reached in	Wind/solar cost	Load growth
		[\$/tCO_2-5yr]	[\$/tCO_2]	[year]		
Reference	Baseline[a]	-	6	2017	Normal[c]	MO[e]
30B	Baseline	10	30	2025	Normal	MO
60B	Baseline	10	60	2040	Normal	MO
100B	Baseline	10	100	2060	Normal	MO
200B	Baseline	20	200	2060	Normal	MO
High Gas	High[b]	-	6	2017	Normal	MO
30H	High	10	30	2025	Normal	MO
60H	High	10	60	2040	Normal	MO
100H	High	10	100	2060	Normal	MO
Low Cost	Baseline	-	6	2017	Low[d]	MO
60B-LC	Baseline	10	60	2040	Low	MO
Low Growth	Baseline	-	6	2017	Normal	Low[f]
[a] EIA AEO 2014 Mountain region, Reference case (67)						
[b] EIA AEO 2014 Mountain region, Low oil and gas resource case (67)						
[c] EIA (64) capital costs with IEA (65) learning rates. See Supplementary material						
[d] Lowest of EIA (64), IEA (65), and NREL (68) costs. See Supplementary material						
[e] AESO 2014 LTO - Main Outlook scenario (42), extrapolated beyond 2034						
[f] AESO 2014 LTO - Low Growth scenario (42), 0% growth after 2034						

Stepped rate increases are a practiced form of carbon tax implementation (47). In most scenarios, increasing carbon tax rates are applied stepwise beginning in 2015 and increasing

[8] http://esrd.alberta.ca/focus/alberta-and-climate-change/regulating-greenhouse-gas-emissions/greenhouse-gas-reduction-program/default.aspx

[9] \$15/tCO_2 applied to 12% of emissions = \$1.80/tCO_2

$10/tCO_2$ every five years up to the specified level. For example, the 30B scenario provides taxes of $1.80/tCO_2$ 2010-2014, increasing to $10/tCO_2$ in 2015, $20/tCO_2$ in 2020, reaching $30/tCO_2$ in 2025 and remaining fixed for the remainder of the model period (Figure 2.3). A more aggressive carbon policy is represented by scenario 200B, which increases by $20/tCO_2$ every five years to reach $200/tCO_2$ in 2060. This scenario is based on the AESO "Environmental Shift" scenario which has strict carbon policy and high load growth (42). These scenarios, summarised in Table 2.3, have *Baseline* natural gas prices from the EIA AEO 2014 "Reference" case.

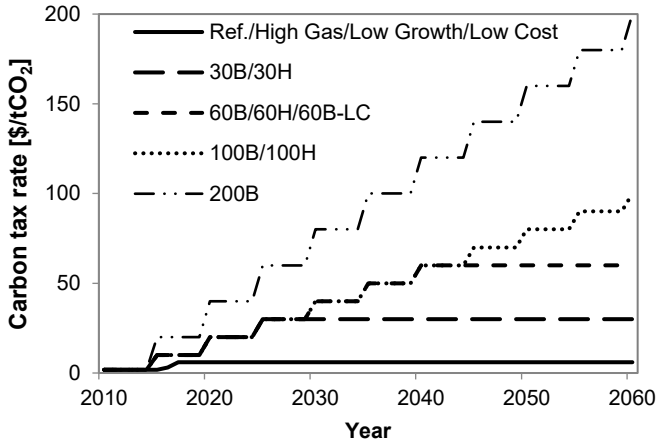

Figure 2.3: Carbon tax scenarios simulated in the model.

An additional cost state of natural gas is analysed considering the historic price volatility of the resource, the uncertain future of unconventional sources, and the impact prices can have on the development of an energy system (69). The sensitivity of the system to higher natural gas prices is explored through four scenarios (i.e. High Gas, 30H, 60H, 100H) with prices from the EIA AEO 2014 "Low oil and gas resource" forecast in which the estimated ultimate recovery of unconventional oil and gas is 50% less than the AEO "Reference" case. Natural gas prices increase at approximately 4.0% annually in the *High* case, compared to 2.7% in the *Baseline* case. The annual average coal price escalation rate is 1% in all scenarios.

Escalated learning rates and lower capital costs for wind and solar PV technologies, as detailed in the Supplementary material, are represented in two scenarios: *Low Cost*, and *60B-LC*. Low Cost assumes the same natural gas price and carbon policy as the Reference scenario, but lower

capital costs for wind and solar PV. As seen in Table 2.3, 60B-LC also assumes lower capital costs for wind and solar PV, but applies the same \$60/tCO_2 tax as the 60B scenario.

The Low Growth scenario, as defined in (42), reflects a future where oil sands growth and overall economic growth in the province are reduced. Annual demand and cogeneration capacity limits for this scenario are based on AESO's *Low Growth Scenario* until 2034, with 2034 values held constant through 2060.

Costs incurred from the carbon tax by the emission of CO_2 in power generation are included in the total system costs. Revenue from the tax can be allocated in different ways, as summarised in (47). This research does not address how the carbon tax revenue would be distributed or the subsequent impacts.

2.3 RESULTS AND DISCUSSION

Total system costs and emissions for the twelve scenarios are summarised in Table 2.4. The effectiveness of carbon taxes is evaluated in Section 2.3.1 by examining CO_2 emissions. Section 2.3.2 compares the generation mixes and discusses the technologies that enable emission reductions. Consideration of fugitive methane emissions from increased natural gas use is addressed in Section 2.3.3. Scenarios exploring sensitivity to high natural gas prices, lower costs of variable renewables, and low load growth are presented in Sections 2.3.4-2.3.6. A discussion of the model limitations is presented in Section 2.3.7.

2.3.1 CO_2 emissions

Simulation results show that carbon taxes incent the decarbonisation of Alberta's power system, with higher taxes triggering lower emissions. Compared to the Reference scenario, scenarios 30B, 60B, and 100B reduce cumulative CO_2 emissions over the model period by 12%, 18%, and 22% respectively. As seen in Table 2.4, higher carbon taxes lead to higher system costs due to tax payments and the shift to higher cost low-carbon technologies.

Table 2.4: Total (2010-2060) system costs and emissions for all scenarios.

Scenario Name	System cost (discounted)	CO_2 emissions	CO_2 reductions[a]	Methane leakage	GHG emissions[b]	2060 Carbon intensity
	[Billion 2010$]	[$MtCO_2$]	[%]	[$MtCH_4$]	[$MtCO_2e$]	[gCO_2/kWh]
Reference	80.0	2435	-	10.5	2698	239
30B	88.8	2132	12%	11.0	2407	225
60B	92.8	2003	18%	10.7	2271	181
100B	93.7	1901	22%	10.3	2159	140
200B	106.0	1385	43%	11.7	1678	105
High Gas	89.1	2274	-	7.6	2464	154
30H	98.0	2065	9%	7.6	2255	151
60H	102.0	2010	12%	7.1	2188	142
100H	102.0	1948	14%	6.9	2121	119
Low Cost	79.4	2368	3%	10.0	2618	234
60B-LC	91.7	1958	20%	10.2	2213	170
Low Growth	57.6	1690	31%	5.8	1835	177

[a] Scenarios with Baseline gas prices are relative to the Reference scenario. Scenarios with High gas prices are relative to the High Gas scenario.
[b] Includes CO_2 and methane (GWP = 25).

Carbon intensity (CI) is a useful metric to evaluate the emission performance of a power system and track its transition away from fossil fuels. CI is calculated as annual carbon emissions divided by annual energy demand.

The CIs for the six Baseline gas price scenarios in Figure 2.4(a) show the impact of the tax on CO_2 emissions. All scenarios have the same CI for the first four years in which generation capacity and carbon taxes are consistent across these scenarios. Divergence begins in 2015 when the different taxation begins and, as expected, higher tax scenarios cause greater CI reductions.

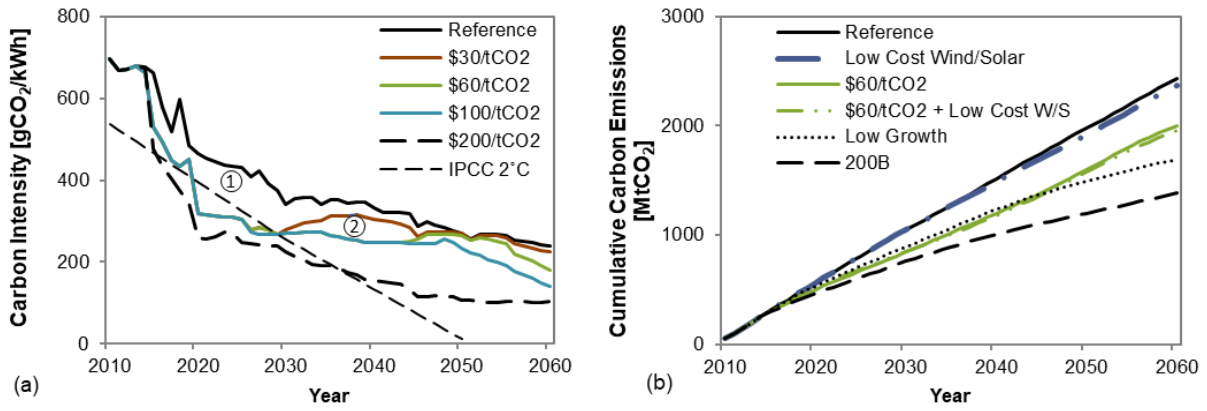

Figure 2.4: Simulated 2010-2060 carbon emissions. (a) Carbon intensity for all Baseline gas price scenarios. IPCC 2˚C line is the median value outlined by the Intergovernmental Panel on Climate Change for the set of 430-530 ppm scenarios contained in the AR5 database (70). Point 1: Divergence of *30B* from *Reference* is due to the absence of coal plants receiving life extensions. Point 2: Divergence of *60B* from *30B* is due to early retirement of coal plants and wind power. See Section 2.3.2. (b) Cumulative CO_2 emissions of selected scenarios.

Further investigation of the CIs reveals that the Reference scenario, without additional carbon policy, realises a CI reduction of nearly 2/3 over the model period. With a carbon intensity of 239 gCO_2/kWh in 2060, the Reference scenario achieves 77% of the CI reduction of the \$200/tCO_2 scenario (105 gCO_2/kWh). The different carbon tax rates and structures drive the system down different paths, but all approach a carbon intensity of 172 gCO_2/kWh ± 67 gCO_2/kWh by 2060.

The Intergovernmental Panel on Climate Change (IPCC) estimates that carbon intensity from power generation must approach zero by 2050 if the increase in global temperature is to be limited to 2˚C this century (Figure 2.4(a)) (70). A carbon tax of \$30/tCO_2 appears to be sufficient for Alberta to meet the global average IPCC recommendation for power systems through to 2030. Beyond 2030, it is increasingly difficult to achieve emission reductions, as none of the scenarios meet the IPCC recommendation from 2040 onward.

Figure 2.4(b) shows the cumulative CO_2 emissions over the model period for selected scenarios. As expected, the scenario with the most aggressive carbon policy (i.e. 200B) has considerably less emissions than the other tax scenarios. Although CIs of all scenarios decrease to similar values in 2060, the cumulative CO_2 emissions for the different scenarios diverge to a wide range of total emissions. For example, scenario 200B has approximately half the total emissions of

the Reference scenario in 2060. This illustrates the significance of reducing CI in the near-term to achieve cumulative reductions in the long-term.

To understand the roles of various technologies in reducing CI, the generation mixes are examined.

2.3.2 Generation mix

Figure 2.5 shows stacked generation plots for six scenarios, illustrating the amount of electrical energy provided by different generation technologies from 2010-2060.

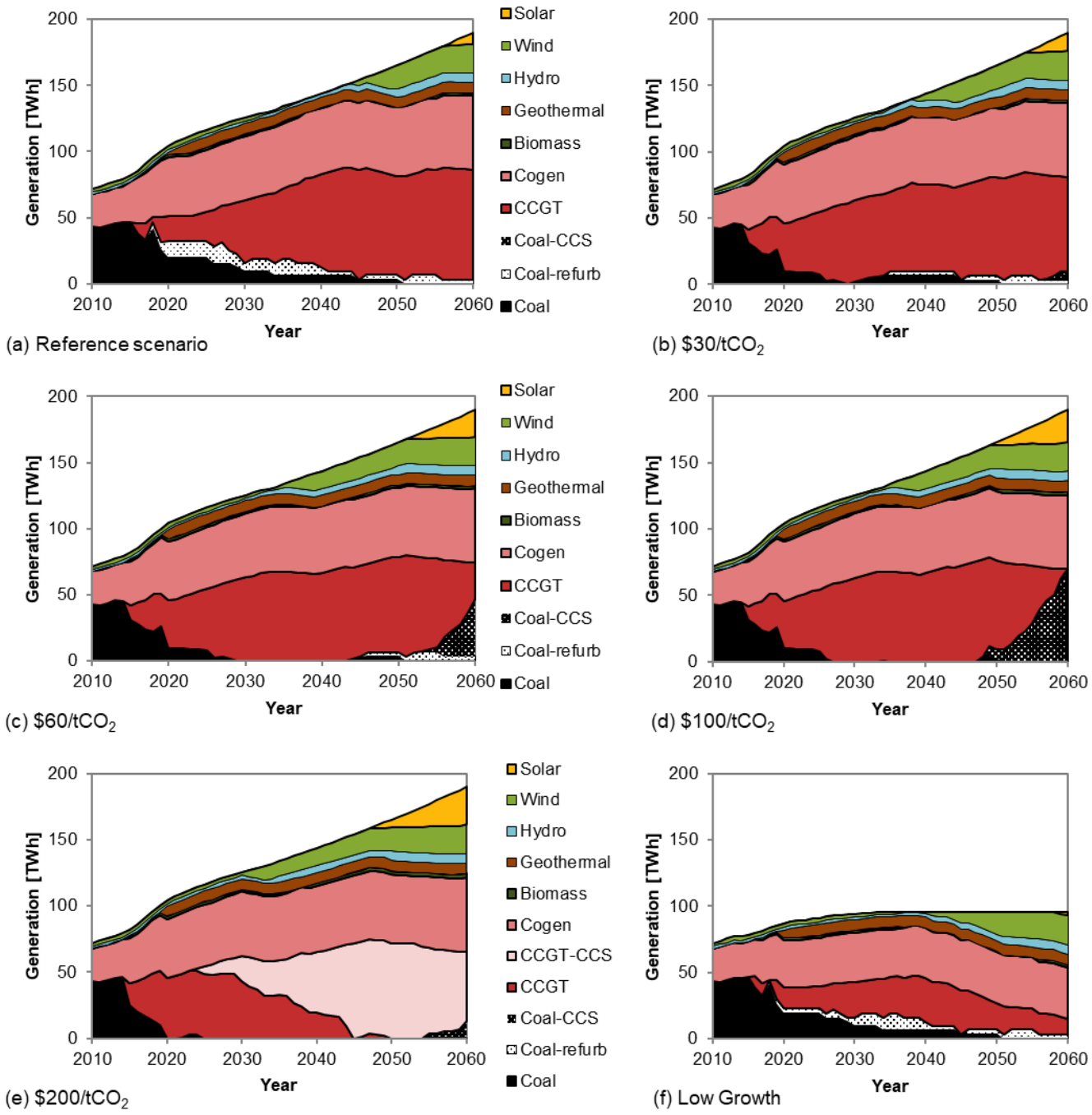

Figure 2.5: Simulated stacked generation by type for six scenarios: (a) Reference, (b) 30B, (c) 60B, (d) 100B, (e) 200B, (f) Low Growth scenario.

The difference in CI between Reference and 30B scenarios in the 2015-2040 timeframe (Point 1, Figure 2.4(a)) is due to fewer life extensions of coal plants as shown in Figure 2.5(a) and (b). In the Reference scenario, eight coal plants, representing 4.2 GW, undergo life extensions, compared to just three plants, representing 1.3 GW, in scenario 30B. In scenario 30B, new

combined cycle natural gas plants make up for the reduced generation from coal plants, and greatly reduce CO_2 emissions. The $30 tax also advances the installation of wind and solar PV, and results in some PC-CCS, but these have minimal impact on the CI compared to the transition from coal to natural gas.

Increasing the carbon tax to $60/t$CO_2$ by 2040 (scenario 60B) forces many coal plants to retire before the end of their expected life (Figure 2.5(c)). This $60 carbon tax also advances the time at which both wind and solar PV become economic. The combination of these two shifts causes the separation in CIs of 60B from the 30B scenario at 2030 (Point 2, Figure 2.4(a)). Escalating fuel prices eventually cause the same technology choices in the 30B scenario, and from 2045 onward emissions remain similar.

The 100B scenario (Figure 2.5(d)) has essentially the same generation mix and emissions as 60B until the mid-2040s when conventional coal and CCGTs are replaced with pulverised coal with CCS. In 2060, 9.4 GW of PC-CCS delivers 70 TWh, while 24 GW of wind and solar PV generate 47 TWh.

The incremental reductions in cumulative CO_2 from increasing the carbon tax from Reference to $30, $30 to $60, and $60 to $100 $/t$CO_2$ are 303, 129, and 102 MtCO_2 respectively. Continued stepwise increase of the carbon tax achieves diminishing incremental emission reductions, as shown in Table 2.4. The greatest reduction of emissions in these scenarios comes from installing new combined cycle natural gas plants rather than extending the lives of coal plants.

A reliance on natural gas with CCS is observed in the 200B scenario (Figure 2.5(e)) because, with the same 85% carbon capture rate as coal with CCS, natural gas fired generation has lower ultimate emissions. In 2042, CCGT-CCS is the largest provider of electricity in this scenario, displacing CCGT without CCS. The rapid tax escalation of $40/t$CO_2$ every five years offsets the price escalation of natural gas so coal with CCS has a reduced role in the latter years. Despite the fact that this tax rate is twice as aggressive as scenario 100B, there is little impact on the date by which wind and solar PV become economic. The early installation of CCGT-CCS enables the lower level of CI and lowest overall carbon emissions (Figure 2.4).

Natural gas acts as a bridge fuel in all scenarios, but scenario 100B demonstrates the transitions most clearly. As seen in Figure 2.5(d), natural gas first facilitates the transition away from coal (~2010-2025), takes on the primary role in the system (~2025-2050), before lower carbon alternatives like CCS and solar PV become economic (~2050-2060). Research modelling future power generation in the US found similar trends (71).

Significant emission reductions caused by switching from coal to gas have been observed in the past. The carbon intensity of the US power system decreased 13% from 2007 to 2012, avoiding 314 $MtCO_2$ emissions (72). Approximately one-third of these reductions can be attributed to the exponential growth of wind and solar generation, which doubled the electricity output of renewables in this five year span. However, it was low gas prices prompting a shift -5% of annual demand - from coal to natural gas for baseload generation that accounted for two-thirds of the reductions (72).

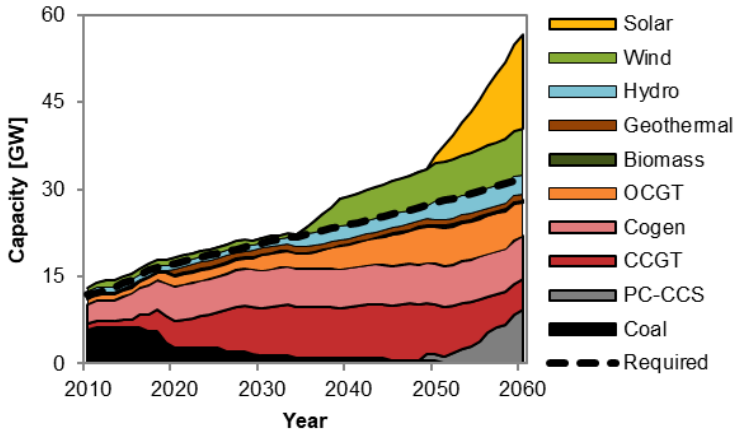

Figure 2.6: Simulated stacked capacity by generation type for scenario100B. The dashed line is the dispatchable capacity required to meet the peak demand and reserve margin.

Wind and solar play minor roles during the first few decades of the model period. Even in scenario 100B, no new wind capacity is installed until 2035 (Figure 2.6) when natural gas is \$7.13/MMBtu and the tax is \$50/tCO_2. Solar PV reaches 16.4 GW of capacity by 2060, but is not installed before 2050. The dashed line in Figure 6 indicates the minimum dispatchable capacity required to meet the reserve margin. Wind and solar PV capacity are in excess of this requirement.

It is generally accepted that on-shore wind and solar PV are cost competitive with conventional generation. However, these results show they are not cost-effective generation options for the Alberta system without an increase in fuel prices and/or carbon taxes. The principal reason for this phenomenon is the non-dispatchable nature of wind and solar power and the backup capacity that must be present to maintain reliability requirements (i.e. reserve margin). When generating, wind and solar PV displace the variable operating costs of other dispatchable generators, but the dispatchable technologies still incur capital and fixed O&M costs. Wind and solar PV become economic when the variable costs of dispatchable technologies increase sufficiently - by fuel price escalation and/or carbon taxes - to offset the investment in wind and solar power.

Emission offsets and tradable renewable energy credits (TRECs) are currently procured by wind farms in Alberta to improve their economics. Compliance with the *Specified Gas Emitters Regulation* (SGER) can be achieved by purchasing offsets from low-carbon generation like wind power for approximately $9/MWh (73). This offset revenue is not included in the model because the offset value is based on the carbon intensity of the system, which will decrease naturally with coal plant retirements, and more quickly if there is rapid installation of zero-carbon generation such as wind power. Wind generators in the province have also been able to obtain money for the offsets by selling them to California utilities as TRECs, but this market is reportedly shrinking so revenue from TRECs are not included (73). Sensitivity to these assumptions was tested by running simulations with a $9/MWh credit to wind power, and the impact was minor. For example, applying the credit in scenario 60B resulted in new wind capacity five years sooner (2030 vs. 2035), and a 0.8% reduction of cumulative CO_2 emissions compared to 60B.

The other generation options make smaller contributions to the generation mixes. Solar PV appears in all scenarios, but always after wind power has reached its capacity limit because, compared to wind, solar PV has a higher capital cost and a lower capacity factor. Biomass power with mill waste as the fuel provides electricity in all scenarios, and all scenarios with carbon taxes incent the use of roadside residues as a fuel. However, with the limited resource availability, the total contribution from biomass does not exceed 2.8 TWh per year, a small

fraction of annual demand. Geothermal and hydropower are quickly installed to their capacity limits in all scenarios, emphasising the value of dispatchable, low-carbon generation even if the capital costs are high. While PC-CCS appears in all scenarios, the more capital intensive IGCC-CCS does not appear because the cost of coal is not high enough to justify the higher efficiencies of these plants.

2.3.3 CO_2 and methane emissions

Despite a nearly threefold increase in demand, the stacked emissions plots in Figure 2.7 show relatively level annual emissions from 2010-2060, even for the Reference scenario. This is consistent with the nearly 2/3 reduction in CI seen in Figure 2.4(a). The emission impact of life extensions for coal plants is seen in Figure 7(a). The combined cycle natural gas plants installed in 30B Figure 2.7(b) have roughly half of the CO_2 emissions of the coal plants they displace. Both scenarios in Figure 2.7 illustrate the shift in primary source of emissions from coal to natural gas.

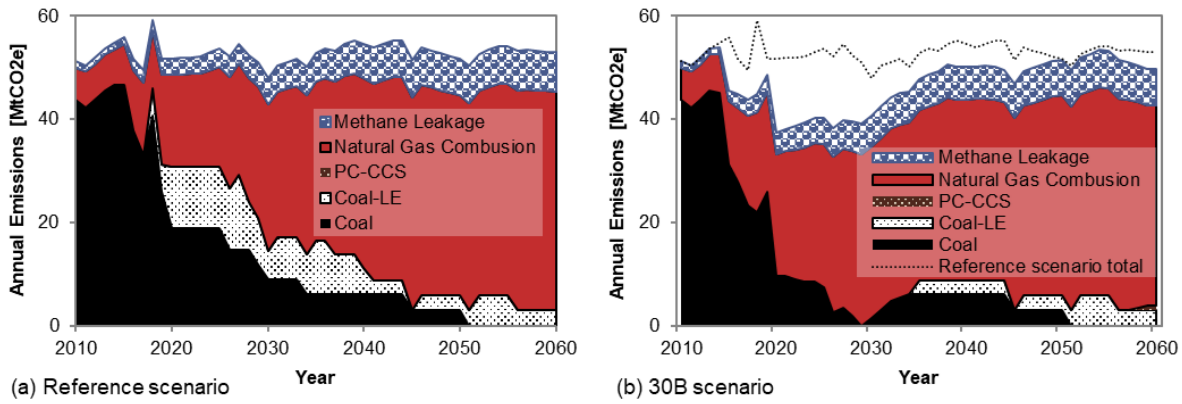

Figure 2.7: Simulated stacked emissions by source for (a) Reference and (b) 30B scenarios.

Uncertainty in the carbon footprint of shale gas has spurred debate over the climate benefits of increased use of natural gas (74–83). To illustrate the relative impact of fugitive methane emissions in the models, a methane leakage rate of 2% is assumed (84), and 100-year global warming potential of 25 is applied (85). Figure 2.7 includes the CO_2 equivalent warming potential of fugitive methane based on the amount of natural gas used for power generation in each scenario. The additional use of natural gas in 30B from 2015 to 2040 increases methane

leakage but does not negate climate benefits of switching from coal. This result is consistent with many other studies (74,76,79,82,83).

2.3.4 High natural gas price scenarios

The results presented to this point have used the *Baseline* price forecast for natural gas. In simulations with the *High* prices, coal remains economic throughout the model time frame with existing coal and PC-CCS overlapping in the middle of the model period, even in the 100H scenario as shown in Figure 2.8.

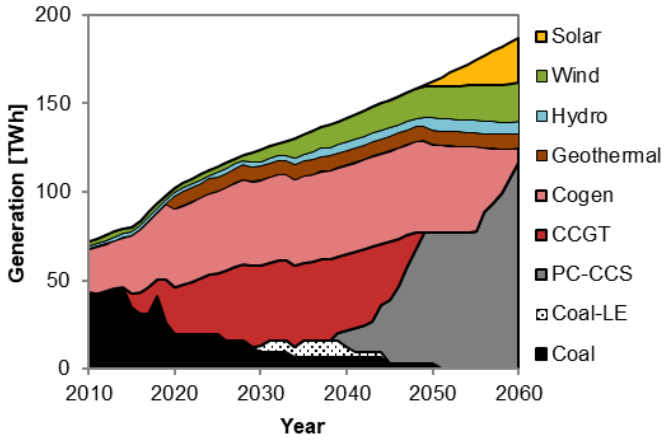

Figure 2.8: Simulated stacked generation by type for 100H scenario.

Compared to the Baseline gas price scenarios (e.g. 30B), annual CO_2 emissions are higher for the High gas price scenarios (e.g. 30H) in the first half of the model period because of persistent conventional coal-fired generation (Figure 2.9). These higher emissions in 30H mean that the IPCC 2˚C target is not met through 2030 with a tax of \$30/tCO_2 as it was in scenario 30B. However, as shown in Figure 2.9, a greater build-out of PC-CCS in the High gas price scenarios results in lower emissions in the final two decades compared to the Baseline gas price scenarios.

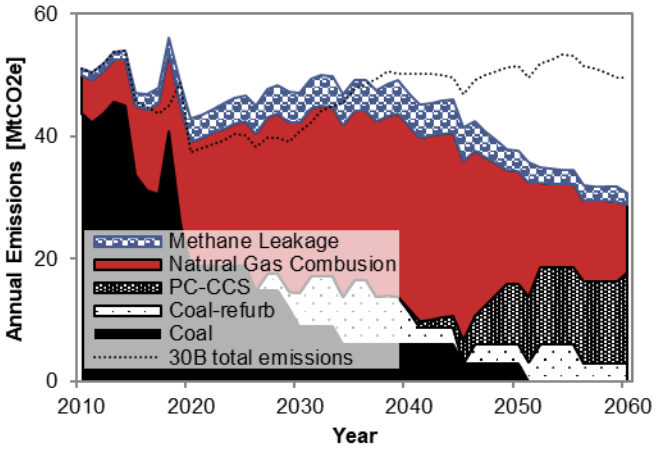

Figure 2.9: Simulated stacked emissions by source for 30H scenario.

2.3.5 Low Cost scenarios

The Low Cost scenario represents high learning rates and optimistic capital costs for wind and solar PV, yet CO_2 emissions over the model period are reduced only 3% compared to the Reference case (Table 2.3). When a carbon tax is applied for the 60B-LC scenario, emissions are reduced by 20% compared to the Reference scenario. This is only marginally better than the 18% reduction achieved in scenario 60B that has the same carbon tax but without the lower costs. This suggests that carbon taxes are more effective at reducing CO_2 emissions than long-term cost reductions on wind and solar PV technologies.

2.3.6 Low Growth scenario

The total electricity demand in the Low Growth scenario is 32% less than the other scenarios, so system costs and emission reductions cannot be fairly compared between different growth scenarios (Table 1). However, even in the absence of additional carbon policy, renewable technologies play an increasing role in the generation mix (Figure 2.5(f)). In 2060, 44% of electricity comes from renewable sources - wind, geothermal, hydro, solar PV, and biomass, from highest to lowest contribution. Cogeneration provides an additional 41%, with CCGT and the Keephills 3 coal plant, after a life extension, providing the remainder. From 2045 onward, annual electricity provided by CCGT decreases as units reach the end of their 30-year lifetime. The escalating cost of natural gas and decreasing capital costs for wind and solar power make renewables with OCGT backup the economic replacement. In the other scenarios with higher

load growth, wind and solar are not sufficient to meet the increasing demand so fossil fuel technologies are also installed.

2.3.7 Model limitations

Bottom-up optimisation models are used to assess the impacts of policy, technology, and resource costs on the development of energy systems. The explicit connection of these inputs to system cost and emissions can offer valuable insight to policy makers' interest in ensuring low-CO_2 electricity at minimal cost. While assumptions about the future are inherently imperfect and optimisation solutions are illusorily precise, multiple simulations can reveal trends and outcomes that, when assessed relative to one another, can support a course of action.

The Alberta power system is a market comprised of companies that make decisions to build, operate, sell, and decommission generators based on a unique portfolio of assets. Decisions are made by a company typically with the goal of maximising shareholder revenue. The model used in this research optimises for lowest net present system cost, and does not represent market characteristics of the system. Although this means different timing of decisions, the overall trends and tendencies for generation technology preferences should be consistent, given the assumed cost and demand profiles.

Results from energy models are highly dependent on capacity and operational limits of the technologies. Recognising the challenges of forecasting these parameters for a long-term outlook, the maximum capacity constraints chosen for this work are intended to be an upper bound on what is possible. This gives the model flexibility to demonstrate preference for specific technologies while staying within realistic limits of construction capability, resource availability, and grid stability.

2.4 CONCLUSIONS

2.4.1 Key findings

Most of the world is faced with the challenge of meeting a pending electricity supply gap while simultaneously decreasing greenhouse gas emissions. The research presented here elucidates

how carbon taxes can be implemented to reduce future emissions from the coal-based Alberta power system.

Simulations indicate that a $30/tCO$_2$ tax on the Alberta power system reduces near-term emissions sufficiently to meet the IPCC 2˚C carbon intensity recommendations until 2030. Reductions are achieved by installing natural gas-fired combined cycle plants instead of extending the lives of ageing coal units. At $60/tCO$_2$, it becomes cost-effective to retire coal plants early and install combined cycle natural gas units in their place. This is the most effective transition that can occur in the power system to reduce emissions - displace coal with natural gas for baseload generation.

While higher carbon taxes result in lower emissions, the incremental reductions decrease as economic low-carbon generation options are depleted. Increasing the carbon tax advances the build-out time of wind and solar PV and causes additional PC-CCS to be installed.

Wind and solar PV are not immediately economic in the system because the technologies require dispatchable backup power. Nevertheless, wind and solar PV are built to their capacity limits by the end of the modelled period. This is part of a shift to renewables that is most clearly seen in the Low Growth scenario (Figure 2.5(f)). In addition to renewables, new fossil fuel generation is necessary in the other scenarios because of the higher load growth.

The aggressive $200 carbon tax (i.e. scenario 200B) reduces cumulative 2010-2060 CO_2 emissions by 43%, and achieves much lower CIs than the other simulations. This is made possible by utilising combined cycle natural gas with CCS - the only modelled scenario to do so.

CCS has been proposed as a technology that will have a key role in future low-carbon power systems (65,86,87). The technology components of CCS are well-established, but it is still an emerging practice with an uncertain future. Alberta has vast coal reserves that could fuel power generation for hundreds of years (88). However, societal and government approval of additional mines required to support extensive coal-fired generation with CCS may be a barrier to the technology's progress (89). It is important to note that, in the model, CCS technology options do not include sequestration cost - the costs are for capture and compression of CO_2 at the power plant only. While the cost of capture and compression are typically the largest

component of CCS, and enhanced oil recovery (EOR) may add value to the process, economic viability hinges upon available storage infrastructure and public acceptance (90).

CCS appears in most of the scenario results as a low-carbon baseload generator to provide increasing amounts of electricity as carbon policy is strengthened. However, this role could be filled by another technology with similar costs and performance, such as nuclear, or some other breakthrough technology yet to be developed.

Higher natural gas costs make it more difficult to achieve early emission reductions because coal is persistently economic. Even with a tax of $\$100/tCO_2$ (scenario 100H), coal plants do not retire before the end of their expected life. However, the quickly escalating cost of natural gas makes PC-CCS economic earlier than in the Baseline scenarios, which reduces CO_2 emissions in latter decades in the model.

Despite the high global warming potential of methane, increased leakage associated with additional natural gas use still results in lower CO_2-equivalent emissions than sustained operation of coal-fired generation.

2.4.2 Implications and considerations

Although Alberta's carbon policy at the time of writing is intensity based, it provides the framework for comprehensive carbon taxes to be implemented in the Alberta power system. This research indicates modest carbon taxes ($\$30/tCO_2$ - $\$60/tCO_2$) have the potential to reduce emissions from the Alberta system by 12-18%. However, the market structure of Alberta's power system and uncertainty of future natural gas prices suggest that companies may be hesitant to quickly build combined cycle gas plants and shutter their coal assets.

Since the most cost-effective emission reductions result from decreasing coal-fired generation, policy targeting the retirement of coal may be a successful alternative to carbon taxes. The federal government's *Reduction of Carbon Dioxide Emissions from Coal-fired Generation of Electricity Regulations* do address this, but permit most plants to operate for 50 years (58). A separate Alberta policy to advance the retirement of coal plants could achieve significant reductions in the coming decades. It would in effect guarantee the mid-term emission

reductions observed by the \$30/tCO_2, or \$60/tCO_2 scenarios, and companies would not have to speculate on the future price of natural gas to determine the economic time to close their coal plants and build CCGTs.

Despite the fact that natural gas-fired generation cannot meet long-term emission targets without CCS, there is no apparent mid-term alternative for baseload generation. Germany's aggressive pursuit of renewable power through feed-in-tariffs has resulted in 74 GW of wind and solar capacity - approximately equivalent to the annual peak demand - that delivers only 16% of annual energy (91). To replace retiring coal and nuclear plants and maintain flexibility in generation, 4.3 GW of new coal and 2.0 GW of new natural gas plants will be commissioned in Germany by 2018 (Bundesnetzagentur, 2014). So while natural gas is not the long-term solution for low-carbon power systems, it provides dispatchable power that is necessary in all systems.

Future resource prices, technology costs and performance, as well as social acceptance of technologies like nuclear power, CCS, and hydraulic fracturing are difficult to predict. Current decisions on carbon policy should aim to phase out coal plants. Policies to assist the transition beyond natural gas will become clearer in the coming decades as technologies and societal priorities evolve. Interconnections and large-scale storage, such as power-to-gas, may facilitate the integration of variable renewables, and should be explored in future research.

Acknowledgments

The authors gratefully acknowledge the financial support of the Pacific Institute for Climate Solutions (PICS). The authors also acknowledge and appreciate the feedback provided by Dr. Amy Sopinka.

3 UTILITY-SCALE P2G ENERGY STORAGE FOR 80% VRE SYSTEM[10]

3.1 INTRODUCTION

Limiting global temperature rise to the 2 ˚C target requires CO_2 emissions from global electricity generation to approach zero by 2050 according to the IPCC and others (70,93). However, with 67% of global electricity generation currently sourced from fossil fuels (94), meeting emission targets will require an extensive build-out of low-carbon generation. The International Energy Agency's (IEA) *450 Scenario*, wherein global warming has a 50% chance of being limited to 2 ˚C, projects renewables will contribute nearly 60% of global power generation in 2040 (95). Even in the IEA and U.S. Energy Information Administration reference scenarios, where the 2 ˚C target is not met, renewables are projected to experience the greatest growth of all generation options for the coming decades, surpassing coal as the largest source of electricity globally by 2040 (96,97).

Variable renewable electricity (VRE) technologies, namely wind and solar, will likely account for the majority of new low-carbon generation in many jurisdictions because of constraints on other options. The future of nuclear power is uncertain amid concerns over reactor accidents, waste disposal, and nuclear proliferation (61). Coal plants outfitted with carbon capture and sequestration (CCS) technology is a low-carbon baseload alternative, but according to the IEA "…progress is far too slow to achieve the widespread commercial deployment envisioned…" (98). Hydropower, currently the largest source of renewable electricity, has limited additional potential, particularly in OECD countries (97,99). Studies exploring the role of bioenergy in future, low-carbon energy systems find its contribution varies greatly depending on the region, competing demands, and, as summarised by Rogner et al., its ultimate use will be "… less a question of the available theoretical potential than of ecological sustainability and socioeconomic desirability" (99–101). The IEA projects that even with breakthroughs in enhanced geothermal systems, geothermal electricity will not exceed 3.5% of global power

[10] An earlier version of this chapter was published in (35)

generation in 2050 (102). These factors, taken together with projections for decreasing costs of wind and solar generation, lead to the conclusion that VRE technologies will contribute significantly in the future of many jurisdictions.

Emerging policies at various levels of government and recent studies of Integrated Assessment Models (IAMs) support the expected growth of VRE technologies. Germany is planning to increase the share of electricity from renewables to at least 80% of gross consumption by 2050 (103), and Denmark aims to be 100% renewable in all sectors by 2050 (104). IAMs such as GCAM (105,106) and IMAGE (107,108), include representations of energy systems, economic structures, and climate systems to study global climate change pathways and policies. Luderer et al. explore the role of renewable energy in limiting global CO_2 concentration to 450-550 ppm by comparing results from a range of IAMs (101). Even when CCS and nuclear are permitted, most IAMs indicate renewables will generate 30-70% of global annual electricity by 2050, largely from wind and solar. Subsequent research improving the representation (i.e. parameterisation of characteristics) of VRE in IAMs found higher wind and solar penetrations than previous versions of all considered models (109).

Integrating these high levels of VRE will be challenging because of the limited ability of existing electrical systems to respond to variation and uncertainty in net load. At timescales less than five minutes, wind and solar power can decrease system inertia and increase the need for power quality and regulation services (22,110). At longer timescales, system operators can be forced to curtail significant amounts of renewable energy generation, even at current penetrations of VRE (111). Depending on contractual arrangements, curtailment can incur costs to the system such as constraint payments, or costs to curtailed generators such as lost energy payments. Expansion of the transmission system to deliver renewable generation to load centres is a common solution to this problem. However, transmission expansion only reduces curtailment due to transmission constraints, not curtailment due to lack of demand.

Curtailment due to lack of demand – the focus of this study – occurs when VRE plus inflexible baseload generation exceed the system demand. Denholm and Hand examine the curtailment that occurs at high levels of VRE penetration under various system flexibilities (21). Defining

flexibility factor as the "fraction below annual peak [demand] to which conventional generators can cycle", they find that "…achieving 80% of the simulated system's electricity from wind generation only (and without storage) requires a system flexibility of close to 100%, and results in a curtailment rate of more than 43%." In this case, the effective capacity factor of the last unit of wind installed would be 6%, making its marginal cost over five times the cost when there is no curtailment. In Europe, under the IEA's *450 Scenario*, curtailment of excess electricity could occur up to one-third of the time in 2040 if integration methods such as storage are not implemented (95).

Energy storage can facilitate VRE integration and reduce curtailment (112–116). Candidate technologies capable of serving long-term energy storage are pumped hydro storage (PHS), compressed air energy storage (CAES), and power-to-gas (PtG) (116–118). Both PHS and CAES require specific geological conditions and, therefore, lack flexibility of location. PtG, whereby hydrogen is produced by electrolysis, is less site-specific. Multiple opportunities exist for PtG to leverage the natural gas grid and integrate with other sectors, as depicted in Figure 3.1. The vast majority of hydrogen - a versatile energy carrier - is currently produced from fossil fuels, but PtG offers a means of production with lower emissions. Furthermore, PtG can be an essential part of a hydrogen economy, which is considered by some to be the ultimate future of energy systems (119–121).

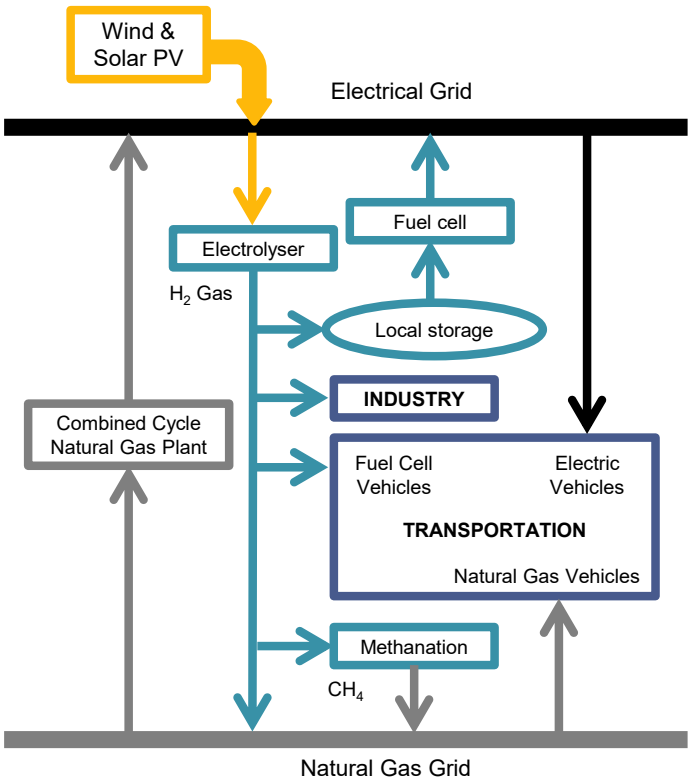

Figure 3.1: Schematic of power-to-gas showing the potential for integration of energy carriers and sectors.

Large-scale PtG in high VRE power systems is an active field of research with many areas yet to be thoroughly explored. This study focusses on PtG storage, assuming the natural gas grid is an unlimited storage reservoir, in an islanded power system targeting 80% VRE penetration. The modelled system, depicted in Figure 3.2, contains wind, solar PV, and combined cycle gas turbines (CCGT) as generators, PtG as the storage technology, and time-varying load in an hourly model of one year. Electrolyser capacity, charging behaviour, curtailment, and hydrogen production are analysed for a range of system configurations that achieve the targeted VRE penetration. Sensitivities to geographic diversity of VRE resources, wind-solar capacity split, and quality of wind year are also explored.

There are many pathways other than storage in Figure 3.1 for PtG hydrogen that are not explored in this study. While this research assumes the natural gas grid to be an infinite storage reservoir, it does not model the injection or interaction with the natural gas grid. Hydrogen can be further processed to create methane before injection into the natural gas grid (122–125).

Alternatively, hydrogen can be used for industrial purposes, displacing fossil fuel-sourced hydrogen and reducing associated emissions such as carbon dioxide (126–128). The global hydrogen market is expected to be valued at several trillion dollars by 2020 (129).

Nomenclature	
CAES	compressed air energy storage
CCS	carbon capture and sequestration
CCGT	combined cycle gas turbine
E_d	annual VRE generation used directly to meet demand [MWh]
E_{load}	annual electricity demand [MWh]
E_{st}	annual energy from storage that serves demand [MWh]
F_{vre}	annual fraction of VRE penetration
LDC	load duration curve

3.2 LITERATURE REVIEW

Existing research on PtG can be divided into four broad categories: small systems (i.e. <1000 MW), nuclear-based systems, natural gas-paired systems, and high VRE systems. Depending on the type of system, the role of PtG can vary from clean hydrogen production to storage. This role, as well as the size of the system, impacts the sizing of PtG and the way in which it is operated.

A recent review of PtG projects reveals that 76% of existing installations are stand-alone systems that are not connected to a bulk power grid (130). Many of these are pilot projects installed on isolated systems to increase VRE penetration and to reduce reliance on fossil fuels. Some studies assess opportunities for PtG on these small, weak, or isolated systems with high wind penetration (131–134). PtG is shown to significantly increase wind penetration (134), and provide a cost-competitive storage option for achieving high penetrations of VRE (133).

Nonetheless, PtG systems would benefit from increased electrolyser flexibility and efficiency (131), and hydrogen production costs are highly sensitive to electrolyser sizing (132). In these studies, VRE and storage are sized for autonomy, system stability, or for reasons not provided. These small-scale systems have unique generation and demand profiles that result in storage operation profiles that differ from the profiles of large-scale systems.

At a larger scale, several studies have explored electrolysis applications in nuclear-based power systems (129,135–140). The focus of these studies is either generation of low-cost hydrogen or operation of the electrolyser as a dispatchable load so that the reactors can operate at constant output. A common finding in these studies is that hydrogen production costs are highly sensitive to electrolyser utilisation. Low utilisation factors and/or operation at high electricity prices result in higher hydrogen production costs. Although the focus of these studies is not storage of excess VRE, results highlight the importance of electrolyser sizing and operation in PtG.

Other research has modelled the impacts of PtG on the power and natural gas sectors (115,141,142). Qadrdan et al. focus on impacts of PtG in the natural gas system with a high resolution model of Great Britain with 30% wind penetration. Electrolyser capacity is not sized; rather its operation is constrained by maximum allowable hydrogen concentrations in the gas grid. The analysis, limited to two days representing high and low demand, finds that PtG decreases the operating costs and emissions of the combined natural gas and power system. Vandewalle et al. model the power, natural gas, and CO_2 sectors in Belgium, with VRE capacity scaled to generate 100% of annual electricity demand, assuming no curtailment. The study's authors find that PtG transfers capacity and flexibility issues from the power system to the natural gas system. Electrolyser capacity is determined based on investment costs and full load hours to produce synthetic methane at a cost competitive with natural gas. Results presented on electrolyser operation are limited to the annual electricity usage.

Previous studies have investigated PtG in electricity systems with high penetrations of VRE (4,14,123,143–146). Most of these studies use cost optimisation models to determine the generation mix, size of storage (MWh), and/or hydrogen production. In a study of a 100% VRE

European power grid with multiple storage options, PtG accounts for 64% of the installed storage charging power (MW) and 99% of the storage capacity (MWh) (143). Another study targeting 100% renewable electricity for a small region in Germany finds that if the capital cost of PtG is less than 2453 €/kW, it is more cost-effective than Li-ion batteries at a cost of 350 €/kW (144). Some of the aforementioned studies of a PtG system coupled to an electrical system with high penetrations of VRE assess several scenarios with different system mixes; however the relationship between electrolyser capacity and VRE capacity is not examined. Furthermore, the temporal characteristics of PtG operation are not assessed and, with the exception of Heide et al. [43], neither is the impact of VRE resource mix on system capacities.

In this study we address these gaps by assessing the VRE-electrolyser capacity trade-off and the associated curtailment. In addition, we characterise the hourly distribution of charging events and discuss its implications for electrolyser operation. We explore impacts of resource diversity in this study by defining six scenarios representing different wind-solar mixes, locations, and wind years. In addition, a brief assessment of hydrogen concentrations in the natural gas grid is presented for selected systems.

To perform this analysis, we develop a method that jointly determines combinations of VRE and electrolyser capacity to achieve 80% VRE penetration. This is done by simulating the hourly operation of hundreds of capacity combinations and selecting ones that have 80% penetration.

3.3 METHODS

The system investigated in this research represents the electric power system in the Canadian province of Alberta with 80% VRE energy penetration in the year 2050. According to the Government of Alberta, “Alberta has one of the most extensive natural gas systems in the world…” and exports over 50% of production (147). This suggests PtG could be broadly deployed and that the hydrogen produced could be accommodated by the natural gas infrastructure.

This study uses the simplified representation of the Alberta electricity system and PtG storage shown in Figure 3.2. A time-varying electricity demand is met by wind, solar PV, and/or CCGT

generators and delivered by the electrical grid. The PtG storage system has three main components: charger, reservoir, and discharger. In our model, the charger is an electrolyser that operates on excess wind and solar generation to produce hydrogen. The reservoir is a proxy for the natural grid, which we assume to be extensive and thus model it simply as an unlimited reservoir for hydrogen. The reservoir storage level increases when hydrogen is produced by the charger (electrolysis), and decreases when the discharger (CCGT) burns hydrogen from the reservoir. The CCGT can also burn natural gas if there is no hydrogen in the storage reservoir. There are no transmission constraints in the model of the power system and, therefore, the effects of siting electrolyser and generation technologies are not assessed.[11]

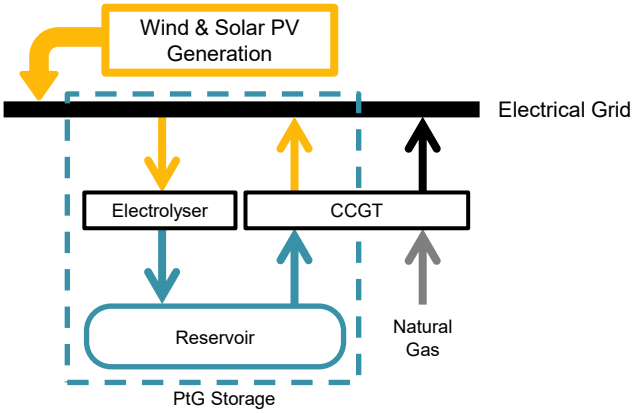

Figure 3.2: Schematic representation of the energy system as modelled.

Assuming an infinitely large natural gas grid, the model does not constrain the rate of hydrogen production (i.e. injection rate into the grid), or the amount of hydrogen in the reservoir (i.e. concentration of hydrogen in the grid). Nonetheless, hydrogen can adversely affect natural gas infrastructure and certain customer end-uses. Therefore we assess the infinite reservoir assumption by determining average hydrogen concentrations that result from selected systems (see Section 3.4.3).

In order to provide 80% of the annual energy by VRE – directly and via storage – there must be sufficient VRE capacity and electrolyser capacity. A wide range of combinations of VRE capacity

[11] Siting of wind and solar generation is examined based on regional resource profiles, but not with regards to energy system infrastructure such as transmission lines.

and electrolyser capacity are simulated to create a contour plot of the VRE penetrations (Figure 3.7). Selected VRE and electrolyser capacity combinations that achieve 80% penetration are then analysed in further detail.

Further explanation of the model is presented in Section 3.3.1. Wind, solar, and load data are provided in Section 3.3.2. Model scenarios are defined in Section 3.3.3, with additional modelling process and details provided in Section 3.3.4.

3.3.1 System model

An hourly dispatch model was developed to simulate operation of the system. For each hour, energy flows are managed in accordance with the flow chart shown Figure 3.3. The model treats wind and solar generation as "must-take" up to the demand in that hour. Therefore, when VRE generation exceeds demand, the energy in storage increases equal to the higher heating value of the hydrogen generated by an 80% efficient electrolyser (124,148,149).[12] If VRE generation is not sufficient to serve the load, the model uses energy from storage before using non-VRE generation. Discharge from storage is assumed to occur at 55% efficiency, representing a CCGT (64). When VRE generation exceeds demand and electrolyser capacity, VRE generation is curtailed. Figure 3.4 illustrates the operation of technologies and energy allocation in the model.

[12] The higher heating value (HHV) is consistent with the assumed efficiency when liquid water is used by the electrolyser and therefore includes the heat of vapourisation.

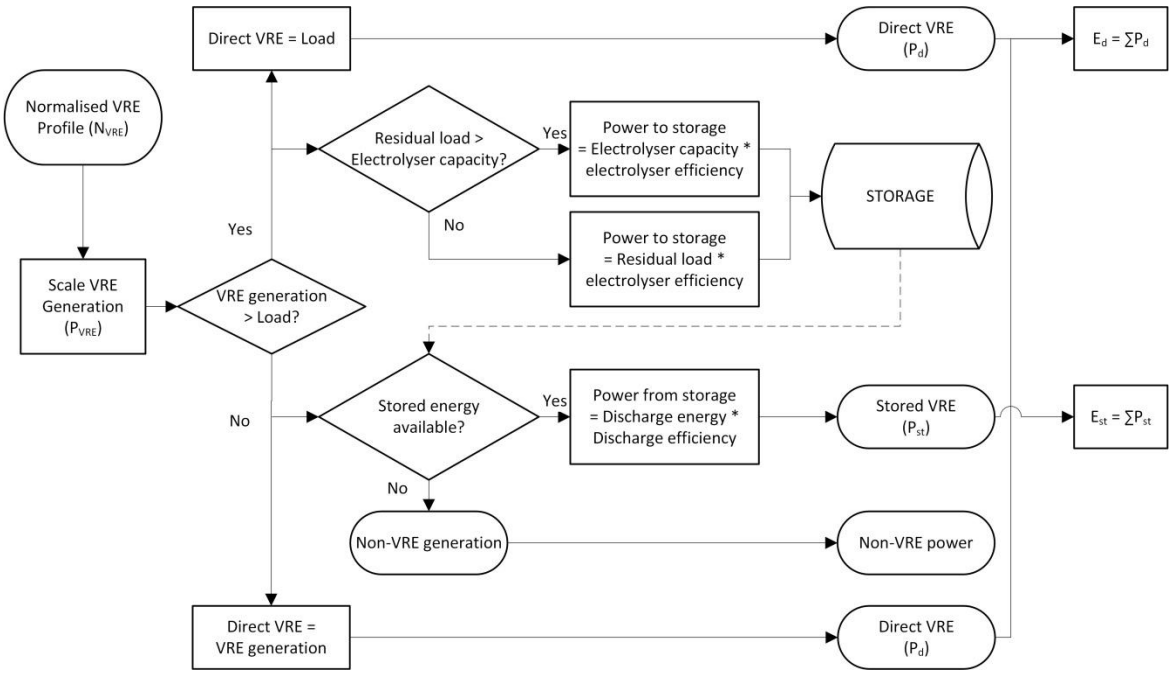

Figure 3.3: Flow chart illustrating the hourly simulation model.

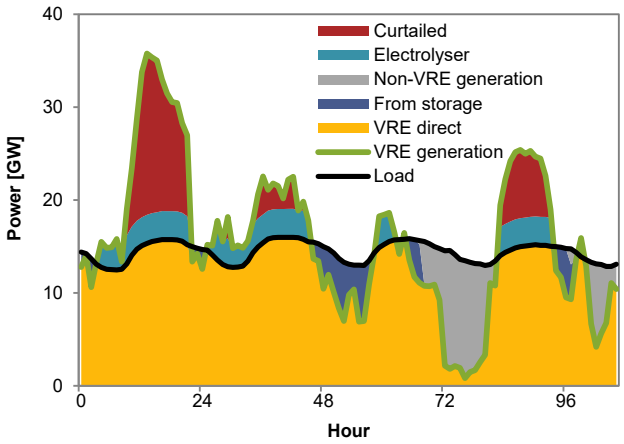

Figure 3.4: Depiction of how energy is allocated in model simulations. Excess generation by VRE up to the maximum electrolyser capacity can be used to create hydrogen for storage. The model will dispatch from storage before relying on non-VRE generation from natural gas-fired combined cycle turbines (CCGT).

To calculate the fraction of annual VRE penetration we include VRE generated energy used directly and energy output from storage. The VRE energy used directly, i.e. instantaneously, to meet hourly demand is denoted as P_d. Hourly energy output from storage, P_{st}, is also considered VRE-sourced because storage was charged with excess VRE generation. The fraction

of annual VRE penetration, F_{vre}, is defined in , where E_{load} is the annual energy demand, and E_d and E_{st} are the annual sums of P_d and P_{st}, respectively.

$$F_{vre} = \frac{E_d + E_{st}}{E_{load}} \quad \text{3-1}$$

It is assumed that the power system has a fleet of CCGT plants with a total capacity equal to the peak demand that can serve as both *storage discharge* and flexible*, non-VRE generation*. In reality, CCGT plants would burn a mixture of electrolysed hydrogen and natural gas as drawn from a pipeline. The CCGT plants are assumed to have no ramping limits or minimum generation level. This duty would more likely be served by a combination of CCGT and open cycle gas turbines in an actual system.

It is also assumed that the electrolysers are perfectly flexible, able to ramp up and down quickly through their full capacity range with constant efficiency. While electrolysers do have minimum load constraints and efficiencies are not constant, hundreds or possibly thousands of electrolysing units would be required for the charging capacities shown here. It is assumed that units are dispatched sequentially and ramp quickly so that each unit can be assumed always to be either off or on at full capacity.

3.3.2 Wind, solar, and load data

Alberta has an area of 662,000 km^2, approximately twice the size of Germany. There are four wind regimes in the province, three in the south and one covering the remainder of the province (150). The diversity in the south results from the mixed geography of the Rocky Mountains in the west to the prairies in the east. The majority of wind development to date has occurred in the southwest region of the province, but an increasing number of farms are currently in various stages of development in other regions.

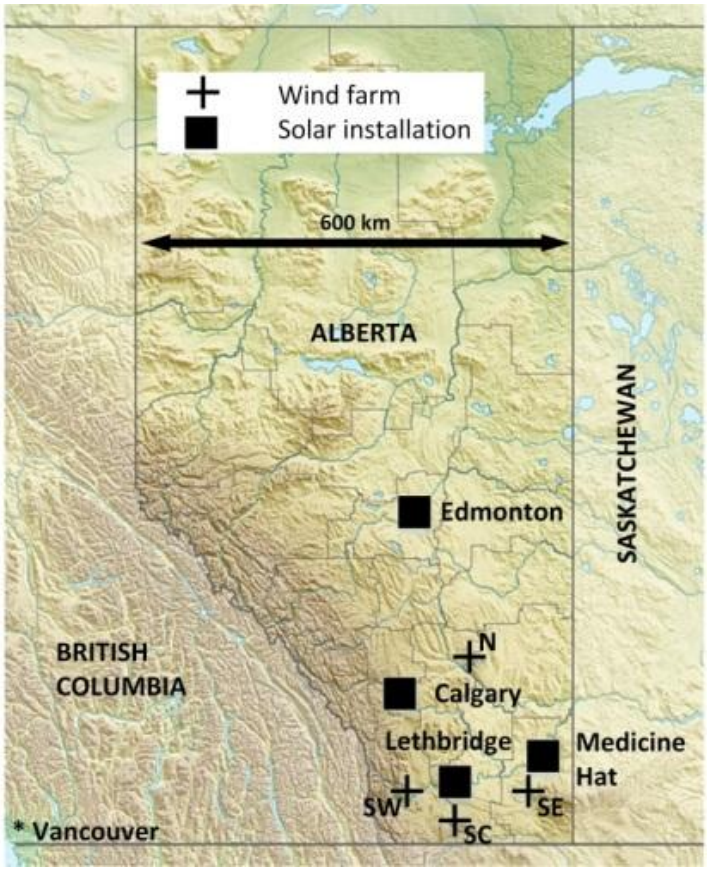

Figure 3.5: Approximate locations of representative wind and solar data[13]. Abbreviations correspond to the wind regions, see Table 3.1.

The hourly wind generation profiles used in the model are constructed from historic hourly data from one representative wind farm in each of the four regions, as shown in Figure 3.5. These wind farms are selected for low cross-correlation of power output with the wind farms in the other regions and high annual capacity factor. Low cross-correlation due to geographic dispersion of generation sites has been shown to be beneficial for integration of VRE (151,152). The selected farms have annual capacity factors of 34-37%, representing the trend to larger, more productive turbines that will likely be installed in the future (153). Data from the year 2013 is selected to represent an average wind year based on annual capacity factors from 2003-2015.

[13] Base map "Canada Alberta relief location map" by Carport is used under CC BY-SA 3.0.

Table 3.1: Representative wind farms for the four regions. Historic hourly generation by wind farm is available from the Alberta Electric System Operator (AESO). Listed capacity factors are for 2013.

Wind region	Wind farm	Capacity [MW]	Capacity Factor [%]
South west (SW)	Soderglen	68	36.9
South central (SC)	Magrath	30	34.8
South east (SE)	Chin Chute	30	34.4
North (N)	Wintering Hills	88	36.8

As of 2016, Alberta has 10.5 MW of installed solar power capacity, mainly in the form of rooftop photovoltaic (PV), with the largest installation being a 2 MW solar farm[14]. For this study, PV Watts[15] is used to simulate hourly solar PV generation at four locations in Alberta, as shown in Table 3.2 and Figure 3.5. Additional details of the solar installations such as tilt angle and efficiency can be found in Appendix A.

Table 3.2: Location and performance of solar installations

Solar installation data location	Type	Annual generation [kWh/kW]	Capacity Factor [%]
Lethbridge (LB)	1-axis tracking	2565	29%
Medicine Hat (MH)	1-axis tracking	2527	29%
Calgary (CG)	Fixed rooftop	1620	18%
Edmonton (ED)	Fixed rooftop	1468	17%

Hourly total system load data from the Alberta Electric System Operator (AESO) for 2013 is used to define the load profile. This load profile is scaled to the projected load for 2050, extrapolated from AESO's 2016 Long-term Outlook (154). The resulting annual electricity demand for this study is 134 TWh, with an average load of 15.3 GW, and a peak load of 19.3 GW.

[14] https://solaralberta.ca/
[15] http://pvwatts.nrel.gov/

3.3.3 Scenarios

A *scenario* is defined by its *normalized VRE generation profile*. The normalised VRE generation profile depends on the mix and locations of wind and solar farms, the wind-solar capacity split, and the wind year. Wind and solar generation profiles are normalised to their nominal rated capacity before an aggregate profile is constructed by the method illustrated in Figure 3.6. The values defining the scenarios, presented in

Table 3.3, are selected to represent a plausible range of resource diversities. The sum of the wind capacity fractions for each of the four wind regions, f_{W_X}, is unity. Similarly, the sum of the capacity fractions for each solar location, f_{S_X}, is unity. The sum of the wind fraction of VRE capacity, f_W, and the solar fraction of VRE capacity, f_S, is unity.

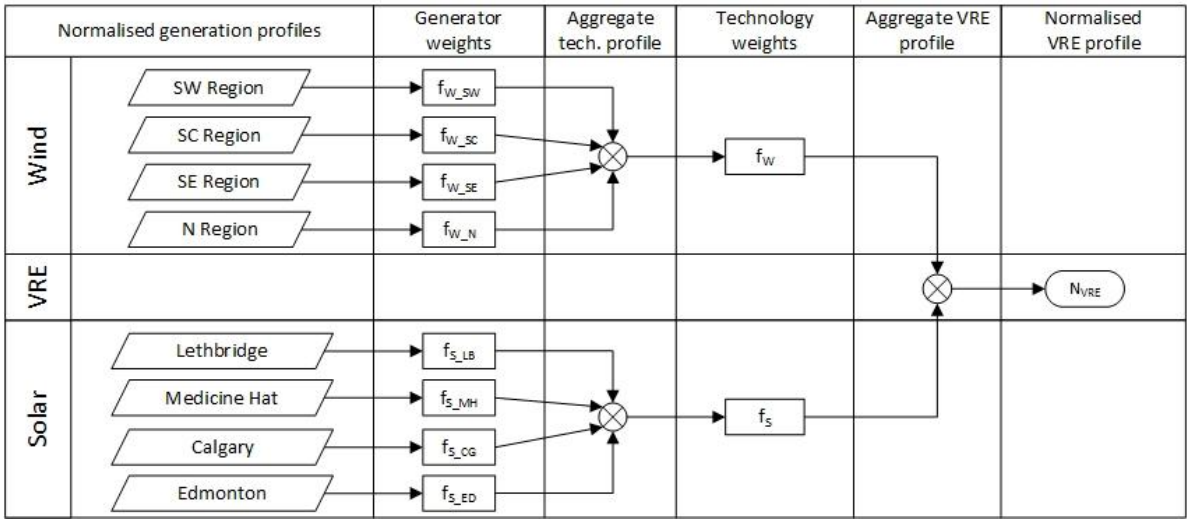

Figure 3.6: The normalised VRE profile, which defines each scenario, is based on the VRE generation mix.

Table 3.3: Parameters defining VRE profile for each scenario. Wind regions and solar locations are described in Section 3.3.2.

Scenario	Wind Year	Wind fraction of VRE capacity	Fraction of wind capacity by region (f_{W_x})				Solar fraction of VRE capacity	Fraction of solar capacity by location (f_{S_x})			
		(f_W)	SW	SC	SE	N	(f_S)	LB	MH	CG	ED
Reference	Avg.	0.5	0.25	0.25	0.25	0.25	0.5	0.5	0.5	0	0
Concentrated Wind	Avg.	0.5	1	0	0	0	0.5	0.5	0.5	0	0
Rooftop Solar	Avg.	0.5	0.25	0.25	0.25	0.25	0.5	0.25	0.25	0.25	0.25
High Solar Fraction	Avg.	0.35	0.25	0.25	0.25	0.25	0.65	0.5	0.5	0	0
2014 Wind	Low	0.5	0.25	0.25	0.25	0.25	0.5	0.5	0.5	0	0
2011 Wind	High	0.5	0.25	0.25	0.25	0.25	0.5	0.5	0.5	0	0

The *Reference Scenario* assumes equal wind and solar capacities, wind capacity spread equally among the four regions, 2013 wind generation data, and solar capacity equally split between two locations in the south of the province. Equally dividing the wind capacity among the four regions results in an aggregate wind generation profile with diversity statistics comparable to that of Nordic countries (151) (see Appendix A).

Three scenarios explore the impact of the wind resource. The *Concentrated Wind* scenario represents the entire wind capacity being built in the region with the highest capacity factor in 2013 and uses 2013 wind generation data. *2014 Wind* and *2011 Wind* scenarios, which are based on data from the namesake years, represent a relatively low and a relatively high wind year, respectively. The average capacity factor of the four representative wind farms for these years are 31.2% and 41.3%, compared to 35.7% in 2013.

The solar generation profile in most scenarios assumes single-axis tracking installations with capacity divided evenly between Lethbridge and Medicine Hat. These cities are in the south of the province where annual solar insolation is highest. The *High Solar Fraction* scenario assumes that 65% of the VRE capacity is solar and 35% is wind, resulting in more annual electricity generation from solar PV than wind. Sensitivity to a large-scale build-out of rooftop PV in

Edmonton and Calgary, the province's two largest cities, is explored in the *Rooftop Solar* scenario. In this scenario, the capacity is spread evenly among the four solar locations.

3.3.4 Combinations and configurations

For each of the six scenarios, 400 *combinations* of VRE capacity and electrolyser capacity are simulated for one year. These combinations consist of 20 capacities of VRE, ranging from zero to six times the average load. For each of these VRE capacities, the electrolyser capacity is varied from zero to half of the average load in 20 increments. For each combination, the fraction of annual energy that can be provided by VRE is determined. This method is used to generate contour plots of system VRE fractions (such as Figure 3.7) that are then used to select configurations for detailed analysis.

A *configuration* specifies a selected VRE capacity and electrolyser capacity combination that achieves exactly 80% VRE penetration. Four configurations are examined in the Reference Scenario and one in each of the other five scenarios.

In the Reference Scenario, the four configurations are determined with electrolyser capacities that are 1%, 10%, 20%, and 50% of the average system demand (MW). The corresponding VRE capacity for each configuration is that which results in 80% VRE penetration. These configurations are used to examine capacity mix, electricity mix, residual load duration curves, hydrogen production, and electrolyser utilisation.

For the other five scenarios, the electrolyser capacity for each configuration is set to 20% of the average system demand (3.06 GW), as in Configuration 3 of the Reference Scenario. In the Concentrated Wind, Rooftop Solar, and High Solar Fraction scenarios, the VRE capacities necessary to reach 80% VRE penetration are determined for each configuration. 2014 Wind and 2011 Wind scenarios are meant to assess the ability of a system to meet the 80% VRE penetration target under different wind years. Therefore, in addition to electrolyser capacity, these scenarios also have the same VRE capacity as Configuration 3 of the Reference Scenario.

3.4 Results and Discussion

3.4.1 Reference Scenario results

For the Reference Scenario, combinations of VRE capacity and electrolyser capacity that enable equivalent penetrations of VRE are plotted as contours in Figure 3.7. For example, the "0.8" line represents the combinations of VRE and electrolyser capacities that achieve 80% VRE penetration. With PtG as the only modelled storage option, there is a trade-off between VRE capacity and electrolyser capacity at high penetrations; increasing electrolyser capacity decreases required wind and solar capacity, and vice versa. Storage has negligible impact when VRE capacity is less than twice the average load. This can be attributed to the diverse mix of VRE and the fully flexible non-VRE generation. Four system configurations, indicated by the numbered points on the 80% curve in Figure 3.7, are selected for more detailed analysis below.

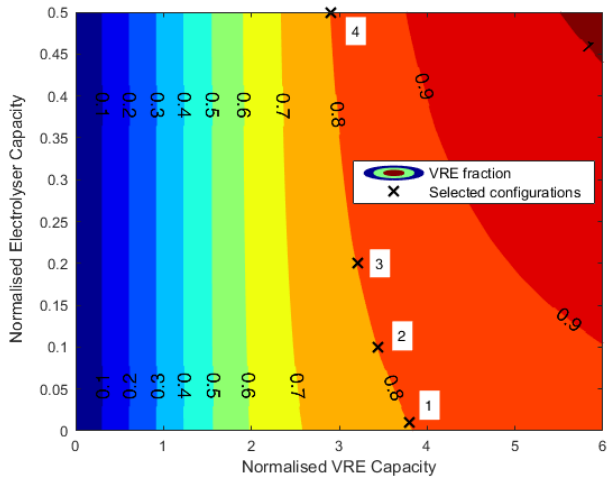

Figure 3.7: Annual energy fractions met by VRE and electrolyser combinations for the Reference Scenario. The four points define different configurations that achieve 80% VRE penetration. Axes are normalised by average system load (MW).

Configuration 1 has little electrolyser capacity, relying almost solely on VRE capacity. Configurations 2, 3 and 4 demonstrate that VRE capacity can be reduced with storage, although at a diminishing rate. Configuration 3 has 16% less VRE capacity than Configuration 1, while Configuration 4 has 23% less. The 80% contour line is nearly vertical at Configuration 4 indicating that additional electrolyser capacity does not significantly decrease VRE capacity.

Combined VRE and electrolyser capacity decreases from Configuration 1 to 2, and again from 2 to 3, but is equal in 3 and 4 (see Figure 3.8(a)). Figure 3.8(b) shows how increasing electrolyser capacity increases the amount of energy from PtG storage, and decreases the amount of curtailed and direct VRE energy. The amount of annual electricity demand met from storage ranges from 0.3% in Configuration 1, to 6.6% in Configuration 4.

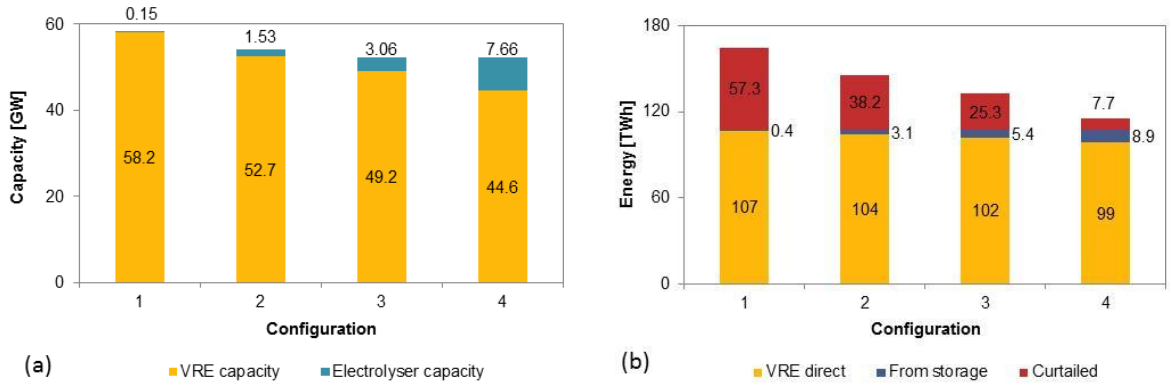

Figure 3.8: (a) VRE and electrolyser capacity for four configurations in the Reference Scenario. (b) Energy distribution for the four configurations.

Charging of storage occurs when the residual load, i.e. demand less VRE generation, is negative. Sorting hourly residual loads in descending order creates a residual load duration curve (RLDC), which is helpful in understanding the behaviour of very high VRE systems with storage. Figure 3.9 presents the RLDCs for the four 80%-configurations. When a RLDC is positive, power from dispatchable generation is used to satisfy demand. This dispatchable generation is from CCGTs and includes both storage discharge and non-VRE generation. Negative residual load charges storage up to the installed charging capacity, beyond which the energy is curtailed.

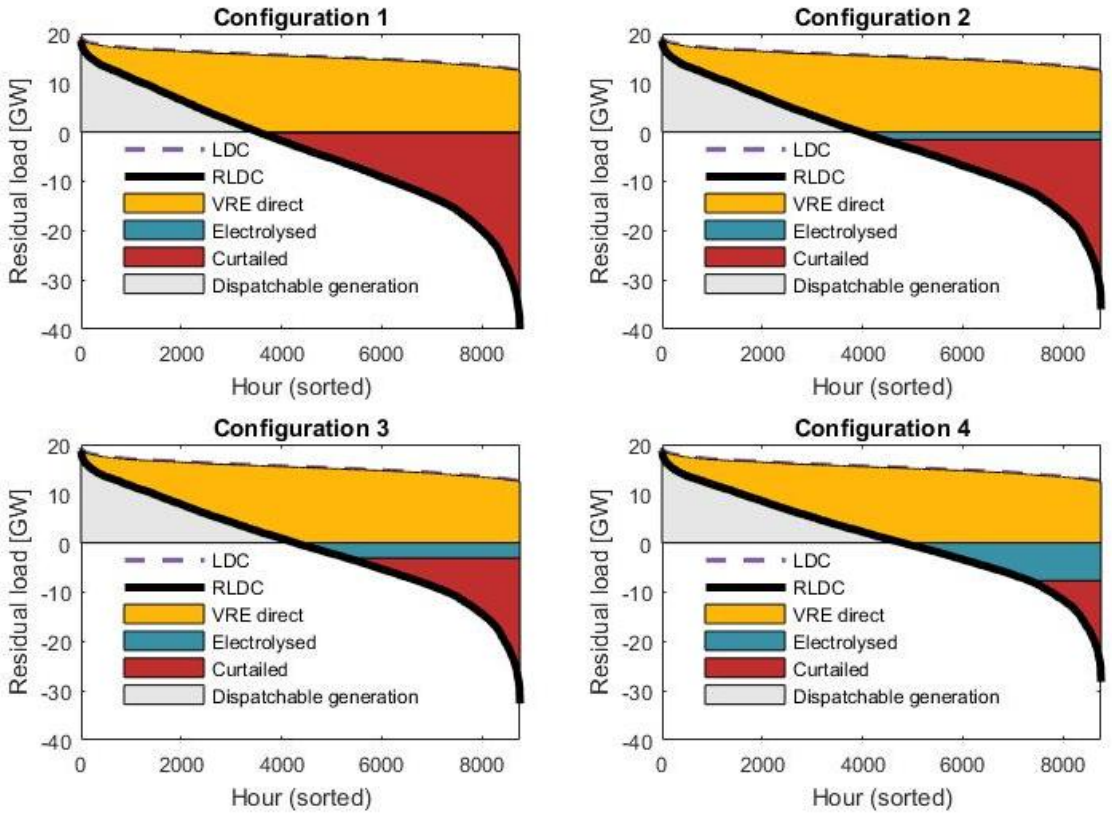

Figure 3.9: Residual load duration curves for the four VRE-electrolyser configurations. Demand met directly by VRE, E_d, is represented by the positive area between the LDC and the RLDC. Dispatchable generation, provided by combined cycle natural gas plants, includes both discharge from storage and nonVRE generation.

These RLDCs illustrate how storage reduces curtailment, albeit at a diminishing rate with increasing electrolyser capacity. The "tails" (highly negative values) of the RLDCs are sharp so the incremental energy available for storage decreases as electrolyser capacity increases. This explains why increasing electrolyser capacity does not proportionally increase energy from storage, as seen in Figure 3.8. On the other hand, increasing electrolyser capacity can greatly reduce the amount of curtailed energy in the tail, a trend also seen in Figure 8. The energy available for storage is significant; however charge and discharge efficiencies reduce the amount that can be delivered back to the power system.

Selection of a preferred PtG system configuration depends on additional factors outside the scope of this study. These include, but are not limited to, relative costs of VRE and storage,

resource availability, and additional benefits of storage such as balancing services. These factors can be unique to each system and should be assessed accordingly.

3.4.2 Electrolyser operation

In this section, electrolysis, i.e. charging, events are examined and implications for the storage technology are discussed. All of the 80%-configurations in the Reference Scenario experience a similar number of charging events, ranging from 435 in Configuration 1 to 477 in Configuration 4. This is expected because all four configurations use the same normalised VRE profile, scaled to different capacities.

Charging events are organised by the number of consecutive hours electrolysis occurs. The majority of charging events are less than 12 hours in duration, as seen by the histogram for Configuration 3 shown in Figure 3.10 (a). This can be largely attributed to the nature of the load, wind, and sun in the summer: system load is lower, winds tend to be lighter, and solar irradiation is higher. Therefore the VRE generation profile is often dominated by solar generation which, on many days, can exceed demand for a number of the daylight hours.

When these events are organised by the cumulative amount of hydrogen that is generated, the contribution of longer duration events is more apparent (Figure 3.10 (b)). For the average wind year in Configuration 3, only 26% of the events have durations of 12 hours or more, but these events account for 54% of the hydrogen produced. The other wind years shown in Figure 3.10 (b) support the same trend. This is why long-term storage technologies like PtG are particularly valuable in very high VRE systems.

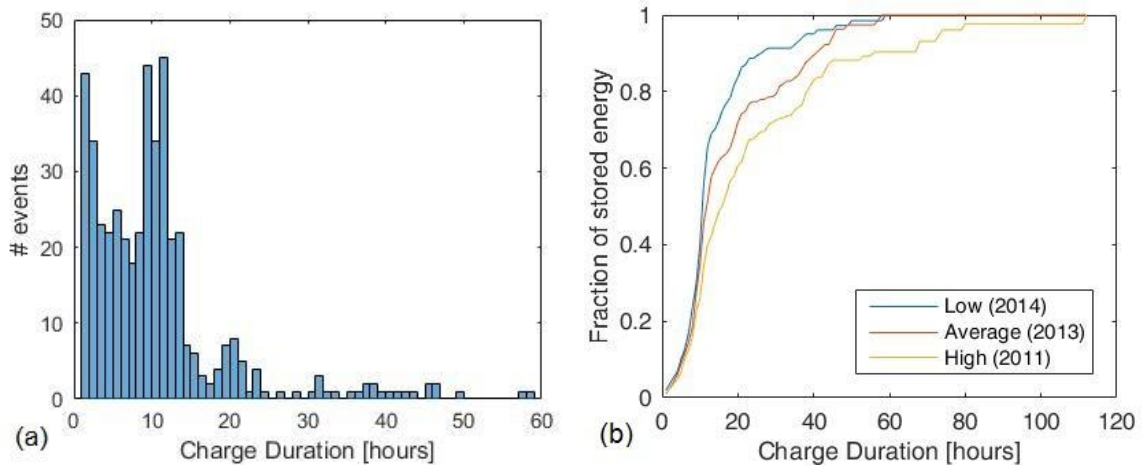

Figure 3.10: (a) Charge durations in Configuration 3 in an average wind year. (b) Cumulative stored energy by charge duration in Configuration 3 for three wind years.

Available storage technologies cover a broad range of energy and power specifications and can be roughly divided into three categories based on energy-to-power ratios (116,155). Stating energy in units of kWh and power in units of kW, the energy-to-power ratio is the number of hours a technology can charge or discharge at its nominal capacity. Short-term storage, such as capacitors and flywheels, has an energy-to-power ratio of less than 1 hour and is used mainly to maintain power quality for seconds or minutes. Medium-term storage, which includes most batteries, has an energy-to-power ratio between 1 and 10 hours and is suitable for peak shaving and time shifting. Long-term storage, such as PtG, has energy-to-power ratios exceeding ten hours and can be suitable for energy management, seasonal storage or unit commitment operation.

The large range in duration of charging events observed in this study may be best served by more than one storage technology. Existing alkaline electrolysers, the most common and lowest cost variety, are slow to reach steady operating temperature (130,131), have exhibited problems when powered by a variable source (124,130,131), and cannot turn down operation below approximately 20% of their rated capacity (124,130,139,156). Nonetheless, continued development of alkaline electrolysers may increase their flexibility to sufficiently manage VRE generation (139,157). Polymer electrolyte membrane (PEM) electrolysers exhibit much greater flexibility in terms of response time and minimum load and would be suitable for the medium-

term storage events (124,130,148). PEM electrolysers are relatively new commercially and likely require cost reductions as well as efficiency and longevity improvements to compete with battery storage technologies for this type of storage duty (124,148). Storage technologies other than PtG for medium-term duty would likely decrease the total storage capacity required to meet the 80% target in this study because of higher round-trip efficiencies. This would be an interesting topic for future research.

3.4.3 Hydrogen and the natural gas grid

Annual hydrogen productions for the Reference Scenario configurations are shown in Table 3.4 and range from 16-408 ktH_2. Globally, over 50 million tonnes of hydrogen are produced annually, mainly from fossil fuels (158). Electrolysers account for just 4% of global production, or approximately 2 Mt (148). Configuration 4 of the Reference Scenario would generate 20% of the current global production of hydrogen by electrolysis. This represents a significant build-out of electrolyser capacity in a relatively small jurisdiction.

Table 3.4: Hydrogen generation and average concentration in Alberta's natural gas grid for the four configurations

Configuration	Annual H_2 generation [MtH_2]	Average annual H_2 concentration [vol.%]
1	0.016	0.17%
2	0.142	1.47%
3	0.247	2.55%
4	0.408	4.21%

One of the principal opportunities of PtG is leveraging the natural gas grid for storage, but there are limits to how much hydrogen can be accommodated. Studies suggest concentrations between 1-20% by volume are possible before the blend adversely impacts end-use devices such as household appliances, public safety, or durability of the existing natural gas network (159–161). Annual average hydrogen concentration in Alberta's extensive natural gas grid from these configurations would be less than 5% and suggests PtG integration with the gas grid at this scale may be feasible (see Table 3.4). Details of the analysis can be found in Appendix B.

The annual average concentrations presented in Table 3.4 suggest feasibility, but there are factors that could lead to hydrogen concentrations that are significantly higher than these averages. Firstly, hydrogen production by the electrolysers will vary throughout the year. Annual utilisation of the electrolysers for the Reference Scenario configurations is between 30-59%. With the exception of Configuration 4, Figure 3.11 shows that most of the hours of operation are at full power. This behaviour can also be seen by the "electrolysed" area of the RLDCs in Figure 3.9. This means instantaneous hydrogen production could be two or three times the annual average. Secondly, natural gas production and system flows vary throughout the year, and times of lower flows will cause higher relative concentrations. Dedicated hydrogen storage near electrolyser plants such as cavern storage could be used to buffer these injection rates.

Another important consideration is the injection points of hydrogen into the natural gas grid. The listed concentrations assume injection of hydrogen such that the concentration is uniformly mixed with natural gas. While electrolysers can be distributed around the electrical and natural gas grids, discrete PtG infrastructure will result in non-uniform concentration.

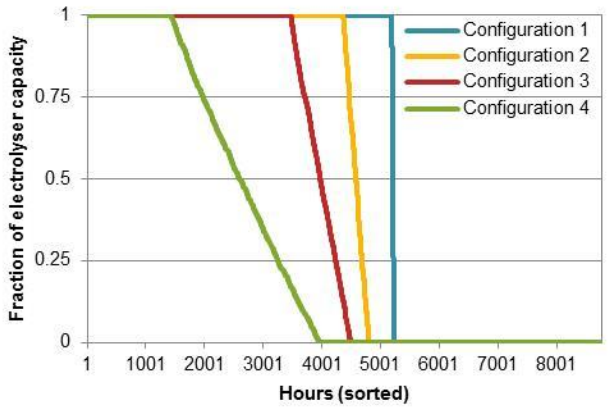

Figure 3.11: Utilisation duration curves of electrolysers configurations in the Reference Scenario.

3.4.4 Resource diversity impacts

The geographic diversity of wind and solar, and the relative capacity mix has an impact on the capacities required to achieve high VRE penetration. To compare across the other scenarios, the electrolyser capacity is fixed at 20% of the average system demand (the same as

Configuration 3 of the Reference Scenario). For each wind and solar scenario the VRE capacity is determined as that which results in 80% VRE penetration.

Figure 3.12 reveals that all of these scenarios require more VRE capacity than Configuration 3 in the Reference Scenario.

Concentrating wind capacity in the location with the best resource, as simulated in the Concentrated Wind scenario, requires 16% more VRE capacity compared to Configuration 3 of the Reference Scenario in which wind is distributed evenly around the regions (

Figure 3.12). Diversity of locations of wind farms smoothes the aggregate generation profile, causing flatter generation duration and RLDC curves, indicating that more VRE is captured, both directly and via storage. The benefit of wind diversity to system balancing requirements has been studied previously (151,162). The current study shows additional benefits of geographic distribution for systems with very high VRE penetrations and storage.

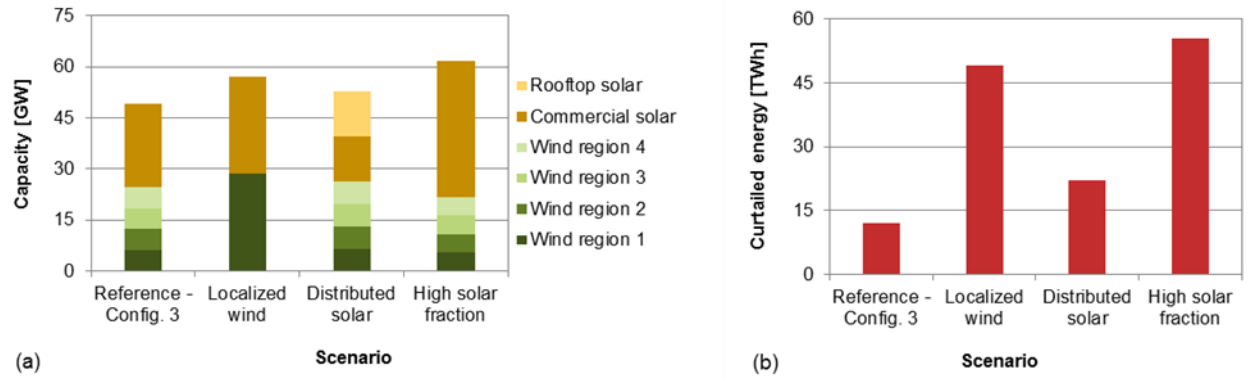

Figure 3.12: (a) VRE capacity required for 80% VRE penetration with an electrolyser capacity of 3.06 GW. (b) The associated curtailed energy in each scenario.

While geographic diversity of wind farms decreases required VRE capacity, geographic diversity of solar PV does not have the same benefit. The Rooftop Solar scenario, in which 50% of the PV capacity is in fixed rooftop systems, requires 7% more VRE capacity than Configuration 3 in the Reference Scenario with the same electrolyser capacity. This can be attributed to the relatively limited East-West distribution of solar sites and to the loss of generation potential from using fixed systems compared to single-axis installations. Solar generation is driven predominantly by

its diurnal pattern, and requires greater distances or unique regional phenomenon to benefit from geographical diversity at this hourly time scale.

The High Solar Fraction scenario (35% wind and 65% solar, by capacity) requires 26% greater total VRE capacity than Configuration 3 in the Reference Scenario to achieve 80% VRE penetration. This is due to the low capacity factor of solar relative to wind, and to the generation profile of solar. Solar has a steep generation duration curve with many hours at or near maximum output, resulting in a RLDC with many highly negative hours. This leads to the high level of curtailment shown in

Figure 3.12. These results are consistent with work by Heide et al., who modelled a highly renewable Europe and concluded that a wind-to-solar energy ratio greater than one reduced storage requirements (163).

The annual resource quality of wind can impact a system's ability to reach its renewable targets. As seen in Table 3.5, Configuration 3 of the Reference Scenario simulated with a Low wind year does not meet the 80% target, while a High wind year results in nearly 84% penetration. Table 3.5 shows that the relative change in energy from storage between the scenarios – approximately 10% – is quite significant. The difference in stored energy comes from charging events lasting longer than 12 hours, which can be seen in Figure 3.10 (b). In the Low wind year, 11% of the annual stored energy comes from events lasting longer than 24 hours. This is compared to 33% in the High wind year, in which one event lasts nearly five days.

Table 3.5: System performance of Reference Scenario Configuration 3 under different wind years.

Wind Year	Annual Capacity Factor	Electrolyser utilisation factor	Charging events	Curtailed energy	Energy from VRE direct (E_d)	Energy from storage (E_s)	VRE penetration (F_{vre})
	[%]	[% full load hours]	[# events]	[TWh]	[% annual energy]	[% annual energy]	[% annual energy]
Low (2014)	31.2%	39.5%	469	22.1	72.3%	3.5%	75.8%
Average (2013)	35.7%	45.3%	448	25.3	76.1%	4.0%	80.1%
High (2011)	41.3%	50.4%	437	31.6	79.3%	4.4%	83.8%

3.5 CONCLUSIONS

This study explores the relationship between VRE and electrolyser capacity, and electrolyser operation under high renewable energy system penetrations. The system investigated in this research represents the electric power system in the Canadian province of Alberta with 80% VRE energy penetration in the year 2050. This study uses the simplified representation of the Alberta electricity system and PtG storage. A time-varying electricity demand is met by wind, solar PV, and/or CCGT generators and delivered by the electrical grid. The PtG storage system has three main components: charger, reservoir, and discharger. In our model, the charger is an electrolyser that operates on excess wind and solar generation to produce hydrogen. The reservoir is a proxy for the natural grid, which we assume to be extensive and thus model it simply as an unlimited reservoir for hydrogen.

We show that, for a system with 80% VRE penetration, PtG storage can reduce VRE capacity by 23% and curtailment by 87% compared to a system without storage. The overall system capacity benefits of including electrolyser capacity are maximized with initial deployments; defined by associated reduction in VRE capacity required to achieve 80% penetration. Incremental electrolyser capacity results in decreasing VRE capacity reductions; however it significantly reduces curtailment.

Analysis of storage operation reveals charging events lasting from one hour to several days. Events lasting 12 hours and longer contribute most of the annual stored energy, demonstrating the value of long-term storage such as PtG. On the other hand, the large number of charging events lasting less than 12 hours suggests that medium-term storage technologies such as batteries, or flexible PEM electrolysers for PtG, may be more appropriate for some of the storage duty.

The hydrogen generated by the systems in this study is between 1% and 20% of the current annual global production of hydrogen by electrolysis; which would be a considerable feat for a small jurisdiction. If injected into Alberta's natural gas grid, the annual average hydrogen concentration would be less than 5%; below the suggested maximum level of blending before adverse effects. Other jurisdictions may require alternative PtG possibilities to avoid high

hydrogen concentrations, such as methanation, fuel cell vehicles, or industrial use of the hydrogen.

Geographic diversity of wind farms is shown to reduce the VRE capacity required to achieve 80% penetration, however, the same benefit is not found for solar PV. Increasing the solar fraction of total VRE capacity from 50% to 65% requires additional VRE capacity to reach 80% penetration. A system designed to achieve 80% penetration in an average wind year is shown to reach 76% penetration in a low wind year, and 84% penetration in a high wind year.

This study has provided a high-level, simplified analysis of the opportunity and challenges associated with meeting high renewable penetrations with PtG. Further research regarding the temporal concentrations of hydrogen, costs of generation and storage capacity, and alternative or complementary storage technologies would provide valuable insights.

3.6 Acknowledgments

The authors gratefully acknowledge the financial support of the Pacific Institute for Climate Solutions (PICS).

4 Optimising Direct Air Capture for a Net-Negative Power System

4.1 Introduction

Negative emissions are part of greenhouse gas accounting in many climate change mitigation studies (1,2,164–168). Net-zero emission targets inherently acknowledge that some form of negative emissions will be required to offset those from parts of the global economy that are particularly hard to decarbonise. Scaling up negative emission technologies (NET) to the levels required to meet strict emission pathways would involve installation growth rates comparable to that of solar PV, with potentially significant impacts to energy systems (169–172). Although commonplace in decarbonisation research, capacity expansion and dispatch models have only recently been expanded to investigate NET impact on power systems (29,30,173,174).

The main mechanism of carbon dioxide removal (CDR) in strict emission pathways is bioenergy with carbon capture and sequestration (165). Bioenergy with carbon capture and sequestration (BECCS) is the processing of biomass for power and/or heat while capturing the associated carbon for permanent removal from the Earth's ecological carbon cycle. The ability to extract work is what makes BECCS particularly attractive among NET options. However, BECCS is land-intensive and its potential varies by region (100,175). The land requirements for BECCS to achieve the cumulative amount of carbon sequestration projected in IPCC emission pathways[16] equates to 5-16% of the planet's total land surface (164). A perspective (171) of negative emissions at this scale suggests that sequestering 6 $GtCO_2$ annually via BECCS could require all the biomass on Earth that could be sustainably sourced, an equivalent of 100 EJ primary energy (172,173).

Another proposed mechanism of CDR is direct air capture (DAC) whereby carbon dioxide is removed from the ambient air through an engineered process. Compared to BECCS, DAC requires 90% less land, and the land does not have to be arable (171,176). Also, compared to more conventional in-situ carbon capture, DAC equipment does not need to be located at the

[16] IPCC SR1.5 °C S2 (middle-of-the-road) and S5 (fossil fuel and BECCS-intensive) pathways

power plant or industrial facility where emissions are released. Unfortunately, these benefits come with an energy penalty for extracting carbon dioxide from ambient air, estimated to be 10-14 GJ per tonne of carbon dioxide (176). Nevertheless, DAC may still outperform BECCS in terms of primary energy per ton of carbon sequestered (171), and the authors "call for research from the energy systems community to sharpen the understanding of the requirements for negative emission technologies to operate in different energy systems" (171).

In this study we apply a declining emission constraint in our energy planning model (17–19,32,37) to force the construction and operation of DAC in a regional power system. We examine generation dispatch and DAC operation across days, seasons, and years to explore energy demands, system flexibility, and VRE integration.

The next section reviews the current state of research on DAC in energy system modelling. Following that, methods of this study are presented, including a description of the modelling framework, scenarios, model enhancements, and the representative days that enable this analysis. Finally, modelling results are presented for generation mixes, annual emissions, DAC operation, and costs.

4.2 Literature Review

There are several DAC technologies in various stages of development, most of which involve chemical sorbents (177–188). These processes require energy inputs, mainly in the form of heat, to regenerate the CO_2 sorbent for cyclical use. McQueen et al. (187) explore meeting heating requirements of DAC with electricity and find total capture costs increase by roughly 2 $/t$CO_2$ per $/MWh increase in electricity price. An assessment by Creutzig et al. states that matching NETs with variable renewable electricity will be required to meet strict emission limits (171).

A 2025 review of negative emissions technologies in energy system models reports the presence of DAC in fourteen of the forty-three models (29). A study of the continental US power grid using a capacity expansion and dispatch model (189) reports DAC reduces the cost of resource portfolios capable of meeting deep decarbonisation targets (173). Bistline and

Blanford assume the bulk of DAC's energy requirement (heating) is met with natural gas, and the US power grid supplies the remaining 15% (173). More recently, Pham and Craig use a capacity expansion model of the US Eastern Interconnect to explore the benefits of advanced planning for DAC in a power system transforming to meet net-negative emission targets (174). Pham and Craig's study assumes electricity from the grid can substitute for all the energy input for DAC, including heating (187,190). In these energy modelling studies the resulting DAC demand is almost exclusively reported as an annual energy value.

The first energy planning study to overtly model DAC operation evaluates the value of load-shifting (30). In this study by Arwa and Schell, flexibility is modelled by decoupling the capture and regeneration portions of the DAC process. DAC capacity and operation is optimised for one year, represented by four 24-hour profiles. The study finds "increasing flexibility in DAC encourages more DAC [capacity] investment and better utilization of solar and wind capacity" (30).

Our study continues the evaluation of DAC operation by enhancing our hybrid capacity expansion and dispatch model (17–19,32,37). We define a new DAC technology in our model that is powered by the grid to "generate negative" carbon dioxide emissions. Like Arwa and Schell (30), we introduce an endogenous electricity demand for DAC by applying a strict emissions constraint.

To better understand DAC's range of daily and annual operations, we examine six years of system dispatch under the strictest emission target. Each year in our model is characterised by six different representative days, increasing the diversity of conditions over which the model must optimize. Our results show DAC's utilisation factor varies significantly over these years, affirming our decision to investigate multiple years of DAC operation. In addition to inter-annual differences, we show DAC operation may be shaped by seasonal and daily fluctuations in wind and solar generation.

4.3 METHODS

This research uses a hybrid capacity expansion and dispatch optimisation model representing the provincial power system in Alberta, Canada. For this study we define a new technology – DAC – that results in negative carbon dioxide emissions when powered by grid-level electricity. The extent to which DAC is powered (megawatts) in each time slice is a decision variable, optimized with the capacity and energy mix. In this section we will provide a description of the model, how DAC technology is represented, and details of other key parameters.

4.3.1 Modelling framework

The bottom-up, techno-economic, supply model, used in other decarbonisation studies (16,19,31–33,37,38,191), is enhanced for this study as depicted in Figure 4.1. The model uses the Open Source Energy Modelling System (OSeMOSYS) (54), a linear optimization platform. The model optimises for the lowest-cost generation mix that meets an exogenously defined load forecast until 2065, subject to future carbon emission limits. When the emission limit is negative, DAC induces an incremental power demand for which the model must also have adequate supply.

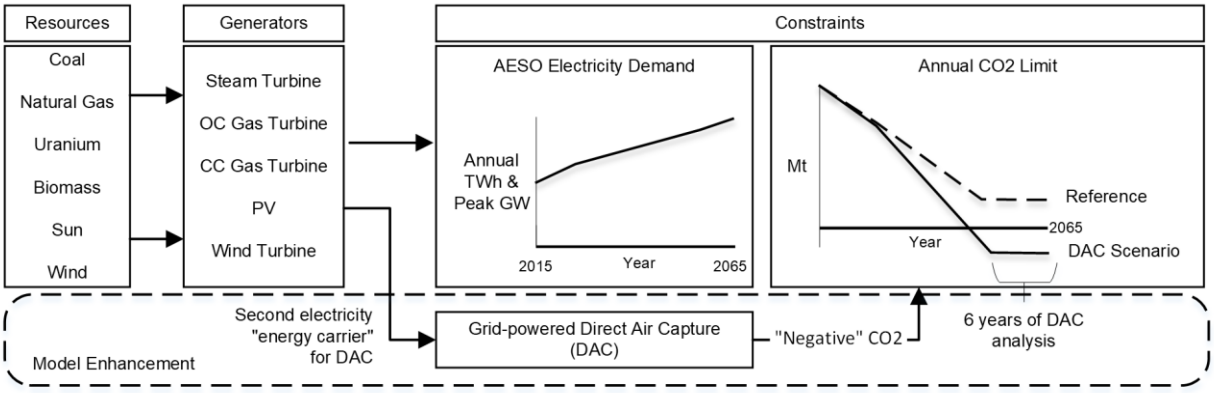

Figure 4.1: Simplified schematic of the hybrid optimisation model used in this study. Enhancements for integration of DAC and negative emissions are presented at the bottom of the figure.

In addition to the annual emissions limit that is the key binding policy constraint in the later model years, three other generic energy policies are modelled. These policies represent policies typically applied by jurisdictions with decarbonisation ambitions: 1) phasing out coal-fired

generation by 2030, 2) 30% renewable energy penetration by 2030, and 3) a carbon tax of 50 $/tCO$_2$ from 2022 to 2065.

4.3.2 Scenarios and emission limits

This study consists of three scenarios with capacity expansion and dispatch modelling:

- *Reference Scenario*, in which the emission constraint declines to 5 MtCO$_2$ by 2060, and
- *two DAC Scenarios,* in which the emission constraint declines to -5 MtCO$_2$ by 2060
    - *DAC Limited Scenario*: constrains the maximum DAC capacity to 3.2 GW[17]; forces higher utilisation rates of DAC technology
    - *DAC Optimised* Scenario: model optimises DAC capacity (no maximum DAC capacity constraint); model may build and operate DAC freely

Figure 4.2 presents the maximum annual emission constraints in our study, along with historic emissions from the Alberta power sector. The Reference emission limit (Figure 4.2, dashed line) is a scaled representation of the median of the 76 IPCC scenarios that limit the global temperature rise to 2°C(192). Similarly, the emission limit in the DAC Scenarios represents negative emissions pathways in strict decarbonisation studies.

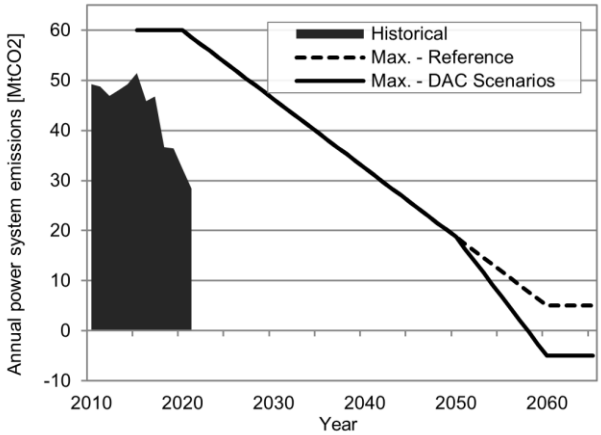

Figure 4.2: Historic emissions from the Alberta grid and maximum emission limits for Reference and DAC Scenarios.

[17] 3.2 GW is the DAC capacity that captures 10 MtCO$_2$/year assuming 90% utilisation factor and 2.5 MWh/tCO$_2$.

4.3.3 DAC technology operation

The DAC technology in our model operates on electricity produced in the same time slice by any of the power generation technologies represented in the model. Applying *modes* of operation in OSeMOSYS introduces a second electricity "energy carrier" to power DAC. This allows us to analyse DAC's energy supply by generation type. With a conversion rate of one tonne of carbon dioxide removed from ambient air per 2.5 MWh electricity, the negative emissions from DAC count toward the annual emission limit.

Our assumption that the bulk power system can provide all the required energy has been assessed and applied in previous studies (30,171,174,187). The theoretical minimum work required to separate a highly concentrated stream of CO_2 from air at 400 ppm is approximately 20 kJ/molCO_2. This study assumes a Second Law efficiency of 5%, or 400 kJ/molCO_2, which equates to 0.40 tCO_2/MWh$_e$ (193).

Capital and fixed operational costs for DAC in this study are based on a $600M facility capturing 1 Mt/year (180,194,195). Energy costs for DAC are endogenously determined by the model. Transportation costs, estimated at 1-10 $/t, and storage and monitoring costs, estimated at 1-5 $/t (196,197), are not included.

4.3.4 Temporal structure

"Representative days" is a strategy for balancing the computational demands of a long duration model period and the short-term dynamics characteristic of wind and solar resources (198). To reduce computational complexity, representative days are selected from a collection of historical days with load, wind, and solar generation data.

Each historical day is represented as a data point in a multi-dimensional vector space, and a k-means clustering algorithm assigns these days to one of six clusters. From each cluster, a representative day is chosen based on its proximity to the cluster centre.

These selected representative days are then further simplified by reducing them from twenty-four to eight time slices. Combinations of time slices within a day are generated, and each time slice is assigned the average value of its constituent hours. The set of eight time slices that best

represents the historical day is determined by minimizing the root-mean-square error between the historical day and the resulting representative day.

The length of each time slice can vary, allowing flexibility in the representation. Time slice durations for years with negative emissions (2060-2065) can be found in Appendix C. Each representative day is assigned a fraction of the model year proportional to the size of the cluster it was selected from.

Finally, the time slices are scaled to match the total annual electricity demand, normalized wind generation, and normalized solar generation of the historical and/or forecast values. A stylised depiction of the wind, solar, and load profiles that define a representative day are presented in Figure 4.3. Each year consists of six representative days, over which the model optimises generation and DAC dispatch to satisfy the annual negative emission constraint. A more detailed explanation of this method is presented in (37).

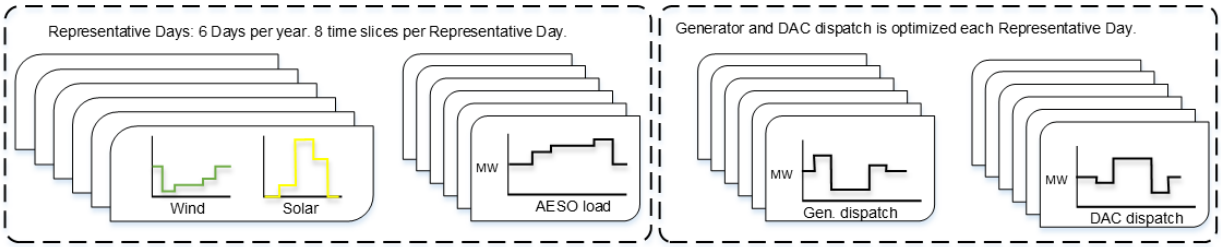

Figure 4.3: Stylised depiction of a set of six representative days that describe the wind, solar and load profiles for one year. The model optimises generation and DAC dispatch for each time slice.

4.3.5 Wind and solar generation profiles

Wind power is defined as five separate technologies, one for existing turbines, and four for new projects. Generation from existing turbines is based on historic fleet generation and the expected lifetimes of the wind farms. New wind power capacity can be installed according to the other four technology definitions, each with a distinct generation profile representing the four wind regimes in the province (150). This allows the model to diversify generation from wind power so that the aggregate generation profile better matches demand, and over-generation can be reduced. Hourly generation for each regime is based on historic generation of wind farms in each area (35,36). These representative wind farms are selected from new,

high performing farms (i.e. capacity factors 35% and higher) reflecting the trend of larger, more productive turbines. Historic hourly generation profiles are normalised from 0 to 1, where 1 is the farm's nominal capacity (megawatts).

PV Watts by NREL (199) is used to generate hourly simulated solar PV generation for different locations in Alberta, representing both rooftop and large-scale, single-axis tilting installations. Previous research did not show benefits of diversifying the location of solar power in province (36). Therefore, the generation profile for solar power in the model is based on the simulated generation from the best-performing location for a largescale single-axis tilting installation (Lethbridge, AB). The hourly generation profile is normalised from 0 to 1, where 1 is the installation's nominal capacity (MW).

4.3.6 Emission intensities

Emission intensities of power generation are a product of the carbon content of the fuel and the efficiency of the generator. Coal in Alberta is a mix of bituminous and subbituminous, and we have assumed a carbon intensity of 0.326 tCO_2/MWh_{th}[18]. The efficiency of the coal fleet changes over the model period as older plants are retired.

Alberta is a producer of natural gas, for which we have assumed a carbon 0.181 tCO_2/MWh_{th}[19]. The corresponding emission intensities from natural gas-fired plants, as modelled, are: 0.257 t/MWh_e for cogeneration facilities, 0.335 t/MWh_e for combined cycle plants, and 0.520 t/MWh_e for open cycle plants.

At the time of writing, cogeneration plants in Alberta's oilsands are the largest type of generation connected to Alberta's grid with a maximum capability over 6000 MW [20]. The efficiency of cogeneration, which directly impacts variable costs and emissions, is determined by the displacement allocation method (200). In this displacement allocation method (M1), the fuel allocated to power generation is calculated as the total required for the combined cycle process less the fuel needed to generate the steam in a separate process with an 80% efficient

[18] https://www.eia.gov/oiaf/1605/coefficients.html
[19] https://www.eia.gov/oiaf/1605/coefficients.html
[20] http://ets.aeso.ca/ets_web/ip/Market/Reports/CSDReportServlet

boiler. Fixed and variable O&M costs for cogeneration are the same as CCGT, and the capital cost for cogeneration is determined from EIA's CCGT by the same relative cost factor between CCGT and cogeneration reported in AESO's 2014 Long-term Outlook[21].

Existing biomass plants on the system burn wood waste so we assume zero emissions associated with current and future biomass power generation.

4.3.7 Generation technologies

Costs and performance of generation technologies have been updated from the original model (32) to reflect more recent estimates. Detailed generator costs can be found in Appendix C:. Wind costs are based on a GIS study of the resource in the province (34) with a linear reduction in capital cost of 15% by 2030, and 20% by 2050. Resource prices for coal and natural gas are based on regional EIA forecasts.

Hydroelectric resource potential is based on the AESO Long-term Outlook 2016 (154); 300 MW of additional potential in the next decade, and a total potential of 2,294 MW from 2034 until the end of the model period. Cogeneration potential is based on the Reference Case forecast in the AESO Long-term Outlook 2016, with an upper limit of 6,000 MW in 2050. Geothermal potential is based on research by Palmer-Wilson et al. (201).

4.4 RESULTS

This section presents key findings from our analysis of Direct Air Capture (DAC) integration into the Alberta power system. We start with the optimised energy and capacity mixes across scenarios. Then we examine how DAC contributes to meeting negative emission targets in years 2060 to 2065. Following that, we analyse DAC operation, including annual, seasonal, and daily dispatch patterns. Lastly, we estimate the cost of energy to serve DAC ($/MWh).

[21] AESO's LTO only provides costs for a few of the generation types that are included in the model. It was judged more important to use internally consistent costs (EIA) than mix data from other sources for the generators not reported on by AESO.

4.4.1 Optimised capacity and energy mixes

Both DAC scenarios require additional low-carbon generation compared to the Reference Scenario to meet the increased energy demands from DAC technology. Figure 4.4(a) presents the installed capacity in 2065 for the Reference Scenario. Figure 4.4(b) presents the relative differences in installed capacity for the DAC scenarios compared to the Reference in 2065.

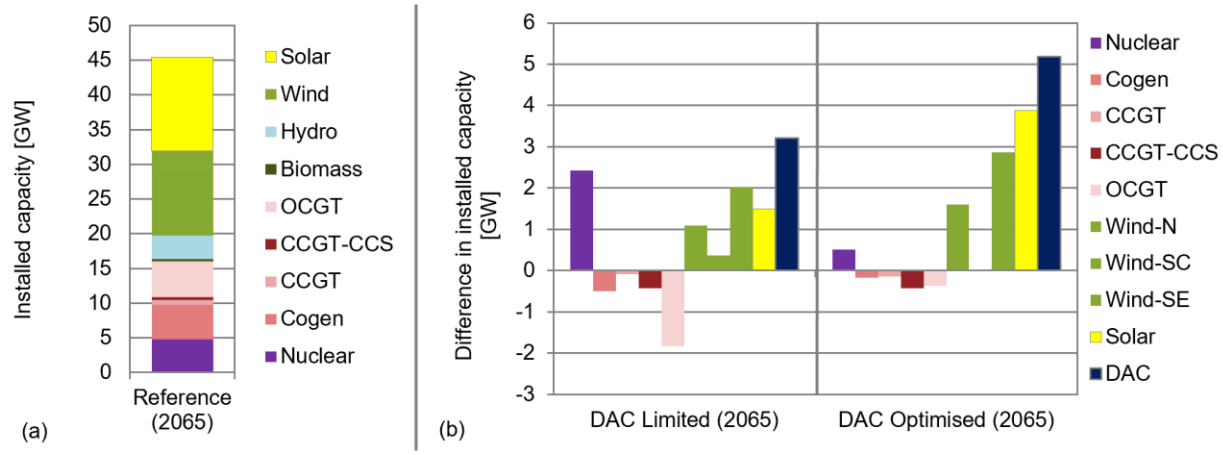

Figure 4.4: (a) Installed capacity in 2065 in the Reference Scenario. (b) Difference in installed capacities for the DAC scenarios relative to the Reference Scenario in year 2065.

Compared to the Reference Scenario in 2065, the DAC Limited Scenario builds an additional 4.6 GW of generation capacity (~10% increase vs Reference), primarily wind and nuclear power. The DAC Optimised Scenario builds an additional 7.7 GW over the Reference Scenario (~17% increase), mainly wind and solar power. As seen in Figure 4.4(b), the DAC scenarios install less natural gas-fired generation capacity. The Reference Scenario installes a few hundred megawatts of combined cycle natural gas with carbon capture and sequestration (CCGT-CCS), but neither DAC scenario builds thermal plants with CCS.

Despite different optimal capacity mixes for the scenarios, the resulting energy mixes serving AESO demand from 2060 to 2065 are similar across scenarios (Figure 4.5(d)). The energy mix serving the AESO demand from years 2060 to 2065 remains relatively constant in the Reference Scenario, as seen in Figure 4.5(a). The DAC scenarios, on the other hand, exhibit larger annual fluctuations in the mix serving AESO demand (Figure 4.5(b) and (c)), most noticeably the portion provided from natural gas-fired generation.

Different annual energy mixes are the result of having unique sets of six representative days drawn to represent each model year. These different combinations will result in different wind-solar-load profiles that impact net load profiles, particularly when installed capacity of wind and solar is high, which can lead to curtailment.

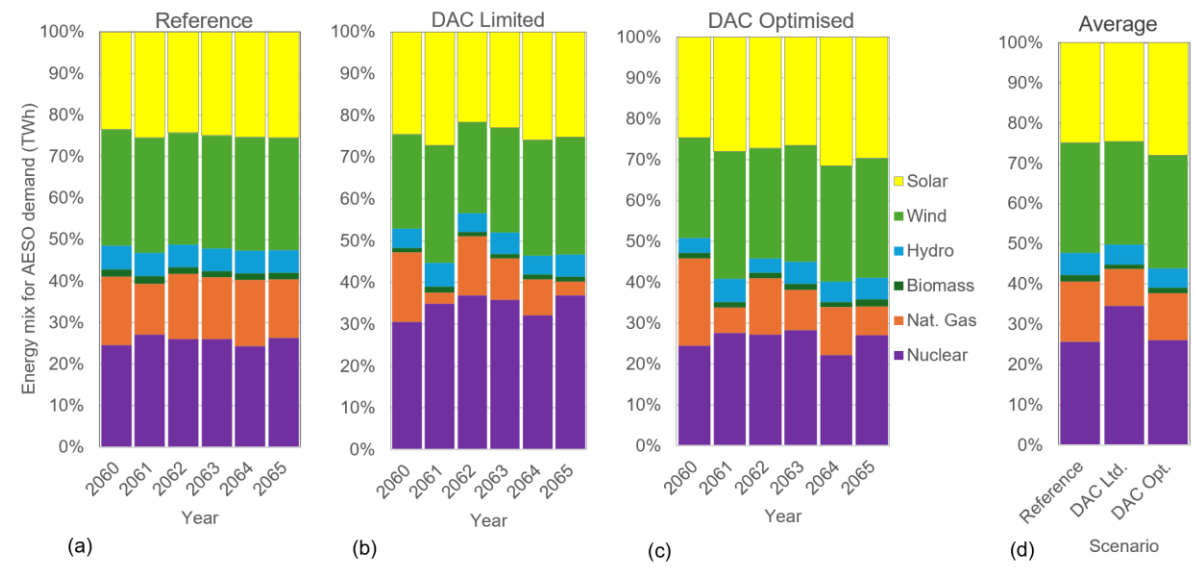

Figure 4.5: Energy supply by resource type for AESO demand in all three scenarios (a) Reference, (b) DAC Limited, (c) DAC Optimised. The 2060-2065 average for each scenario is presented in (d). AESO demand is the same across scenarios; 125 TWh in 2060, rising to 131 TWh in 2065.

4.4.2 Annual DAC energy

Annual electricity supply presented in Figure 4.6 shows DAC Scenarios require up to 30 TWh more generation than the Reference Scenario, although annual differences are significant. In 2061, DAC demand is just 15 TWh in the Limited Scenario and 18 TWh in the Optimised Scenario, approximately half of peak annual demand observed in 2060. The annual DAC load represents increases of approximately 13% to 25% to the forecasted provincial (AESO) demand.

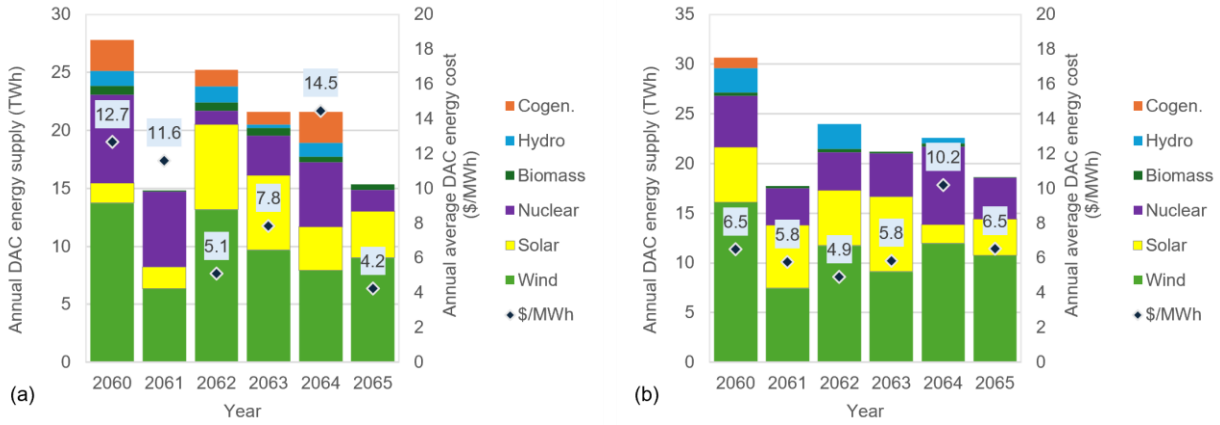

Figure 4.6: Annual energy mixes powering DAC from 2060 to 2065 as allocated by model, for (a) DAC Limited Scenario, and (b) DAC Optimised Scenario. Weighted average variable cost of each year's energy mix presented as $/MWh.

As intended, utilisation factors of DAC are higher in the DAC Limited scenario than the DAC Optimised Scenario. The average annual utilisation factor of DAC from 2060 to 2065 is 75% in the DAC Limited Scenario and 52% in the DAC Optimised Scenario.

4.4.3 Emissions

Figure 4.7 presents the annual CO_2 emissions for the DAC and Reference scenarios from 2015 to 2065. Additional low-carbon generation resources in the DAC scenarios enter the system starting 2045, resulting in earlier emission reductions than in the Reference Scenario. Both DAC scenarios demonstrate accelerated emission reductions starting 2055, ultimately reaching net emissions of -5 $MtCO_2$ in 2060, compared to the Reference Scenario's 5 $MtCO_2$/yr.

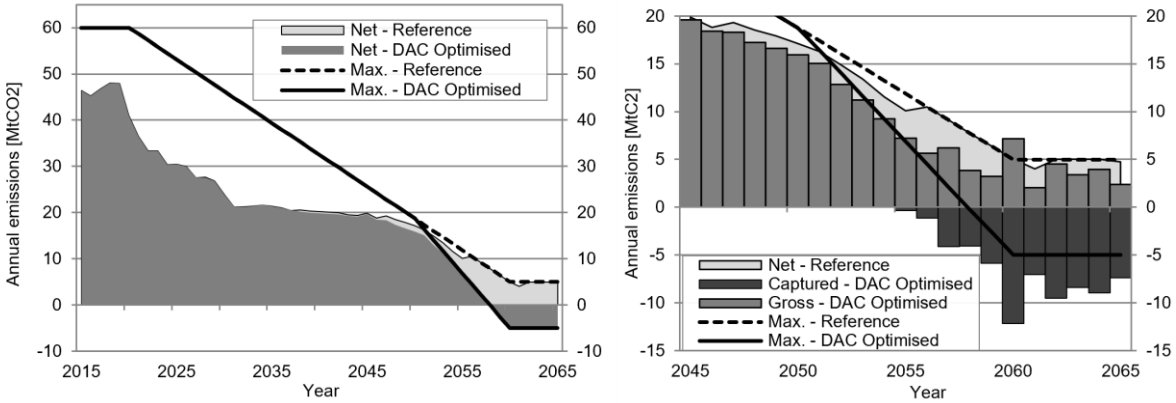

Figure 4.7: Annual CO_2 emissions for the Reference Scenario and DAC Optimised Scenario. The right half of the figure examines years 2045 to 2065, presenting gross and captured emissions.

Table 4.1 details the carbon dioxide generation and reduction from 2060 to 2065 for each scenario. From 2060 to 2065, the DAC Optimised Scenario generates more emissions than the DAC Limited Scenario. To meet the emission constraint, the DAC Optimised Scenario also captures more emissions than the DAC Limited Scenario over the same period. The amount of carbon dioxide captured each year ranges from 7.0 to 12.1 $MtCO_2$ in the DAC Optimised Scenario as shown in Figure 4.7, and from 5.9 to 11.0 $MtCO_2$ in the DAC Limited Scenario. The bulk of emission reduction in both DAC Scenarios comes from DAC itself, not cleaner electricity mixes.

Table 4.1: Breakdown of average annual emissions (2060-2065).

Scenario	Average annual gross emissions		Average annual emissions reduction due to lower-carbon generation mix		Average annual emissions reduction due to DAC	Average annual net emissions
	[$MtCO_2$]	[$MtCO_2$]	% of reduction	[$MtCO_2$]	% of reduction	[$MtCO_2$]
Reference	4.8	-	-	-	-	4.8
DAC Limited	3.3	1.4	15%	8.3	85%	-5.0
DAC Optimised	3.9	0.9	9%	8.9	91%	-5.0

4.4.4 Seasonal DAC operation

Seasonal differences in load, wind, and solar generation also impact the operation of DAC. Figure 4.8 presents variation in load and VRE generation by season for (a) Reference and (b) DAC Optimised Scenarios. DAC load is highest in the spring, consistent with moderate load and high VRE generation. Low wind generation in the summer means DAC operation is more dependent on solar generation, impacting the DAC Optimised Scenario more than the DAC Limited Scenario due to its higher portion of solar capacity.

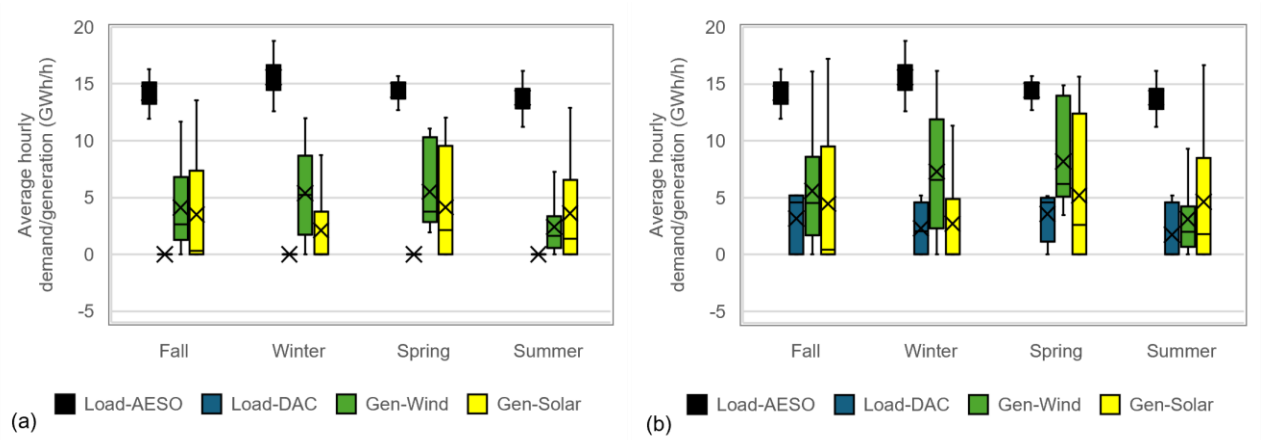

Figure 4.8: Seasonal variation in load and VRE generation for (a) Reference Scenario, and (b) DAC Optimised Scenario.

4.4.5 Daily system dispatch

Figure 4.9 presents system dispatch results for one representative day modelled across scenarios. This representative day (January 22, 2011), one of six representative days for 2061 in all scenarios, exhibits high AESO demand (15.1 GW peak), fluctuating wind generation (Figure 4.9, green bars), and high mid-day solar generation (Figure 4.9, yellow bars). Figure 4.9, the colour of the bar indicates the generator type, while the load can be distinguished by the fill or pattern of the bar. Bars with solid-colour fill represents AESO demand, striped or lined pattern segments indicates DAC load, and the hatched pattern represents curtailed generation.

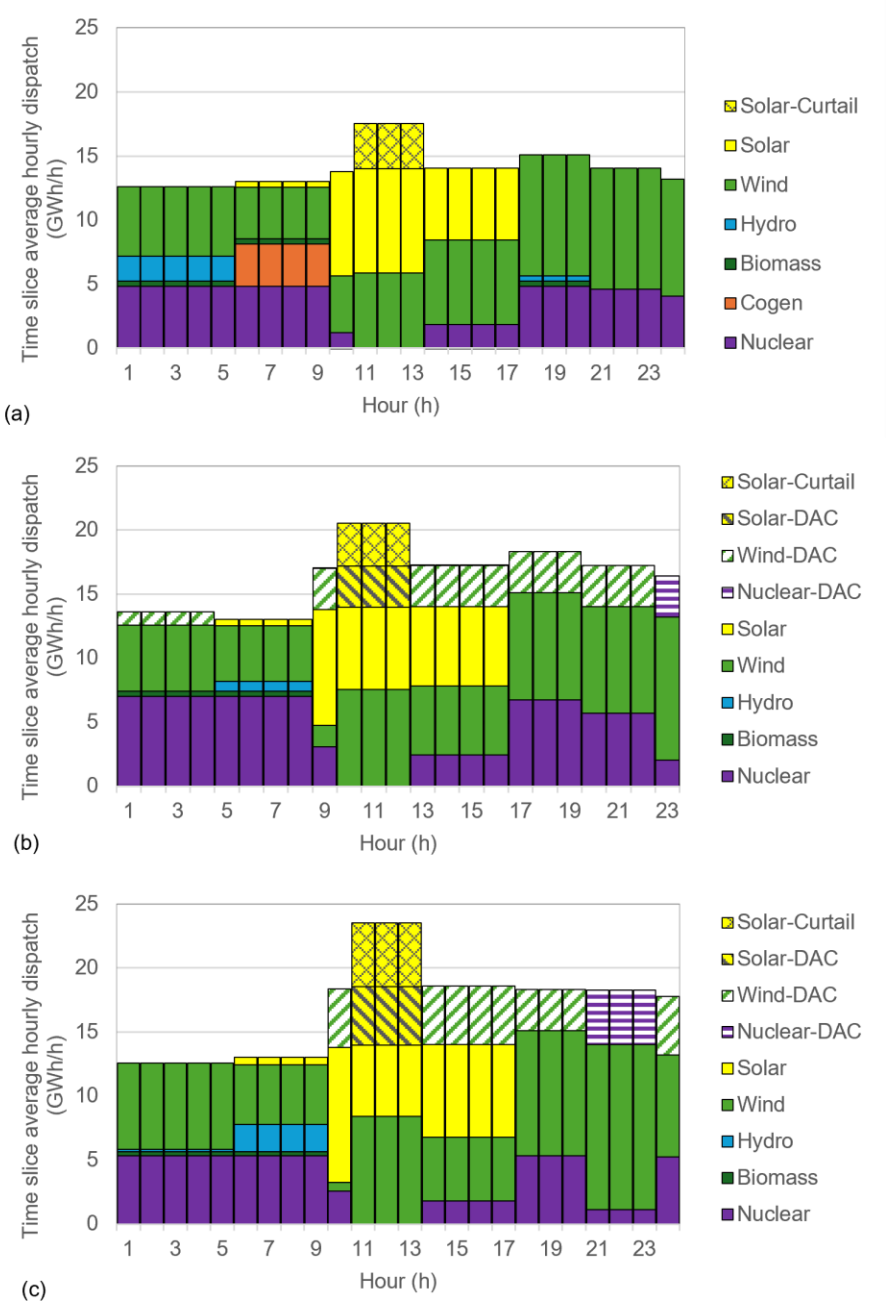

Figure 4.9: System dispatches for one of the representative days in 2061 (January 22), for (a) Reference, (b) DAC Limited Scenario, and (c) DAC Optimised Scenario. Colours represent different generator types; solid-fill bars are meeting AESO load; striped or lined segments are allocated to DAC; hatched pattern represents curtailed energy.

Curtailment of VRE occurs in all three scenarios, shown in Figure 4.9 as hatched yellow bars at the top of the fourth time slice. In the DAC Limited Scenario, DAC is dispatched in seven of the

eight time slices. In the DAC Optimised Scenario, DAC is dispatched in six of the eight time slices. Next, we will present typical DAC dispatch across all representative days.

4.4.6 Typical daily DAC operation

In Figure 4.10 we present DAC operation by daily time slice for all representative days modelled for years 2060 through 2065. Each of the six years has six representative days, for a total of 36 data points for each time slice. Each data point represents the average power (GWh/h) supplied to DAC by the modelled power system for that time slice. For example, the hight of the DAC load segments in Figure 4.9 (striped pattern) would comprise one series of data in Figure 4.10.

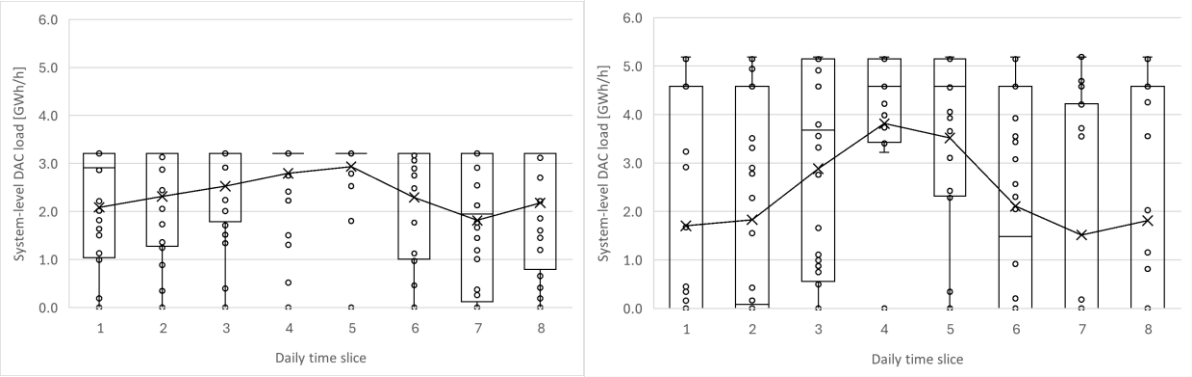

Figure 4.10: Histogram of system-level DAC operation by time slice for all 288 time slices in 2060-2065, for (a) DAC Limited Scenario and, (b) DAC Optimised Scenario.

The baseload-type operation of DAC in the Limited Scenario is reflected by the flatter average DAC load across the daily time slices presented in Figure 4.10(a). This contrasts with the more variable DAC dispatch exhibited by the Optimised Scenario presented in Figure 4.10 (b). These results are consistent with the different capacity and generation mixes presented in Figure 4.4, where the Limited Scenario had more nuclear, and the Optimised Scenario had more solar power. In both Scenarios, DAC load tends to be highest at mid-day.

4.4.7 Curtailment

Results across all three scenarios indicate negligible curtailment of wind energy, but approximately 5% curtailment of solar energy (Figure 4.11). Analysis shows the least curtailment from 2060 to 2065 occurs in the DAC Limited Scenario, and the most curtailment

over the same six years occurs in the DAC Optimised Scenario, although the annual variations are more significant than the differences between scenario.

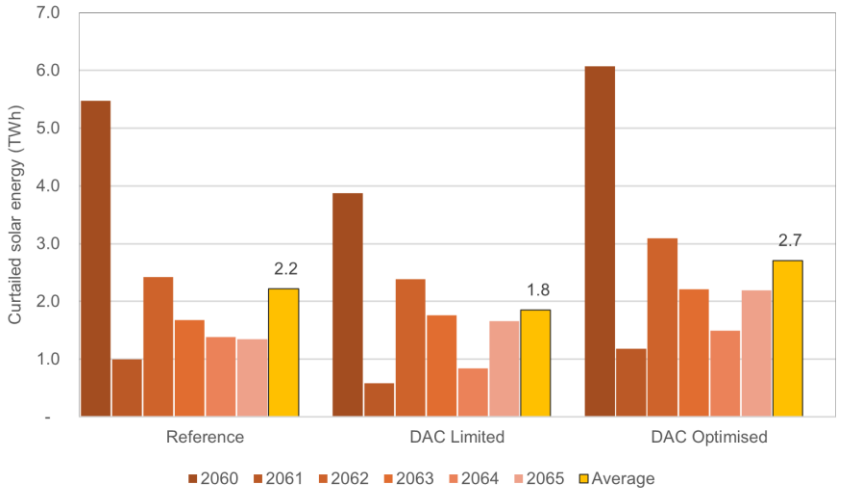

Figure 4.11: Curtailed solar energy from 2060 to 2065 for all three scenarios.

4.4.8 System costs and energy costs

Total system cost is lowest in the Reference Scenario, which includes capital, fixed operation and maintenance, variable operation and maintenance, fuel, and the carbon tax. Over the 51 years modelled, the total non-discounted costs[22] are 7.9% higher in the Limited Scenario and 6.5% higher in the Optimised Scenario. Most of the increase in total system costs in both DAC scenarios can be attributed to capital for the additional generation capacity (i.e. wind, solar, nuclear) and DAC (Figure 4.12), a result consistent with (173,174).

[22] All costs in this section are "total non-discounted system costs".

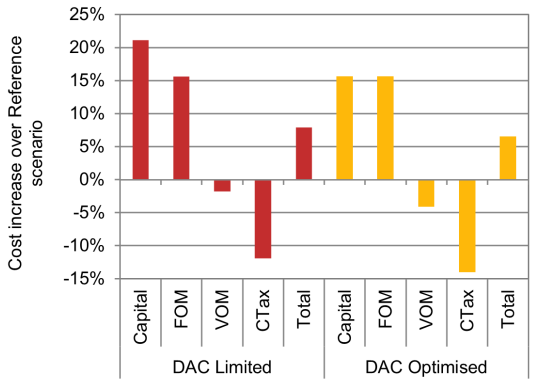

Figure 4.12: Non-discounted cost difference for DAC scenarios compared to the Reference scenario.

Analysis of the energy supplied to DAC in Figure 4.6 provides insight to DAC's average energy costs. The annual average cost ($/MWh) of the energy mix serving DAC load in Figure 4.6 is calculated by summing the variable operating costs each year (fuel and plant VOM) and dividing by the total annual DAC energy supply that year. The resulting energy supply costs range from 4.2 to 14.5 $/MWh in the DAC Limited Scenario, and 4.9 to 10.2 $/MWh in the DAC Optimised Scenario. The weighted average DAC energy cost for 2060 to 2065 is 9.5 $/MWh in the DAC Limited Scenario, and 6.6 $/MWh in the DAC Optimised Scenario.

(202)Figure 4.13 presents the system generation costs over the model period for Reference and DAC Scenarios. In both Scenarios shown in Figure 4.13, and the DAC Optimised Scenario the total generation cost increases over time, driven mainly by capital costs. The largest difference in generation costs occurs in the 2054 to 2059 time frame, when Limited DAC Scenario generation costs are $20/MWh more than the Reference Scenario over the same period. Similarly, generation costs in the DAC Optimised Scenario are $17/MWh more than the Reference Scenario over the same period.

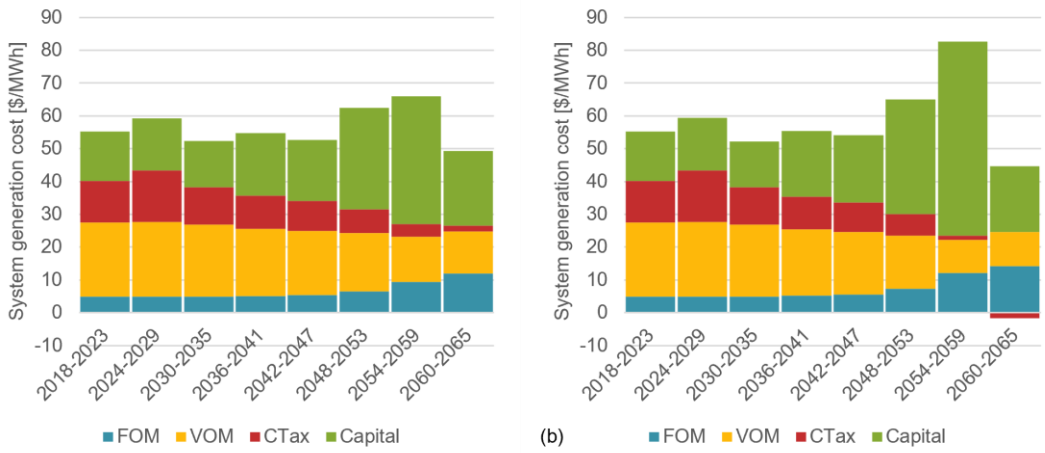

Figure 4.13: Average system (AESO and DAC) generation costs for (a) Reference Scenario, and (b) DAC Optimised Scenario. Legend costs: FOM=Fixed Operation and Maintenance, VOM=Variable Operation and Maintenance (incl. fuel), CTax=Carbon Tax ($50 t/$CO_2$ as defined in 4.4.1), Capital=Overnight Capital.

4.5 Discussion

Negative emissions technologies including DAC are increasingly a part of climate mitigation pathways despite technological challenges, environmental concerns, and potential over-reliance in decarbonisation plans (192,203–208). Their deployment would introduce complex interactions with energy systems already balancing VRE integration with declining fossil fuel use while maintaining system stability. Powering DAC with low variable cost wind and solar power is an intriguing possibility, however, many DAC processes in development are better suited to steady-state operation (177–186). This study examines how DAC might be optimally integrated into a regional power grid under strict net-negative emission targets. Using a capacity expansion and dispatch model we analyse the energy requirements for DAC over several years, highlighting key considerations for generation mix, system flexibility, and dispatch considerations.

Across all scenarios, DAC drives additional investment in low-carbon generation, most notably wind, solar, and nuclear power. In the DAC Limited Scenario, DAC is primarily powered by nuclear and wind power, resulting in high DAC utilisation factors. Electricity from nuclear power, with a variable cost of $2.29/MWh, is the lowest variable cost carbon-free dispatchable generation modelled. With DAC's assumed capture rate of 2.5 MWh/tCO_2, nuclear-powered capture costs are less than $6 per tonne. In contrast, at a hypothetical electricity cost of

$30/MWh, the energy cost alone for DAC rises to $75/t$CO_2$. These results demonstrate the sensitivity of DAC cost-effectiveness to the marginal cost of electricity, and the generation mix that supplies it.

A key finding of this work is the variation in DAC operation over multiple timescales. In the DAC Limited Scenario, DAC operates more uniformly, resembling a baseload demand. In the DAC Optimised Scenario, the greater reliance on solar power drives a clear diurnal daily operation pattern for DAC. This diurnal pattern is like the charging profiles of battery storage technologies, suggesting competition between DAC and storage resources for access to low-cost carbon-free energy.

One of the novel contributions of this study is the explicit modelling of inter-annual and seasonal differences in DAC operation. While other studies analyse a single year, we optimise six distinct net-negative years, revealing meaningful differences in generation, DAC dispatch, and curtailment. For example, 2060 DAC demand is approximately double the 2061 DAC demand for the same negative emission target while the Reference Scenario energy mix remains largely unchanged over those years. Driven by different sets of representative days (wind, solar, and load profiles), this variability suggests that system planning with DAC is particularly sensitive to inter-annual differences and multi-year analysis should be considered in net-negative energy studies.

Seasonal differences in VRE generation are also shown to impact DAC operation. Our results reveal higher utilisation of DAC in the winter and spring compared to the summer because wind generation is typically higher in the winter and spring. This insight could be valuable when it comes to planning annual maintenance of DAC or the generation technologies.

The interaction between DAC and VRE curtailment is nuanced. In the DAC Limited Scenario, additional DAC load helps reduce curtailment by consuming otherwise unused generation. However, in the DAC Optimised Scenario, increased DAC capacity drives additional solar deployment, which in turn increases overall curtailment. This finding highlights the importance of aligning DAC capacity with system needs. DAC could be a flexibility option on the system to reduce curtailment, or it could be a load that simply increases VRE capacity.

An unexpected outcome of the study is the simultaneous dispatch of fossil fuel generation and DAC. In these time slices, natural gas-fired cogeneration creates 0.257 tCO_2/MWh_e while DAC captures 0.4 tCO_2/MWh_e , resulting in net negative emissions. This outcome stems from defining the system boundary between the electricity product and thermal product from cogeneration and including only the emissions associated with the electricity portion. Other studies, including those that assume natural gas with CCS can meet the thermal demand of DAC, arrive at similar conclusions (171,173,187,190). These findings indicate continued use of fossil fuel generation in net negative futures, and highlights the need for emission accounting frameworks.

The topic of grid-powered DAC is broad, and many assumptions were made to limit the scope of this study. Operation of DAC in this study should be interpreted with the understanding that the optimisation model in this study has perfect foresight. The objective function minimises total discounted system costs subject to the strict negative emission that must be met. The model will build generation capacity and dispatch DAC with full knowledge of the year's load, solar, and wind profiles. Our results, while representing idealised system operation and planning, provide insights into generation mixes and DAC operation.

Energy planning environments often require simple, explainable models for long-term planning. Complex market models or transmission-rich nodal models may offer more detailed system representation, but they often sacrifice transparency, replicability, and trust from key stakeholders. Our hybrid model balances details and tractability, capturing the system parameters and dynamics essential to resource planning while remaining accessible to a wider audience. Importantly, our findings suggest that the strategic insights on temporal variation, DAC dispatch patterns, VRE impacts, and cost differences, that do not hinge on specific pieces of grid infrastructure that can result from detailed transmission or discrete unit representations. For long-term planners and policy designers, clarity can be more valuable that precise representation.

In summary, this study advances understanding of how DAC interacts with power systems across multiple timescales. By modelling six years of operation under net-negative emission

constraints, we identify important trends in system mix, DAC operation, curtailment, and system costs. Future work could explore alternative dispatch strategies for DAC, for example limiting operation to times of excess VRE generation, or using any available nuclear capacity to power DAC. Nonetheless, the results presented here support the growing body of research identifying DAC as a cost-competitive NET when paired with low-carbon electricity.

5 CONTRIBUTIONS AND RECOMMENDATIONS

5.1 CONTRIBUTIONS

In Chapter 2, the OSeMOSYS model representing the Alberta power system is introduced and explained. Carbon taxes are applied at increasing levels to explore transitions, emission reductions, technologies, and costs as the system expands to 2060. Key contributions are:

1. Capacity expansion model of Alberta's power system
   A detailed techno-economic supply model is developed for the Alberta power system, based on the Open Source Energy Modelling System (OSeMOSYS), that serves as a key modelling tool for several researchers and multiple peer-reviewed publications.
2. Assessment of carbon pricing on decarbonisation
   Applying various levels of carbon pricing, from $30 to $200 per tonne, accelerates decarbonisation but with diminishing returns. Coal-to-gas switching is shown to be the most cost-effective way to reduce emissions.
3. Role of renewables and low-carbon generation
   Wind and solar expand to displace carbon-intensive fossil fuel generation, but resource adequacy requirements keep fossil-fuel generation as part of the resource mix.

Chapter 3 examines high penetrations of wind and solar with power-to-gas (PtG) serving as long-duration energy storage. For this study, an hourly storage simulation model is developed in MATLAB to accurately represent VRE variability and chronology, a limitation of the capacity expansion model. This research co-sizes VRE capacity and electrolyser capacity in different combinations to reach 80% energy penetration of wind and solar. Part of this research includes an extensive literature on power-to-gas, presented in Appendix B:. Key contributions are:

4. Reduction in VRE capacity and curtailment
   Integrating power-to-gas storage to achieve 80% VRE penetration can reduce the necessary VRE capacity to by up to 23% and curtailment by as much as 87%.

5. Analysis of electrolyser operation and energy storage needs
   While most charging events in a year last less than 12 hours, the majority of annual stored energy comes from longer events.
6. Feasibility of using the natural gas grid for hydrogen storage
   PtG generates massive quantities of hydrogen gas, which Alberta's extensive natural gas grid can accommodate while keeping annual hydrogen concentrations below 5%.

Chapter 4 expands the capacity expansion model introduced in Chapter 2 to study net-negative emission pathways, direct air capture, and optimal system operation. Key contributions are:

7. Hybrid capacity expansion and dispatch model for negative emission planning
   Several enhancements including representative days, DAC as a new technology, and annual net-load variability enables negative emission planning with an established model.
8. DAC flexibility and operation
   DAC's future deployment likely depends on its ability to integrate with a transforming power system. Net-negative emission constraints create an endogenous demand for DAC that can result in its dispatch over a range of conditions, including alongside fossil fuel generation. Inter-annual and season differences can be significant and should be part of future net-negative studies.
9. Minimising DAC's energy cost
   Optimising DAC expansion and operation with a grid's generation mix can decrease the energy supply costs for DAC. However, low-cost energy resources like solar power do not provide firm capacity and increase reliance on the rest of the grid for balancing.

5.2 Reflection and Recommendations

When this research began in 2012, a carbon tax in Alberta seemed like a purely academic idea. Coal-fired generation was providing more than half of the provincial demand, and wind project

development often relied on the sale of their renewable energy credits to outside jurisdictions. Since then, policies enacted by the provincial government, including carbon pricing and renewable energy supports, have transformed province's generation mix. Although the exact suite of policies has not been replicated in the model, results from this dissertation are consistent with changes observed in the AESO system over the last decade: coal-fired plants have been decommissioned or converted to burn natural gas, and wind and solar power have experienced rapid growth.

Many energy planning models in 2012 explored how far and how fast decarbonisation could occur. Results showing VRE substituting for baseload generation highlighted the need for modellers to better understand flexibility in power systems. Consequently, modelling methods to represent grid reliability expanded beyond annual energy and peak capacity requirements. The impact of VRE on flexibility emerged as a key problem in VRE-dominant grids.

Batteries, riding the cost declines driven by electric vehicles, were shown in many studies to cost-effectively increase VRE penetration. While effective for daily balancing, other studies have shown storage or demand flexibility lasting less than 10 hours is insufficient to serve prolonged VRE-droughts, such as Dunkelflaute. Year-round reliability in high VRE systems will require dispatchable resources that are not energy limited.

Long-duration energy storage can provide dispatchable power to serve prolonged net-demand events, but feasible projects remain rare. Pumped hydro storage can be cost-effective, but projects are particularly location dependent. Power-to-X and flow batteries are innovative storage alternatives but require further development before large-scale deployment is possible.

Resource adequacy – having sufficient resources available to the system operator to meet future load – is one of the biggest challenges facing energy planning. Conventional risk metrics, like loss of load expectation (LOLE), assume discrete independent failures and provide only an average measure of risk. As weather dependent resources increase their share of the generation mix, weather-influenced correlated events must be considered. It will likely require several metrics that quantify frequency, size, duration, and timing of resource inadequacy.

Integrating advanced resource adequacy metrics in energy planning models is going to be crucial for increasing VRE shares and decreasing reliance on natural gas generation.

6 REFERENCES

1. Rogelj J, D. Shindell, K. Jiang, S. Fifita, P. Forster, V. Ginzburg, et al. Mitigation Pathways Compatible with 1.5°C in the Context of Sustainable Development. In: Global Warming of 1.5°C. An IPCC Special Report on the impacts of global warming of 1.5°C above pre-industrial levels and related global greenhouse gas emission pathways, in the context of strengthening the global response to the threat of climate change, sustainable development, and efforts to eradicate poverty. In: Global Warming of 15°C [Internet]. Cambridge University Press; 2022. p. 93–174. Available from: https://www.cambridge.org/core/product/identifier/9781009157940%23c2/type/book_part

2. IEA. Net Zero by 2050 [Internet]. Paris; 2021 [cited 2023 Mar 11]. Available from: https://www.iea.org/reports/net-zero-by-2050

3. Jenkins JD, Mayfield EN, Larson ED, Pacala SW, Greig C. Mission net-zero America: The nation-building path to a prosperous, net-zero emissions economy. Joule [Internet]. 2021 Nov 17;5(11):2755–61. Available from: https://doi.org/10.1016/j.joule.2021.10.016

4. Karlsson K, Meibom P. Optimal investment paths for future renewable based energy systems-Using the optimisation model Balmorel. Int J Hydrogen Energy. 2008;33(7):1777–87.

5. Amorim F, Pina A, Gerbelová H, Pereira da Silva P, Vasconcelos J, Martins V. Electricity decarbonisation pathways for 2050 in Portugal: A TIMES (The Integrated MARKAL-EFOM System) based approach in closed versus open systems modelling. Energy [Internet]. 2014;69:104–12. Available from: https://www.sciencedirect.com/science/article/pii/S0360544214000735

6. Sepulveda NA, Jenkins JD, de Sisternes FJ, Lester RK. The Role of Firm Low-Carbon Electricity Resources in Deep Decarbonization of Power Generation. Joule [Internet]. 2018;2(11):2403–20. Available from: https://www.sciencedirect.com/science/article/pii/S2542435118303866

7. Denholm P, Arent DJ, Baldwin SF, Bilello DE, Brinkman GL, Cochran JM, et al. The challenges of achieving a 100% renewable electricity system in the United States. Joule [Internet]. 2021;5(6):1331–52. Available from: https://www.sciencedirect.com/science/article/pii/S2542435121001513

8. Ruhnau O, Qvist S. Storage requirements in a 100% renewable electricity system: extreme events and inter-annual variability. Environmental Research Letters. 2022 Apr 1;17(4):044018.

9. McPherson M, Monroe J, Jurasz J, Rowe A, Hendriks R, Stanislaw L, et al. Open-source modelling infrastructure: Building decarbonization capacity in Canada. Energy Strategy Reviews [Internet]. 2022;44:100961. Available from: https://www.sciencedirect.com/science/article/pii/S2211467X22001559

10. McPherson M, Rhodes E, Stanislaw L, Arjmand R, Saffari M, Xu R, et al. Modeling the transition to a zero emission energy system: A cross-sectoral review of building, transportation, and electricity system models in Canada. Energy Reports [Internet]. 2023;9:4380–400. Available from: https://www.sciencedirect.com/science/article/pii/S2352484723002330

11. Niet T, Arianpoo N, Kuling K, Wright AS. Increasing the reliability of energy system scenarios with integrated modelling: a review. Environmental Research Letters [Internet]. 2022;17(4):043006. Available from: https://dx.doi.org/10.1088/1748-9326/ac5cf5

12. Motalebi S, Barnes T, Lu L, Leibowicz BD, Niet T. The role of U.S.-Canada electricity trade in North American decarbonization pathways. Energy Strategy Reviews [Internet]. 2022;41:100827. Available from: https://www.sciencedirect.com/science/article/pii/S2211467X2200027X

13. Arianpoo N, Islam ME, Wright AS, Niet T. Electrification policy impacts on land system in British Columbia, Canada. Renewable and Sustainable Energy Transition [Internet].

2024;5:100080. Available from: https://www.sciencedirect.com/science/article/pii/S2667095X24000047

14. Meibom P, Karlsson K. Role of hydrogen in future North European power system in 2060. Int J Hydrogen Energy [Internet]. 2010;35(5):1853–63. Available from: http://www.sciencedirect.com/science/article/pii/S036031990902120X

15. Karlsson H, Delahaye T, Johnsson F, Kjärstad J, Rootzén J. Immediate deployment opportunities for negative emissions with BECCS: a Swedish case study. 2017.

16. English J, Niet T, Lyseng B, Keller V, Palmer-Wilson K, Robertson B, et al. Flexibility requirements and electricity system planning: Assessing inter-regional coordination with large penetrations of variable renewable supplies. Renew Energy. 2020;145.

17. English J, Niet T, Lyseng B, Palmer-Wilson K, Keller V, Moazzen I, et al. Impact of electrical intertie capacity on carbon policy effectiveness. Energy Policy. 2017;101.

18. Niet T, Lyseng B, English J, Keller V, Palmer-Wilson K, Moazzen I, et al. Hedging the risk of increased emissions in long term energy planning. Energy Strategy Reviews. 2017;16.

19. Keller V, Lyseng B, English J, Niet T, Palmer-Wilson K, Moazzen I, et al. Coal-to-biomass retrofit in Alberta –value of forest residue bioenergy in the electricity system. Renew Energy. 2018;125.

20. Impram S, Varbak Nese S, Oral B. Challenges of renewable energy penetration on power system flexibility: A survey. Energy Strategy Reviews. 2020 Sep 1;31:100539.

21. Denholm P, Hand M. Grid flexibility and storage required to achieve very high penetration of variable renewable electricity. Energy Policy [Internet]. 2011 Mar [cited 2015 Jan 13];39(3):1817–30. Available from: http://www.sciencedirect.com/science/article/pii/S0301421511000292

22. Lund PD, Lindgren J, Mikkola J, Salpakari J. Review of energy system flexibility measures to enable high levels of variable renewable electricity. Renewable and Sustainable Energy

Reviews [Internet]. 2015 May [cited 2015 Feb 28];45:785–807. Available from: http://www.sciencedirect.com/science/article/pii/S1364032115000672

23. Degefa M, Sperstad I, Sæle H. Comprehensive classifications and characterizations of power system flexibility resources. Electric Power Systems Research [Internet]. 2021;194:107022. Available from: https://libkey.io/10.1016/j.epsr.2021.107022

24. Hillberg E, Zegers A, Herndler B, Wong S, Pompee J, Bourmaud JY, et al. Power Transmission & Distribution Systems Flexibility needs in the future power system Discussion paper Disclaimer. 2019.

25. Albertus P, Manser JS, Litzelman S. Long-Duration Electricity Storage Applications, Economics, and Technologies. Joule. 2020 Jan 15;4(1):21–32.

26. Twitchell J, DeSomber K, Bhatnagar D. Defining long duration energy storage. J Energy Storage [Internet]. 2023;60:105787. Available from: https://www.sciencedirect.com/science/article/pii/S2352152X22017753

27. Sepulveda NA, Jenkins JD, Edington A, Mallapragada DS, Lester RK. The design space for long-duration energy storage in decarbonized power systems. Nat Energy [Internet]. 2021;6(5):506–16. Available from: https://doi.org/10.1038/s41560-021-00796-8

28. Dowling JA, Rinaldi KZ, Ruggles TH, Davis SJ, Yuan M, Tong F, et al. Role of Long-Duration Energy Storage in Variable Renewable Electricity Systems. Joule [Internet]. 2020 Sep 16;4(9):1907–28. Available from: https://doi.org/10.1016/j.joule.2020.07.007

29. Xie W, Aryanpur V, Deane P, Daly HE. Negative emissions technologies in energy system models and mitigation scenarios - a systematic review. Appl Energy [Internet]. 2025;380:125064. Available from: https://www.sciencedirect.com/science/article/pii/S0306261924024486

30. Arwa EO, Schell KR. Impact of direct air capture process flexibility and response to ambient conditions in net-zero transition of the power grid. Appl Energy [Internet].

2025;386:125549. Available from: https://www.sciencedirect.com/science/article/pii/S030626192500279X

31. Lyseng B, Rowe A, Wild P. Emission reduction through carbon taxes on Alberta's electrical system. In: Proceedings of the 3rd EIC Climate Change Technology Conference [Internet]. Montreal, Canada; 2013. Available from: http://www.cctc2013.ca/Papers/CCTC2013 MIT2-2 Lyseng.pdf

32. Lyseng B, Rowe A, Wild P, English J, Niet T, Pitt L. Decarbonising the Alberta power system with carbon pricing. Energy Strategy Reviews. 2016;10:40–52.

33. Niet T, Lyseng B, English J, Keller V, Palmer-Wilson K, Moazzen I, et al. Hedging the risk of increased emissions in long term energy planning. Energy Strategy Reviews. 2017;16:1–12.

34. English J, Niet T, Lyseng B, Keller V, Palmer-Wilson K, Robertson B, et al. Flexibility requirements and electricity system planning: Assessing inter-regional coordination with large penetrations of variable renewable supplies. Renew Energy [Internet]. 2020;145:2770–82. Available from: https://www.sciencedirect.com/science/article/pii/S0960148119311176

35. Lyseng B, Niet T, English J, Keller V, Palmer-Wilson K, Robertson B, et al. System-level power-to-gas energy storage for high penetrations of variable renewables. Int J Hydrogen Energy. 2017;

36. Lyseng B, Niet T, English J, Palmer-Wilson K, Rowe A, Wild P, et al. Resource diversity impacts on storage in a high variable renewable power system. In: Proceedings of the 35th International Energy Workshop. Cork, Ireland; 2016.

37. Palmer-Wilson K, Donald J, Robertson B, Lyseng B, Keller V, Fowler M, et al. Impact of land requirements on electricity system decarbonisation pathways. Energy Policy [Internet]. 2019;129:193–205. Available from: https://www.sciencedirect.com/science/article/pii/S0301421519300576

38. Keller V, Lyseng B, Wade C, Scholtysik S, Fowler M, Donald J, et al. Electricity system and emission impact of direct and indirect electrification of heavy-duty transportation. Energy. 2019;172.

39. Ringkjøb HK, Haugan PM, Solbrekke IM. A review of modelling tools for energy and electricity systems with large shares of variable renewables. Renewable and Sustainable Energy Reviews [Internet]. 2018;96:440–59. Available from: https://www.sciencedirect.com/science/article/pii/S1364032118305690

40. Gacitua L, Gallegos P, Henriquez-Auba R, Lorca Á, Negrete-Pincetic M, Olivares D, et al. A comprehensive review on expansion planning: Models and tools for energy policy analysis. Renewable and Sustainable Energy Reviews [Internet]. 2018;98:346–60. Available from: https://www.sciencedirect.com/science/article/pii/S1364032118306269

41. Environment Canada. National Inventory Report 1990–2012: Greenhouse Gas Sources and Sinks in Canada. 2014.

42. AESO. 2014 Long-term Outlook [Internet]. Calgary, Canada; 2014 [cited 2015 Jan 10]. Available from: http://www.aeso.ca/downloads/AESO_2014_Long-term_Outlook.pdf

43. Government of Alberta. Alberta's Carbon Capture and Storage projects [Internet]. [cited 2015 Sep 2]. Available from: http://www.energy.alberta.ca/CCS/3822.asp

44. AUC. Alberta Utilities Commission: Annual electricity data collection: Total generation [Internet]. 2014 [cited 2015 Feb 17]. Available from: http://www.auc.ab.ca/market-oversight/Annual-Electricity-Data-Collection/Pages/default.aspx

45. IEA. Key World Energy Statistics 2014. International Energy Agency, Paris, France; 2014.

46. IEA. World Energy Outlook 2014 - Presentation to the Press [Internet]. London, UK: International Energy Agency; 2014 [cited 2015 Feb 19]. Available from: http://www.worldenergyoutlook.org/media/weowebsite/2014/WEO2014_LondonNovember.pdf

47. Sumner J, Bird L, Dobos H. Carbon taxes: a review of experience and policy design considerations. Climate Policy. 2011 Mar;11(2):922–43.

48. Lin B, Li X. The effect of carbon tax on per capita CO2 emissions. Energy Policy. 2011 Sep;39(9):5137–46.

49. Bruvoll A, Larsen BM. Greenhouse gas emissions in Norway: Do carbon taxes work? Energy Policy. 2004 Mar;32(4):493–505.

50. Nakata T, Lamont A. Analysis of the impacts of carbon taxes on energy systems in Japan. Energy Policy. 2001;29(2):159–66.

51. Yang C, Yeh S, Zakerinia S, Ramea K, McCollum D. Achieving California's 80% greenhouse gas reduction target in 2050: Technology, policy and scenario analysis using CA-TIMES energy economic systems model. Energy Policy. 2015 Feb;77:118–30.

52. AUC. Alberta Utilities Commission: Annual electricity data collection: Total generation [Internet]. 2015 [cited 2015 Aug 24]. Available from: http://www.auc.ab.ca/market-oversight/Annual-Electricity-Data-Collection/Pages/default.aspx

53. AESO. 2013 Annual Market Statistics [Internet]. Calgary, Canada; 2014 [cited 2014 Apr 11]. Available from: http://www.aeso.ca/downloads/2013_Annual_Market_Statistics.pdf

54. Howells M, Rogner H, Strachan N, Heaps C, Huntington H, Kypreos S, et al. OSeMOSYS: The Open Source Energy Modeling System. Energy Policy [Internet]. 2011;39(10):5850–70. Available from: http://dx.doi.org/10.1016/j.enpol.2011.06.033

55. Welsch M, Howells M, Bazilian M, DeCarolis JF, Hermann S, Rogner HH. Modelling elements of Smart Grids – Enhancing the OSeMOSYS (Open Source Energy Modelling System) code. Energy and Exergy Modelling of Advance Energy Systems. 2012;46(1):337–50.

56. DeCarolis JF, Hunter K, Sreepathi S. The case for repeatable analysis with energy economy optimization models. Energy Econ. 2012 Nov;34(6):1845–53.

57. AESO. Long Term Adequacy Metrics, Threshold and Threshold Actions Recommendation Paper. Calgary, Canada; 2008.

58. Environment Canada. Reduction of Carbon Dioxide Emissions from coal-fired Generation of Electricity Regulation. Canada Gazette Part II, SOR/2012-167; 2012.

59. Government of Alberta. Alberta's 2008 Climate Change Strategy: Responsibility/Leadership/Action. Vol. ISBN : 978. Edmonton: Ministry of Environment and Sustainable Resource Development; 2008.

60. Adamantiades A, Kessides I. Nuclear power for sustainable development: Current status and future prospects. Energy Policy. 2009 Dec;37(12):5149–66.

61. Sailor W, Bodansky D, Braun C, Fetter S, van der Zwaan B. Vol. 288, Science. 2000. p. 1177–8 A Nuclear Solution to Climate Change? Available from: http://www.sciencemag.org/content/288/5469/1177.short

62. Grape S, Jacobsson Svärd S, Hellesen C, Jansson P, Åberg Lindell M. New perspectives on nuclear power—Generation IV nuclear energy systems to strengthen nuclear non-proliferation and support nuclear disarmament. Energy Policy. 2014 Oct;73:815–9.

63. AESO. Alberta Reliability Standards. 2015.

64. EIA. Updated Capital Cost Estimates for Utility Scale Electricity Generating Plants. Washington, DC; 2013.

65. IEA. Energy Technology Perspectives 2014: Harnessing Electricity's Potential. International Energy Agency, Paris, France; 2014.

66. IEA. Projected Costs of Generating Electricity: 2010 Edition [Internet]. 2010 [cited 2014 Jan 21]. Available from: http://www.iea.org/publications/freepublications/publication/projected_costs.pdf

67. EIA. Annual Energy Outlook Interactive Table Viewer: Energy Prices by Sector and Source [Internet]. 2014 [cited 2015 Sep 2]. Available from: http://www.eia.gov/oiaf/aeo/tablebrowser/

68. Black & Veatch. Cost and performance data for power generation technologies. Overland Park: Black & Veatch Holding Company; 2012.

69. Capros P, De Vita A, Fragkos P, Kouvaritakis N, Paroussos L, Fragkiadakis K, et al. The impact of hydrocarbon resources and GDP growth assumptions for the evolution of the EU energy system for the medium and long term. Energy Strategy Reviews. 2015 Jan;6:64–79.

70. IPCC. Energy Systems. In: Climate Change 2014: Mitigation of Climate Change. Contribution of Working Group III to the Fifth Assessment Report of the Intergovernmental Panel on Climate Change. Cambridge, United Kingdom and New York, USA; 2014.

71. Nichols C, Victor N. Examining the relationship between shale gas production and carbon capture and storage under CO2 taxes based on the social cost of carbon. Energy Strategy Reviews. 2015 Apr;7:39–54.

72. EIA. U.S. Energy-Related Carbon Dioxide Emissions, 2012. Energy Information Administration, Washington, DC; 2013.

73. Goetz J. The Impact of Offsets and REC's on the Economics of Wind Projects in Alberta. In: 2011 Canadian Wind Energy Association Annual Conference. Vancouver, Canada; 2011.

74. Alvarez RA, Pacala SW, Winebrake JJ, Chameides WL, Hamburg SP. Greater focus needed on methane leakage from natural gas infrastructure. Proc Natl Acad Sci U S A. 2012 Apr 24;109(17):6435–40.

75. Howarth RW, Santoro R, Ingraffea A. Methane and the greenhouse-gas footprint of natural gas from shale formations. Clim Change. 2011 Apr 12;106(4):679–90.

76. NREL. Natural Gas and the Transformation of the U.S. Energy Sector: Electricity. Joint Institute for Strategic Energy Analysis - Technical Report. NREL/TP-6A50-55538. Golden, USA; 2012.

77. Cathles LM, Brown L, Taam M, Hunter A. A commentary on “The greenhouse-gas footprint of natural gas in shale formations” by R.W. Howarth, R. Santoro, and Anthony Ingraffea. Clim Change. 2012 Jan 3;113(2):525–35.

78. Howarth RW, Santoro R, Ingraffea A. Venting and leaking of methane from shale gas development: response to Cathles et al. Clim Change. 2012 Feb 1;113(2):537–49.

79. Howarth RW. A bridge to nowhere: methane emissions and the greenhouse gas footprint of natural gas. Energy Sci Eng. 2014 Jun 15;2(2):47–60.

80. Myhrvold NP, Caldeira K. Greenhouse gases, climate change and the transition from coal to low-carbon electricity. Environmental Research Letters. 2012 Mar 1;7(1):014019.

81. McJeon H, Edmonds J, Bauer N, Clarke L, Fisher B, Flannery BP, et al. Limited impact on decadal-scale climate change from increased use of natural gas. Nature. 2014 Oct 23;514(7523):482–5.

82. Hultman N, Rebois D, Scholten M, Ramig C. The greenhouse impact of unconventional gas for electricity generation. Environmental Research Letters. 2011 Oct 1;6(4):044008.

83. Levi M. Climate consequences of natural gas as a bridge fuel. Clim Change. 2013 Jan 3;118(3–4):609–23.

84. Heath GA, O’Donoughue P, Arent DJ, Bazilian M. Harmonization of initial estimates of shale gas life cycle greenhouse gas emissions for electric power generation. Proc Natl Acad Sci U S A. 2014 Aug 5;111(31):E3167-76.

85. IPCC. Changes in Atmospheric Constituents and in Radiative Forcing, In: Climate Change 2007: The Physical Science Basis. Contribution of Working Group I to the Fourth Assessment Report of the Intergovernmental Panel on Climate Change. Cambridge, United Kingdom and New York, USA; 2007.

86. Metz B, Davidson O, de Coninck H, Loos M, Meyer L. IPCC Special Report on Carbon Dioxide Capture and Storage. Vol. ISBN 13-97. New York, USA: Cambridge University Press, New York, NY; 2005.

87. Mishra MK, Khare N, Agrawal AB. Scenario analysis of the CO2 emissions reduction potential through clean coal technology in India's power sector: 2014–2050. Energy Strategy Reviews. 2015 Apr;7:29–38.

88. Government of Alberta. Coal Statistics [Internet]. 2015 [cited 2015 Sep 7]. Available from: http://www.energy.alberta.ca/coal/643.asp

89. Thorbjörnsson A, Wachtmeister H, Wang J, Höök M. Carbon capture and coal consumption: Implications of energy penalties and large scale deployment. Energy Strategy Reviews. 2015 Apr;7:18–28.

90. IPCC. IPCC Special Report on Carbon Dioxide Capture and Storage. Prepared by Working Group III of the Intergovernmental Panel on Climate Change [Metz, B., O. Davidson, H. C. de Coninck, M. Loos, and L. A. Meyer (eds.)]. Cambridge, United Kingdom and New York, USA; 2005.

91. Burger B. Fraunhofer Institute. 2014 [cited 2015 Mar 2]. Electricity production from solar and wind in Germany in 2014. Available from: http://www.ise.fraunhofer.de/en/downloads-englisch/pdf-files-englisch/data-nivc-/electricity-production-from-solar-and-wind-in-germany-2014.pdf

92. Bundesnetzagentur. Bundesnetzagentur List of Power Plants. 2014 [cited 2015 Mar 21]. Kraftwerksliste der Bundesnetzagentur - Stand: 29.10.2014. Available from: http://www.bundesnetzagentur.de/EN/Areas/Energy/Companies/SpecialTopics/PowerPlantList/PubliPowerPlantList_node.html

93. Kriegler E, Weyant JP, Blanford GJ, Krey V, Clarke L, Edmonds J, et al. The role of technology for achieving climate policy objectives: overview of the EMF 27 study on global technology and climate policy strategies. Clim Change. 2014;123:353–67.

94. IEA. Key World Energy Statistics. Paris, France; 2016.

95. IEA. World Energy Outlook 2016. Paris, France; 2016.

96. IEA. World Energy Outlook 2015. Paris, France; 2015.

97. EIA. International Energy Outlook 2016. Washington, DC; 2016.

98. IEA. Tracking Clean Energy Progress 2013: IEA Input to the Clean Energy Ministerial. Vol. Directorat. Paris and Washington, DC: Organisation for Economic Co-operation and Development; 2013.

99. Rogner HH, Aguilera RF, Archer C, Bertani R, Bhattacharya SC, Dusseault MB, et al. Chapter 7 - Energy Resources and Potentials. In: Global Energy Assessment - Toward a Sustainable Future. Cambridge University Press, Cambridge, UK and New York, NY, USA and the International Institute for Applied Systems Analysis, Laxenburg, Austria; 2012. p. 423–512.

100. Rose SK, Kriegler E, Bibas R, Calvin K, Popp A, Van Vuuren DP, et al. Bioenergy in energy transformation and climate management. Clim Change. 2014;123:477–93.

101. Luderer G, Krey V, Calvin K, Merrick J, Mima S, Pietzcker R, et al. The role of renewable energy in climate stabilization: results from the EMF27 scenarios. Clim Change. 2014;123:427–41.

102. IEA. Technology Roadmap: Geothermal Heat and Power. Paris, France; 2011.

103. German Federal Ministry for Economic Affairs and Energy. Renewable Energy Sources Act - RES Act 2014. Berlin, Germany; 2014.

104. Government of Denmark. Independent from fossil fuels by 2050 [Internet]. [cited 2016 Oct 14]. Available from: http://denmark.dk/en/green-living/strategies-and-policies/independent-from-fossil-fuels-by-2050

105. GCAM Wiki documentation [Internet]. [cited 2017 Nov 2]. Available from: http://jgcri.github.io/gcam-doc/

106. Fawcett AA, Iyer GC, Clarke LE, Edmonds JA, Hultman NE, McJeon HC, et al. Can Paris pledges avert severe climate change? Science. 2015 Dec 4;350(6265):1168–9.

107. MNP. Integrated modelling of global environmental change. An overview of IMAGE 2.4. A.F. Bouwman, T. Kram, K. Klein Goldewijk, editors. Bilthoven, The Netherlands: Netherlands Environmental Assessment Agency (MNP); 2006.

108. van Vuuren DP, Stehfest E, den Elzen MGJ, Kram T, van Vliet J, Deetman S, et al. RCP2.6: exploring the possibility to keep global mean temperature increase below 2°C. Clim Change. 2011 Nov 5;109(1–2):95–116.

109. Pietzcker R, Ueckerdt F, Luderer G, Scholz Y, Gils H, Carrara S, et al. Evaluating the capacity of Integrated Assessment Models (IAMs) to represent system integration challenges of wind and solar power. In: International Energy Workshop 2016. Cork, Ireland; 2016.

110. Lopes JAP, Hatziargyriou N, Mutale J, Djapic P, Jenkins N. Integrating distributed generation into electric power systems: A review of drivers, challenges and opportunities. Electric Power Systems Research. 2007 Jul;77(9):1189–203.

111. Fink S, Mudd C, Porter K, Morgenstern B. Wind Energy Curtailment Case Studies: May 2008 - May 2009. Columbia, USA; 2010.

112. Bathurst GN, Strbac G. Value of combining energy storage and wind in short-term energy and balancing markets. Electric Power Systems Research. 2003;67(1):1–8.

113. Zhang G, Wan X. A wind-hydrogen energy storage system model for massive wind energy curtailment. Int J Hydrogen Energy. 2014;39(3):1243–52.

114. Loisel R, Mercier A, Gatzen C, Elms N, Petric H. Valuation framework for large scale electricity storage in a case with wind curtailment. Energy Policy. 2010;38(11):7323–37.

115. Qadrdan M, Abeysekera M, Chaudry M, Wu J, Jenkins N. Role of power-to-gas in an integrated gas and electricity system in Great Britain. Int J Hydrogen Energy. 2015;40(17):5763–75.

116. Díaz-González F, Sumper A, Gomis-Bellmunt O, Villafáfila-Robles R. A review of energy storage technologies for wind power applications. Renewable and Sustainable Energy Reviews. 2012;16(4):2154–71.

117. de Boer HS, Grond L, Moll H, Benders R. The application of power-to-gas, pumped hydro storage and compressed air energy storage in an electricity system at different wind power penetration levels. Energy. 2014;72:360–70.

118. International Electrotechnical Commission. Electrical Energy Storage. White paper. Geneva; 2011.

119. Bockris J. The hydrogen economy: Its history. Int J Hydrogen Energy. 2013 Feb 27;38(6):2579–88.

120. Scott DS. Smelling land: the hydrogen defense against climate catastrophe. Queen's Printer Publishing; 2008.

121. Winter CJ. Hydrogen energy — Abundant, efficient, clean: A debate over the energy-system-of-change. Int J Hydrogen Energy. 2009 Jul;34(14):S1–52.

122. Dickinson RR, Battye DL, Linton VM, Ashman PJ, Nathan GGJ. Alternative carriers for remote renewable energy sources using existing CNG infrastructure. Int J Hydrogen Energy. 2010;35(3):1321–9.

123. Varone A, Ferrari M. Power to liquid and power to gas: An option for the German Energiewende. Renewable and Sustainable Energy Reviews. 2015;45:207–18.

124. Götz M, Lefebvre J, Mörs F, McDaniel Koch A, Graf F, Bajohr S, et al. Renewable Power-to-Gas: A technological and economic review. Renew Energy. 2016;85:1371–90.

125. Gutiérrez-Martín F, Rodríguez-Antón LM. Power-to-SNG technology for energy storage at large scales. Int J Hydrogen Energy. 2016 Nov 9;41(42):19290–303.

126. Olateju B, Kumar A. Hydrogen production from wind energy in Western Canada for upgrading bitumen from oil sands. Energy. 2011;36(11):6326–39.

127. Olateju B, Monds J, Kumar A. Large scale hydrogen production from wind energy for the upgrading of bitumen from oil sands. Appl Energy. 2014;118:48–56.

128. Walker SB, van Lanen D, Fowler M, Mukherjee U. Economic analysis with respect to Power-to-Gas energy storage with consideration of various market mechanisms. Int J Hydrogen Energy. 2016;41(19):7754–65.

129. Naterer G, Fowler M, Cotton J, Gabriel K. Synergistic roles of off-peak electrolysis and thermochemical production of hydrogen from nuclear energy in Canada. Int J Hydrogen Energy. 2008 Dec;33(23):6849–57.

130. Gahleitner G. Hydrogen from renewable electricity: An international review of power-to-gas pilot plants for stationary applications. Int J Hydrogen Energy. 2012;38:2039–61.

131. Ulleberg Ø, Nakken T, Eté A. The wind/hydrogen demonstration system at Utsira in Norway: Evaluation of system performance using operational data and updated hydrogen energy system modeling tools. Int J Hydrogen Energy. 2010;35(5):1841–52.

132. Genç G, Çelik M, Serdar Genç M. Cost analysis of wind-electrolyzer-fuel cell system for energy demand in Pnarbaş-Kayseri. Int J Hydrogen Energy. 2012;37(17):12158–66.

133. Kaldellis JK, Zafirakis D. Optimum energy storage techniques for the improvement of renewable energy sources-based electricity generation economic efficiency. Energy. 2007;32(12):2295–305.

134. Korpås M, Greiner CJ. Opportunities for hydrogen production in connection with wind power in weak grids. Renew Energy. 2008;33(6):1199–208.

135. Bennoua S, Le Duigou A, Quéméré MM, Dautremont S. Role of hydrogen in resolving electricity grid issues. Int J Hydrogen Energy. 2015;40(23):7231–45.

136. Floch PH, Gabriel S, Mansilla C, Werkoff F. On the production of hydrogen via alkaline electrolysis during off-peak periods. Int J Hydrogen Energy. 2007;32(18):4641–7.

137. Mansilla C, Dautremont S, Shoai Tehrani B, Cotin G, Avril S, Burkhalter E. Reducing the hydrogen production cost by operating alkaline electrolysis as a discontinuous process in the French market context. Int J Hydrogen Energy. 2011;36(11):6407–13.

138. Mansilla C, Louyrette J, Albou S, Barbieri G, Collignon N, Bourasseau C, et al. Electric system management through hydrogen production-A market driven approach in the French context. Int J Hydrogen Energy. 2012;37(15):10986–91.

139. Mansilla C, Louyrette J, Albou S, Bourasseau C, Dautremont S. Economic competitiveness of off-peak hydrogen production today - A european comparison. Energy. 2013;55:996–1001.

140. Cany C, Mansilla C, da Costa P, Mathonniere G. Adapting the French nuclear fleet to integrate variable renewable energies via the production of hydrogen: Towards massive production of low carbon hydrogen? Int J Hydrogen Energy. 2017 May 11;42(19):13339–56.

141. Vandewalle J, Bruninx K, D'haeseleer W. Effects of large-scale power to gas conversion on the power, gas and carbon sectors and their interactions. Energy Convers Manag. 2015 Apr;94:28–39.

142. Mukherjee U, Elsholkami M, Walker S, Fowler M, Elkamel A, Hajimiragha A. Optimal sizing of an electrolytic hydrogen production system using an existing natural gas infrastructure. Int J Hydrogen Energy. 2015 Aug 17;40(31):9760–72.

143. Bussar C, Stöcker P, Cai Z, Moraes Jr. L, Magnor D, Wiernes P, et al. Large-scale integration of renewable energies and impact on storage demand in a European renewable power system of 2050—Sensitivity study. J Energy Storage. 2016;6:1–10.

144. Kötter E, Schneider L, Sehnke F, Ohnmeiss K, Schröer R. The future electric power system: Impact of Power-to-Gas by interacting with other renewable energy components. J Energy Storage. 2016;5:113–9.

145. Jentsch M, Trost T, Sterner M. Optimal use of Power-to-Gas energy storage systems in an 85% renewable energy scenario. In: Energy Procedia. Elsevier B.V.; 2014. p. 254–61.

146. Heide D, von Bremen L, Greiner M, Hoffmann C, Speckmann M, Bofinger S. Seasonal optimal mix of wind and solar power in a future, highly renewable Europe. Renew Energy. 2010;35(11):2483–9.

147. Government of Alberta. Natural Gas Facts and Stats [Internet]. 2015 [cited 2016 Sep 13]. Available from: http://www.energy.alberta.ca/NaturalGas/Gas_Pdfs/FactSheet_NGFacts.pdf

148. Ursua A, Gandia LM, Sanchis P. Hydrogen Production From Water Electrolysis: Current Status and Future Trends. Proceedings of the IEEE. 2012;100(2):410–26.

149. Carmo M, Fritz DL, Mergel J, Stolten D. A comprehensive review on PEM water electrolysis. Int J Hydrogen Energy. 2013 Apr;38(12):4901–34.

150. Frost W, McCrank D. Wind Integration in Alberta: Market & Operational Framework Implementation. AESO Stakeholder Information Session. Calgary, Canada; 2007.

151. Holttinen H. Hourly wind power variations in the nordic countries. Wind Energy. 2005;8(2):173–95.

152. MacDonald AE, Clack CTM, Alexander A, Dunbar A, Wilczak J, Xie Y. Future cost-competitive electricity systems and their impact on US CO2 emissions. Nat Clim Chang. 2016;(January):1–6.

153. Staffell I, Pfenninger S. Using bias-corrected reanalysis to simulate current and future wind power output. Energy. 2016;114:1224–39.

154. AESO. AESO 2016 Long-term Outlook [Internet]. Calgary, Canada; 2016. Available from: http://www.aeso.ca/downloads/AESO_2016_Long-term_Outlook_WEB.pdf

155. IEA. Technology Roadmap: Energy storage. Paris, France; 2014.

156. Sherif SA, Barbir F, Veziroglu TN. Wind energy and the hydrogen economy—review of the technology. Solar Energy. 2005;78(5):647–60.

157. Bertuccioli L, Chan A, Hart D, Lehner F, Madden B, Standen E. Development of Water Electrolysis in the European Union. Lausanne, Switzerland; 2014.

158. U.S. Department of Energy. Report of the Hydrogen Production Expert Panel: A Subcommittee of the Hydrogen & Fuel Cell Technical Advisory Committee. Washington, DC; 2013.

159. Melaina MW, Antonia O, Penev M. Blending Hydrogen into Natural Gas Pipeline Networks: A Review of Key Issues. 2013.

160. Altfeld K, Pinchbeck D. Admissible hydrogen concentrations in natural gas systems. 2013;

161. NaturalHY European Project (FP6). Using the Existing Natural Gas System for Hydrogen. 2004.

162. Soder L, Hofmann L, Orths A, Holttinen H, Wan Y huei, Tuohy A. Experience From Wind Integration in Some High Penetration Areas. Energy. 2007;22(1):4–12.

163. Heide D, von Bremen L, Greiner M, Hoffmann C, Speckmann M, Bofinger S. Seasonal optimal mix of wind and solar power in a future, highly renewable Europe. Renew Energy. 2010;35(11):2483–9.

164. Hanssen S V, Daioglou V, Steinmann ZJN, Doelman JC, Van Vuuren DP, Huijbregts MAJ. The climate change mitigation potential of bioenergy with carbon capture and storage. Nat Clim Chang [Internet]. 2020;10(11):1023–9. Available from: https://doi.org/10.1038/s41558-020-0885-y

165. Rose S, Scott M. Review of 1.5˚C and Other Newer Global Emissions Scenarios Insights for Company and Financial Climate Low-Carbon Transition Risk Assessment and Greenhouse Gas Goal Setting. Palo Alto; 2020.

166. Luderer G, Vrontisi Z, Bertram C, Edelenbosch OY, Pietzcker RC, Rogelj J, et al. Residual fossil CO2 emissions in 1.5–2 °C pathways. Nat Clim Chang [Internet]. 2018;8(7):626–33. Available from: https://doi.org/10.1038/s41558-018-0198-6

167. Hilaire J, Minx JC, Callaghan MW, Edmonds J, Luderer G, Nemet GF, et al. Negative emissions and international climate goals—learning from and about mitigation scenarios. Clim Change [Internet]. 2019;157(2):189–219. Available from: https://doi.org/10.1007/s10584-019-02516-4

168. Minx JC, Lamb WF, Callaghan MW, Fuss S, Hilaire J, Creutzig F, et al. Negative emissions—Part 1: Research landscape and synthesis. Environmental Research Letters [Internet]. 2018 Jun 1;13(6):063001. Available from: https://iopscience.iop.org/article/10.1088/1748-9326/aabf9b

169. Smith P, Davis SJ, Creutzig F, Fuss S, Minx J, Gabrielle B, et al. Biophysical and economic limits to negative CO2 emissions. Nat Clim Chang [Internet]. 2015 Dec 7 [cited 2017 Feb 8];6(1):42–50. Available from: http://www.nature.com/doifinder/10.1038/nclimate2870

170. Nemet GF, Callaghan MW, Creutzig F, Fuss S, Hartmann J, Hilaire J, et al. Negative emissions - Part 3: Innovation and upscaling. Vol. 13, Environmental Research Letters. 2018.

171. Creutzig F, Breyer C, Hilaire J, Minx J, Peters GP, Socolow R. The mutual dependence of negative emission technologies and energy systems. Energy Environ Sci [Internet]. 2019;12(6):1805–17. Available from: http://dx.doi.org/10.1039/C8EE03682A

172. Edwards MR, Thomas ZH, Nemet GF, Rathod S, Greene J, Surana K, et al. Modeling direct air carbon capture and storage in a 1.5 °C climate future using historical analogs. Proceedings of the National Academy of Sciences [Internet]. 2024 May 14;121(20):e2215679121. Available from: https://doi.org/10.1073/pnas.2215679121

173. Bistline JET, Blanford GJ. Impact of carbon dioxide removal technologies on deep decarbonization of the electric power sector. Nat Commun [Internet]. 2021;12(1):3732. Available from: https://doi.org/10.1038/s41467-021-23554-6

174. Pham AT, Craig MT. Cost and deployment consequences of advanced planning for negative emissions with direct air capture in the U.S. Eastern Interconnection. Appl Energy [Internet]. 2023;350:121649. Available from: https://www.sciencedirect.com/science/article/pii/S0306261923010139

175. Wise M, Calvin K, Thomson A, Clarke L, Bond-Lamberty B, Sands R, et al. Implications of limiting CO2 concentrations for land use and energy. Science. 2009 May 29;324(5931):1183–6.

176. National Academies of Sciences and Medicine E. Negative Emissions Technologies and Reliable Sequestration: A Research Agenda [Internet]. Washington, DC: The National Academies Press; 2019. Available from: https://nap.nationalacademies.org/catalog/25259/negative-emissions-technologies-and-reliable-sequestration-a-research-agenda

177. Baciocchi R, Storti G, Mazzotti M. Process design and energy requirements for the capture of carbon dioxide from air. Chemical Engineering and Processing: Process Intensification. 2006 Dec;45(12):1047–58.

178. Barkakaty B, Sumpter BG, Ivanov IN, Potter ME, Jones CW, Lokitz BS. Emerging materials for lowering atmospheric carbon. Environ Technol Innov. 2017;7:30–43.

179. Duyar MS, Trevi?o MAA, Farrauto RJ. Dual function materials for CO2 capture and conversion using renewable H2. Appl Catal B. 2015 Jun;168–169:370–6.

180. Holmes G, Keith DW. An air-liquid contactor for large-scale capture of CO2 from air. Philosophical Transactions of the Royal Society A: Mathematical, Physical and Engineering Sciences [Internet]. 2012 Sep 13 [cited 2017 Feb 8];370(1974):4380–403. Available from: http://rsta.royalsocietypublishing.org/cgi/doi/10.1098/rsta.2012.0137

181. Mahmoudkhani M, Keith DW. Low-energy sodium hydroxide recovery for CO2 capture from atmospheric air—Thermodynamic analysis. International Journal of Greenhouse Gas Control. 2009 Jul;3(4):376–84.

182. Stolaroff JK, Keith DW, Lowry G V. Carbon Dioxide Capture from Atmospheric Air Using Sodium Hydroxide Spray. Environ Sci Technol. 2008 Apr;42(8):2728–35.

183. Veselovskaya J V., Derevschikov VS, Kardash TYu, Stonkus OA, Trubitsina TA, Okunev AG. Direct CO2 capture from ambient air using K2CO3/Al2O3 composite sorbent. International Journal of Greenhouse Gas Control. 2013 Sep;17:332–40.

184. Wang T, Liu J, Lackner KS, Shi X, Fang M, Luo Z. Characterization of kinetic limitations to atmospheric CO_2 capture by solid sorbent. Greenhouse Gases: Science and Technology. 2016 Feb;6(1):138–49.

185. Zhang W, Liu H, Sun C, Drage TC, Snape CE. Capturing CO2 from ambient air using a polyethyleneimine–silica adsorbent in fluidized beds. Chem Eng Sci. 2014 Sep;116:306–16.

186. Sanz-Pérez ES, Murdock CR, Didas SA, Jones CW. Direct Capture of CO_2 from Ambient Air. Chem Rev. 2016 Oct 12;116(19):11840–76.

187. McQueen N, Desmond MJ, Socolow RH, Psarras P, Wilcox J. Natural Gas vs. Electricity for Solvent-Based Direct Air Capture. Frontiers in Climate [Internet]. 2021;2. Available from: https://www.frontiersin.org/journals/climate/articles/10.3389/fclim.2020.618644

188. Sanz-Pérez ES, Murdock CR, Didas SA, Jones CW. Direct Capture of CO2 from Ambient Air. Chem Rev [Internet]. 2016 Oct 12;116(19):11840–76. Available from: https://doi.org/10.1021/acs.chemrev.6b00173

189. EPRI. US-REGEN Model Documentation. EPRI; 2020.

190. Daggash HA, Heuberger CF, Mac Dowell N. The role and value of negative emissions technologies in decarbonising the UK energy system. International Journal of Greenhouse Gas Control [Internet]. 2019;81:181–98. Available from: https://www.sciencedirect.com/science/article/pii/S1750583618305024

191. English J, Niet T, Lyseng B, Palmer-Wilson K, Keller V, Moazzen I, et al. Impact of electrical intertie capacity on carbon policy effectiveness. Energy Policy. 2016;

192. Anderson K, Peters G. The trouble with negative emissions. Science [Internet]. 2016 Oct 14 [cited 2017 Sep 20];354(6309):182–3. Available from: http://www.ncbi.nlm.nih.gov/pubmed/27738161

193. House KZ, Baclig AC, Ranjan M, van Nierop EA, Wilcox J, Herzog HJ. Economic and energetic analysis of capturing CO2 from ambient air. Proc Natl Acad Sci U S A. 2011 Dec 20;108(51):20428–33.

194. IEAGHG. Global Assessment of Direct Air Capture Costs. 2021 May.

195. Keith DW, Ha-Duong M, Stolaroff JK. Climate strategy with CO2 capture from the air. Clim Change. 2006;74(1–3):17–45.

196. Küng L, Aeschlimann S, Charalambous C, McIlwaine F, Young J, Shannon N, et al. A roadmap for achieving scalable, safe, and low-cost direct air carbon capture and storage. Energy Environ Sci [Internet]. 2023;16(10):4280–304. Available from: http://dx.doi.org/10.1039/D3EE01008B

197. Galeazzi C, Lam G, Holdren JP. Carbon Capture, Utilization, and Storage: Carbon Dioxide Transport Costs and Network-Infrastructure Considerations for a Net-Zero United States. 2023.

198. Blanford GJ, Merrick JH, Bistline JET, Young DT. Simulating Annual Variation in Load, Wind, and Solar by Representative Hour Selection. The Energy Journal. 2018 Jul 1;39(3).

199. Dobos AP. PVWatts Version 5 Manual (NREL/TP-6A20-62641). 2014;(September):20.

200. Doluweera GH, Jordaan SM, Moore MC, Keith DW, Bergerson JA. Evaluating the role of cogeneration for carbon management in Alberta. Energy Policy. 2011;39(12):7963–74.

201. Palmer-Wilson K, Banks J, Walsh W, Robertson B. Sedimentary basin geothermal favourability mapping and power generation assessments. Renew Energy [Internet]. 2018;127:1087–100. Available from: https://www.sciencedirect.com/science/article/pii/S0960148118305032

202. Fuss S, Lamb WF, Callaghan MW, Hilaire J, Creutzig F, Amann T, et al. Negative emissions - Part 2: Costs, potentials and side effects. Vol. 13, Environmental Research Letters. Institute of Physics Publishing; 2018.

203. Pritchard C, Yang A, Holmes P, Wilkinson M. Thermodynamics, economics and systems thinking: What role for air capture of CO2? Process Safety and Environmental Protection. 2015 Mar;94:188–95.

204. Ranjan M, Herzog HJ. Feasibility of air capture. In: Energy Procedia. 2011. p. 2869–76.

205. Ruthven DM. CO2 capture: Value functions, separative work and process economics. Chem Eng Sci. 2014 Jul;114:128–33.

206. Ruthven DM, Farooq S, Brandani S. Work of separation in CO2 capture: Applicability of the value function. Chem Eng Sci. 2015 Apr;126:604–7.

207. Simon AJ, Kaahaaina NB, Julio Friedmann S, Aines RD. Systems analysis and cost estimates for large scale capture of carbon dioxide from air. Energy Procedia. 2011;4:2893–900.

208. American Physical Society. Direct Air Capture of CO2 with Chemicals: A Technology Assessment for the APS Panel on Public Affairs. 2011.

209. Ellerman DA. The competition between coal and natural gas the importance of sunk costs. Resources Policy. 1996 Mar;22(1–2):33–42.

210. BC Hydro. 2013 Resource Options Report Update Appendix 6: Wood Biomass Energy Potential of British Columbia. 2013.

211. Bradley D. Canada Report on Bioenery 2010. [Internet]. Ottawa, Canada; 2010. Available from: http://www.canbio.ca/upload/documents/canada-report-on-bioenergy-2010-sept-15-2010.pdf

212. Lipman TE. What Will Power the Hydrogen Economy ? Present and Future Sources of Hydrogen Energy. UCD-ITS-RR-04-10. Davis, CA; 2004.

213. Bockris JO, Conway BE, Yeager E. Comprehensive Treatise of Electrochemistry. Volume 2: Electrochemical Processing. New York: Plenum Press; 1981.

214. Dieguez P, Ursua A, Sanchis P, Sopena C, Guelbenzu E, Gandia L. Thermal performance of a commercial alkaline water electrolyzer: Experimental study and mathematical modeling. Int J Hydrogen Energy. 2008 Dec;33(24):7338–54.

215. Onda K, Kyakuno T, Hattori K, Ito K. Prediction of production power for high-pressure hydrogen by high-pressure water electrolysis. J Power Sources. 2004 May;132(1–2):64–70.

216. LeRoy RL. The Thermodynamics of Aqueous Water Electrolysis. J Electrochem Soc. 1980 Sep 1;127(9):1954.

217. NREL. Current (2009) State-of-the-Art Hydrogen Production Cost Estimate Using Water Electrolysis: Independent Review. 2009;(NREL/BK-6A1-46676):1–43.

218. Ivy J. Summary of Electrolytic Hydrogen Production: Milestone Completion Report. NREL Tech. Rep. MP-560-36734. NREL Tech. Rep. MP-560-36734; 2004.

219. Götz M, Lefebvre J, Mörs F, McDaniel Koch A, Graf F, Bajohr S, et al. Renewable Power-to-Gas: A technological and economic review. Renew Energy. 2015 Aug;

220. Laguna-Bercero MA. Recent advances in high temperature electrolysis using solid oxide fuel cells: A review. J Power Sources. 2012 Apr;203:4–16.

221. Vad Mathiesen B, Ridjan I. Technology Data for High Temperature Solid Oxide Electrolyser Cells , Alkali and Pem Electrolysers. 2013.

222. Prince-Richard S, Whale M, Djilali N. A techno-economic analysis of decentralized electrolytic hydrogen production for fuel cell vehicles. Int J Hydrogen Energy. 2005;30(11):1159–79.

223. Holladay JD, Hu J, King DL, Wang Y. An overview of hydrogen production technologies. Catal Today. 2009;139(4):244–60.

224. Salzano F. Water vapor electrolysis at high temperature: Systems considerations and benefits. Int J Hydrogen Energy. 1985;10(12):801–9.

225. Zahid M, Schefold J, Brisse A. High-Temperature Water Electrolysis Using Planar Solid Oxide Fuel Cell Technology: a Review. In: 18th World Hydrogen Energy Conference 2010 - WHEC 2010. Essen Germany; 2010.

226. Smolinka T, Günther M, Garche J. NOW-Studie: Stand und Entwicklungspotenzial der Wasserelektrolyse zur Herstellung von Wasserstoff aus regenerativen Energien. http://www.hs-ansbach.de/uploads/tx_nxlinks/NOW-Studie-Wasserelektrolyse-2011.pdf; 2011.

227. Woo CK, Horowitz I, Moore J, Pacheco a. The impact of wind generation on the electricity spot-market price level and variance: The Texas experience. Energy Policy. 2011;39(7):3939–44.

228. Nicolosi M. Wind power integration and power system flexibility-An empirical analysis of extreme events in Germany under the new negative price regime. Energy Policy. 2010;38(11):7257–68.

229. Korpaas M, Holen AT, Hildrum R. Operation and sizing of energy storage for wind power plants in a market system. International Journal of Electrical Power and Energy System. 2003;25(8):599–606.

230. Mantz RJ, De Battista H. Hydrogen production from idle generation capacity of wind turbines. Int J Hydrogen Energy. 2008;33(16):4291–300.

231. Takahashi R, Kinoshita H, Murata T, Tamura J, Sugimasa M, Komura a., et al. Output Power Smoothing and Hydrogen Production by Using Variable Speed Wind Generators. IEEE Transactions on Industrial Electronics. 2010;57(2):485–93.

232. Segura I, Pérez-Navarro A, Sánchez C, Ibáñez F, Payá J, Bernal E. Technical requirements for economical viability of electricity generation in stabilized wind parks. Int J Hydrogen Energy. 2007;32(16):3811–9.

233. Shaw S, Peteves E. Exploiting synergies in European wind and hydrogen sectors: A cost-benefit assessment. Int J Hydrogen Energy. 2008;33(13):3249–63.

234. Genç G, Çelik M, Serdar Genç M. Cost analysis of wind-electrolyzer-fuel cell system for energy demand in Pınarbaşı-Kayseri. Int J Hydrogen Energy. 2012;

235. Zhang G, Wan X. A wind-hydrogen energy storage system model for massive wind energy curtailment. Int J Hydrogen Energy. 2014;39(3):1243–52.

236. Lund H, Salgi G, Elmegaard B, Andersen AN. Optimal operation strategies of compressed air energy storage (CAES) on electricity spot markets with fluctuating prices. Appl Therm Eng. 2009;29(5–6):799–806.

237. Foley A, Díaz Lobera I. Impacts of compressed air energy storage plant on an electricity market with a large renewable energy portfolio. Energy. 2013;57:85–94.

238. Nyamdash B, Denny E, O'Malley M. The viability of balancing wind generation with large scale energy storage. Energy Policy. 2010;38(11):7200–8.

239. Sioshansi R, Denholm P, Jenkin T, Weiss J. Estimating the value of electricity storage in PJM: Arbitrage and some welfare effects. Energy Econ. 2009 Mar;31(2):269–77.

240. Guandalini G, Campanari S, Romano MC. Power-to-gas plants and gas turbines for improved wind energy dispatchability: Energy and economic assessment. Appl Energy. 2015;147:117–30.

241. Guinot B, Montignac F, Champel B, Vannucci D. Profitability of an electrolysis based hydrogen production plant providing grid balancing services. Int J Hydrogen Energy. 2015 Aug;40(29):8778–87.

242. Gutiérrez-Martín F, Guerrero-Hernández I. Balancing the grid loads by large scale integration of hydrogen technologies: The case of the Spanish power system. Int J Hydrogen Energy. 2012;37(2):1151–61.

243. Steward D, Saur G, Penev M, Ramsden T. Lifecycle cost analysis of hydrogen versus other technologies for electrical energy storage. Vol. NREL/TP-56. Golden: National Renewable Energy Laboratory; 2009.

244. Bussar C, Moos M, Alvarez R, Wolf P, Thien T, Chen H, et al. Optimal allocation and capacity of energy storage systems in a future European power system with 100% renewable energy generation. Energy Procedia. 2014;46:40–7.

245. Ruth M, Joseck F. Hydrogen Threshold Cost Calculation. Program Record (Offices of Fuel Cell Technologies). 2011.

246. Levene JI, Mann MK, Margolis RM, Milbrandt A. An analysis of hydrogen production from renewable electricity sources. Solar Energy. 2007;81(6):773–80.

247. Jørgensen C, Ropenus S. Production price of hydrogen from grid connected electrolysis in a power market with high wind penetration. Int J Hydrogen Energy. 2008;33(20):5335–44.

248. Beccali M, Brunone S, Finocchiaro P, Galletto JM. Method for size optimisation of large wind-hydrogen systems with high penetration on power grids. Appl Energy. 2013;102(0):534–44.

249. Jensen SH, Larsen PH, Mogensen M. Hydrogen and synthetic fuel production from renewable energy sources. Int J Hydrogen Energy. 2007 Oct;32(15):3253–7.

Appendix A: CHAPTER 2 ASSUMPTION DETAILS

(209)(210)(211)**Decarbonising the Alberta power system with carbon taxes**

B. Lyseng*, A. Rowe, P. Wild, J. English, T. Niet, L. Pitt

Appendix A: Supplementary Material

I. Temporal structure

On-peak times are defined as when load is more than half of one standard deviation above the monthly median load for summer and winter, or one quarter standard deviation for spring and fall (because of lower peaks in shoulder seasons). Off-peak times are defined as times when demand is more than half of one standard deviation below the monthly median. Mid-peak times occur when the demand is greater than the off-peak and lower than the on-peak. A graphical representation of the three daily time slices for one month is presented in Figure A.1.

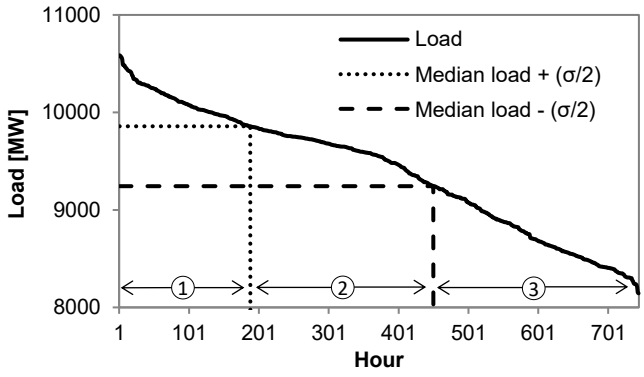

Fig. A.1. An historic Alberta load duration curve (January 2013) indicating how time slices are determined for one season. Point 1: On-peak slice; Point 2: Mid-peak slice; Point 3: Off-peak slice.

For each of the thirty-six time slices, both *year fractions* and *demand fractions* are calculated. The year fraction (*YF*) is the percentage of the year the slice occupies, and demand fraction (*DF*) is the percentage of the annual demand occurring in the year fraction. Demand fraction is calculated by summing loads in each time slice and dividing by the total annual demand. To determine the five representative profiles from historic hourly data, the following equations are used:

$$YF_{y,m,l} = n(L_{y,m,l}) / H_y \quad (1)$$

$$LF_{y,m,l} = \Sigma L_{y,m,l}(x) / \Sigma L_y(x) \quad (2)$$

Where y is the year, m is the month, l is the time slice type (on-peak, mid-peak, off-peak), and H is the total number of hours in the year. $L_{y,m,l}$ is the set of hourly loads in one time slice. Notation $n(A_i)$ is the number of elements in set A with consistent values of i.

The modelled load (*ML*) that must be met in each future time slice is calculated by Equation 3, where the AESO forecast annual demand (D_y) is multiplied by a load fraction. The year fraction of the time slice is from the corresponding profile (i.e. same *y,m,l*).

$$ML_{y,m,l} = D_y * LF_{y,m,l} \quad (3)$$

This structure captures the daily and seasonal load profiles while permitting reasonable computation times for a model with a 50 year scope. To capture the annual peak hour that is lost by aggregating load into 36 time slices, the maximum modelled on-peak load (*MP*), determined by Equation 4, is compared with AESO annual peak load predictions[23], and a peak factor (*PF*) is calculated (Eqution 5). This factor is applied with the historic average AESO reported reserve

[23] The AESO 2014 Long-term Outlook estimates both annual energy (GWh) and system peak load (MW)

margin when defining the reserve margin in the model to ensure that sufficient capacity is installed.

$$MP_y = \max(LF_{y,m,l} / YF_{y,m,l}) \quad (4)$$

$$PF_y = AP_y / MP_y \quad (5)$$

$$RM_y = PF_y * (1 + HRM) - 1 \quad (6)$$

Where *AP* is the peak predicted by AESO, *RM* is the reserve margin specified in the model, and *HRM* is the historic reserve margin (18%, which excludes wind and intertie capacity [1]).

II. Assumptions regarding existing generation assets

Assumed retirement dates for existing coal plants are based on a combination of several sources: Canada's *Reduction of Carbon Dioxide Emissions from Coal-fired Generation of Electricity Regulations*[24], AEUB Decision U97065[25], AESO 2012 Long-Term Outlook Update[26], JEM Energy report[27], and KPMG report[28]. For life extensions, units are assumed to be taken offline for one year following their assumed retirement year for the refurbishment, and are then eligible to operate for an additional ten years with a 5% improvement in HR. Assumptions are presented in Table A.1.

[24] http://www.gazette.gc.ca/rp-pr/p2/2012/2012-09-12/html/sor-dors167-eng.html
[25] http://www.auc.ab.ca/applications/decisions/Decisions/1997/U97065-v2.pdf
[26] http://www.aeso.ca/downloads/AESO_LTO_Update_Final.pdf
[27] http://www.hme.ca/reports/CASA_Report_--_The_Efficiency_of_Alberta%27s_Electrical_Supply_System_EEEC-02-04.pdf
[28] https://www.kpmg.com/Ca/en/IssuesAndInsights/ArticlesPublications/Documents/KPMG-Issue3-Alberta-FINAL-web-Jul2014.pdf

Table A.1

Coal plant capacities, retirements and heat rates.

Unit Name	Capacity [MW]	Assumed Retirement[a] [Year]	Heat Rate [Btu/kWh]	Life extension option
Battle River #3	149	2019	11.5	No
Battle River #4	155	2025	11.5	No
Battle River #5	385	2018	10.1	Yes
Genesee #1	400	2028	10.5	Yes
Genesee #2	400	2033	10.5	Yes
Genesee #3	466	2044	9.5	Yes
H.R. Milner	144	2019	15.5	No
Keephills #1 & #2	806	2018	10.3	Yes
Keephills #3	450	2050	9.2	Yes
Sheerness #1	390	2025	10.3	Yes
Sheerness #2	390	2029	10.3	Yes
Sundance #1 & #2	576	2019	10.9	No
Sundance #3 & #4	768	2016	11.1	Yes
Sundance #5 & #6	807	2018	10.7	Yes

[a] Plant is assumed to be operation for entire retirement year

The capital cost of refurbishing a coal plant, based on Ellerman [2], is determined by:

$$CapEx_{refurb} = CapEx_{Ellerman,refurb} \times \frac{US2010\$}{US1994\$} \times \frac{CapEx_{EIA,new\ coal,US2010\$}}{CapEx_{\ Ellerman,new\ coal} \times \frac{US2010\$}{US1994\$}}$$

Assumed residual capacities for existing generation are presented in Table A.2.

Table A.2

Residual capacity of existing generation as modelled [GW].

	Coal	CCGT	OCGT	Cogen	Hydro	Biomass	Wind
2010	5.81	1.005	0.93	3.416	0.884	0.354	0.723
2011	6.286	1.012	0.939	3.6	0.894	0.356	0.896
2012	6.286	1.064	0.963	3.6	0.894	0.404	1.087
2013	6.286	1.064	0.963	3.6	0.894	0.404	1.087
2014	6.286	1.064	0.963	3.6	0.894	0.404	1.087
2015	6.286	1.064	0.963	3.6	0.894	0.404	1.087
2016	6.286	1.064	0.963	3.6	0.894	0.352	1.087

2017	5.518	1.064	0.963	3.6	0.894	0.352	1.087
2018	5.518	1.064	0.963	3.6	0.894	0.352	1.087
2019	3.52	1.064	0.963	3.6	0.894	0.352	1.087
2020	2.651	1.064	0.963	3.6	0.894	0.327	1.087
2021	2.651	1.064	0.963	3.6	0.894	0.327	1.087
2022	2.651	1.064	0.963	3.6	0.894	0.316	1.087
2023	2.651	1.064	0.963	3.6	0.894	0.316	1.087
2024	2.651	1.064	0.963	3.6	0.894	0.298	1.087
2025	2.651	1.064	0.963	3.6	0.894	0.298	1.087
2026	2.106	1.064	0.963	3.6	0.894	0.298	1.087
2027	2.106	1.064	0.963	3.6	0.894	0.236	1.01
2028	2.106	1.064	0.963	3.6	0.894	0.236	1.01
2029	1.706	1.064	0.963	3.6	0.894	0.236	0.935
2030	1.316	1.064	0.963	3.6	0.894	0.236	0.839
2031	1.316	1.064	0.963	3.6	0.894	0.209	0.839
2032	1.316	1.064	0.963	3.6	0.894	0.209	0.678
2033	1.316	1.064	0.963	3.561	0.894	0.209	0.597
2034	0.916	1.064	0.915	3.466	0.894	0.209	0.597
2035	0.916	1.064	0.787	2.63	0.894	0.209	0.531
2036	0.916	1.064	0.781	2.06	0.894	0.209	0.315
2037	0.916	0.604	0.605	1.965	0.894	0.131	0.227
2038	0.916	0.394	0.593	1.785	0.894	0	0
2039	0.916	0	0.593	1.294	0.894	0	0
2040	0.916	0	0.593	1.109	0.894	0	0
2041	0.916	0	0.593	1.096	0.894	0	0
2042	0.916	0	0.593	0.195	0.894	0	0
2043	0.916	0	0.593	0.195	0.894	0	0
2044	0.916	0	0.376	0.092	0.894	0	0
2045	0.45	0	0.131	0	0.894	0	0
2046	0.45	0	0	0	0.894	0	0
2047	0.45	0	0	0	0.894	0	0
2048	0.45	0	0	0	0.894	0	0
2049	0.45	0	0	0	0.894	0	0
2050	0.45	0	0	0	0.894	0	0
2051	0	0	0	0	0.894	0	0
2052	0	0	0	0	0.894	0	0
2053	0	0	0	0	0.894	0	0
2054	0	0	0	0	0.894	0	0
2055	0	0	0	0	0.894	0	0
2056	0	0	0	0	0.894	0	0
2057	0	0	0	0	0.894	0	0
2058	0	0	0	0	0.894	0	0
2059	0	0	0	0	0.894	0	0
2060	0	0	0	0	0.894	0	0

III. Biomass resource

Costs for the three biomass fuel types are derived from the BC Hydro *2013 Resource Options Report Update* [3]. "Exhibit 3" in this report provides costs for the three different biomass types for two different periods, which are adjusted for US2010$ and presented in Table A.3. "Exhibit 2" gives the annual energy available from each resource in BC, which is adjusted for Alberta's industry size with information from the *Canada Report on Bioenergy 2010* [4]. The Mill waste availability is based on historic biomass-fired generation in Alberta, averaging 2TWh$_e$ annually and a plant efficiency of 25%.

Table A.3

Assumed costs and availability for the biomass resource.

	Cost [$/MWh]	Annual availability [GWh/yr]	
	2010-2024	2010-2024	2025-2060
Mill waste	5.42	8000.0	8000.0
Roadside residues	11.30	845.7	771.1
Standing timber	27.57	2050.4	1567.2

IV. Determining the solar resource

The solar power technology is defined using NREL's PVWatts[29] Calculator with the parameters in Table A.4 to generate average hourly AC output (W). With the same method as is used for wind power, this hourly output is processed to generate capacity factors for each of the 36 time slices. However, unlike the five annual profiles for wind power, solar power only has the one annual capacity factor profile.

[29] http://pvwatts.nrel.gov/

Table A.4

Parameters used in PVWatts to determine solar resource

Location:	CALGARY, ALBERTA
Lat (deg N):	51.12
Long (deg W):	114.02
Elev (m):	1077
DC System Size (kW):	1000
Module Type:	Standard
Array Type:	1-Axis Tracking
Array Tilt (deg):	51
Array Azimuth (deg):	180
System Losses:	14
Invert Efficiency:	96
DC to AC Size Ratio:	1.3
Ground Coverage Ratio:	0.4

V. Technology costs

Generator performance, overnight capital costs, fixed operations and maintenance (O&M) costs, and variable O&M costs are taken from the U.S. Energy Information Administration (EIA) *Updated Capital Cost Estimates for Utility Scale Electricity Generating Plants* [5]. These costs are presented in US2010$ in Table A.5, with the exceptions as noted. Learning rates are applied to generator technologies according to long-term estimates by the International Energy Agency (IEA) [6]. Cost decreases are assumed linear, and extrapolated to 2060. The low cost (LC) values are the lowest capital costs predicted by either the EIA, IEA, or NREL.

Table A.5

Capital cost for generation technologies. Values are from the EIA unless noted.

	2015	2050
Coal-life extension	539	539
PC-CCS	4966	4966
IGCC-CCS	6269	6269
CCGT	972	972
OCGT	642	642
Cogen[d]	1203	1203
CCGT-CCS	1990	1990
Biomass	3908	3908
Hydro	2789	2789
Geothermal	4144	4144
Wind	2102	1897[a]
Solar	3679	1818[a]
Wind-LC	1383[b]	1248[b]
Solar-LC	2620[c]	1654[b]

[a] EIA [5] with IEA [6] learning rate
[b] IEA [6]
[c] NREL [7]
[d] Based on CCGT with adjustment from AESO.

Costs for generation technologies with CCS include the additional capital for capture and compressor equipment, as well as the increased fixed and variable costs associated with managing, operating, and maintaining the compressor and sequestration equipment.

Cogeneration is the only plant type for which the EIA does not provide characteristics. The model definition of this technology is based on the combined cycle natural gas plant. Fixed and variable O&M costs for cogeneration are the same as CCGT, and the capital cost for cogeneration is determined from EIA's CCGT by the same relative cost factor between CCGT and cogeneration reported in AESO's 2014 Long-term Outlook30. The efficiency of cogeneration, which directly impacts variable costs and emissions, is determined by the displacement allocation method, whereby the fuel allocated to power generation is calculated as

[30] AESO's LTO only provides costs for a few of the generation types that are included in the model. It was judged more important to use internally consistent costs (EIA) than mix data from other sources for the generators not reported on by AESO.

the total required for the combined cycle process less the fuel needed to generate the steam in a separate process with an 80% efficient boiler [8].

References

[1] AESO, 2013 Annual Market Statistics, (2014). http://www.aeso.ca/downloads/2013_Annual_Market_Statistics.pdf (accessed April 11, 2014).

[2] D.A. Ellerman, The competition between coal and natural gas the importance of sunk costs, Resour. Policy. 22 (1996) 33–42. doi:10.1016/S0301-4207(96)00017-7.

[3] BC Hydro, 2013 Resource Options Report Update Appendix 6: Wood Biomass Energy Potential of British Columbia, 2013. https://www.bchydro.com/energy-in-bc/meeting_demand_growth/irp/document_centre/reports/2013-ror-update.html (accessed December 11, 2014).

[4] D. Bradley, Canada Report on Bioenery 2010., (2010). http://www.canbio.ca/upload/documents/canada-report-on-bioenergy-2010-sept-15-2010.pdf.

[5] EIA, Updated Capital Cost Estimates for Utility Scale Electricity Generating Plants, Washington, DC, 2013. http://www.eia.gov/forecasts/capitalcost/pdf/updated_capcost.pdf.

[6] IEA, Energy Technology Perspectives 2014: Harnessing Electricity's Potential, International Energy Agency, Paris, France, 2014.

[7] Black & Veatch, Cost and performance data for power generation technologies, Black & Veatch Holding Company, Overland Park, 2012. http://bv.com/docs/reports-studies/nrel-cost-report.pdf.

[8] G.H. Doluweera, S.M. Jordaan, M.C. Moore, D.W. Keith, J.A. Bergerson, Evaluating the role of cogeneration for carbon management in Alberta, Energy Policy. 39 (2011) 7963–7974.

Appendix B: POWER-TO-GAS LITERATURE REVIEW

INTRODUCTION

Power-to-gas (PtG) is the process of producing hydrogen by water electrolysis. Its potential applications can be divided into three general categories: balancing electrical systems, large-scale electricity storage, and clean hydrogen production. Increasing amounts of variable renewable energy (VRE), like wind and solar power, places additional pressure on the grid to manage the unreliable nature of VRE. PtG provides flexibility to the system as a dispatchable load that can absorb "excess" electricity, either from the entire system, or regionally because of transmission constraints. PtG can be used for daily arbitrage, but is particularly well-suited for seasonal storage. Unlike pumped hydro and compressed air energy storage, the other large-scale storage options, PtG is not dependent on requisite geography. While the vast majority of hydrogen gas is produced from fossil fuels, PtG offers a means of production with lower carbon emissions. Furthermore, PtG can be an essential part of a hydrogen economy, which many believe is the future of energy systems (120,121).

ELECTROLYSIS OF WATER

Electrolysis is used for just 4% of global hydrogen production (212). The rest is generated from fossil fuels, primarily natural gas via steam reforming of methane (SRM). Electrolysis is more expensive than the alternatives, so it is typically only used when high purity – up to 99.999% – is required for applications such as fuel cells. There are three main types of electrolysers: alkaline, proton exchange (PEM), and solid oxide (SOE).

Fundamentals

Electrolysis produces hydrogen and oxygen gases by running direct current through water to separate its molecules. An electrolyser consists of several electrolytic cells that convert electric and thermal energy into chemical energy. Each cell consists of electrodes where

the half-reactions occur, a diaphragm to keep the created gases separate, and an electrolyte to increase ionic conductivity. The global electrolysis reaction is given in Equation 1.

$$H_2O_{(l)} \rightarrow \frac{1}{2}O_{2(g)} + H_{2(g)} \qquad \Delta H^0 = +285.8\ kJ/mol \qquad (1)$$

The enthalpy change for electrolysis (ΔH) is the minimum amount of energy required for the endothermic, nonspontaneous reaction to occur. As defined by the thermodynamic relationship in Equation 2, both heat (Q) and Gibbs' free energy (G) are necessary. The thermal energy input (Q) equals the product of the process temperature (T) and the change in entropy (ΔS).

$$\Delta G = \Delta H - Q = \Delta H - T \cdot \Delta S \qquad (2)$$

At standard temperature and pressure (298.15 K and 1 atm) the reversible voltage required for Gibbs' free energy is 1.229 V for 237.2 kJ of electrical energy. The corresponding thermal energy requirement is 48.6 kJ. Irreversibility caused by ohmic loses, electrode kinetics, and mass transport processes means higher voltage, or "overpotential", is required in order for the reaction to actually occur. Increasing the temperature at which the reaction occurs decreases the electricity required, whereas increasing the pressure slightly increases the electricity demand. Additional details of the thermodynamics and electrochemistry can be found in (148,213–216).

Electrolyser Configuration

Hydrogen production per unit of active electrode area is proportional to the current density. Lower current densities result in higher cell efficiency but a lower rate of hydrogen production. Higher voltages increase the rate of hydrogen production, but at the expense of efficiency (156).

Electrolysis cells are connected in either series or parallel. Most manufacturers use a series configuration, referred to as bipolar, which requires much lower current (148). Although bipolar electrolysers have a more complex configuration they take up considerably less space and are considered more suitable for hydrogen production. The

parallel configuration, known as monopolar or unipolar modules, requires lower voltage (typically 1.9 - 2.5 V) and their modular construction makes maintenance of individual cells possible.

Equipment in addition to the electrolysis module is required for hydrogen production. Feed water must be purified to remove minerals and have an electric conductivity below 5 µS/cm, subject to the type of electrolyser (148). At 100% efficiency, 8.9 litres of feed water are required to produce 1 kg of hydrogen. Air or water cooling is required of the electrolyser to evacuate excess heat generation. Depending on the use of hydrogen, it is typically purified of oxygen and moisture, cooled, compressed, and stored. This additional equipment can require significant upfront investment, but relatively low ongoing costs. Balance-of-plant costs are estimated to comprise 34% to 86% of total system installation costs (excluding storage) (217).

The three main types of electrolysers are alkaline, proton exchange membrane, and solid oxide. An introduction to each of these technologies are presented in the following sections.

Alkaline Electrolysers

Alkaline water electrolysers have been in use for over 100 years, are the most common type of electrolyser, and are considered a mature technology (218). They are named for the liquid electrolyte that increases the ionic conductivity, typically a solution of KOH of 25-30 wt.% concentration. Water is reduced at the cathode (Equation 3) to produce hydrogen gas, and hydroxide ions that cross the diaphragm. The hydroxide ions combine on the anode according to Equation 4 to create oxygen gas and electrons that complete the externally powered circuit.

Cathode: $$2H_2O_{(l)} + 2e^- \rightarrow H_{2(g)} + 2OH^-{}_{(aq)} \quad (3)$$

Anode: $$2OH^-{}_{(aq)} \rightarrow \frac{1}{2}O_{2(g)} + H_2O_{(l)} + 2e^- \quad (4)$$

Alkaline electrolysers are more economic than the other types, offer reasonable efficiency, and are the most suitable for large-scale hydrogen production. The corrosive nature of alkaline electrolysers is a challenge, but they have proven to be reliable and can operate for up to 15 years (218). The main characteristics of the electrolyser types are presented in Table C.6.1.

Table C.6.1: Characteristics of alkaline, PEM, and SOE electrolysers, based on (148,149,212,219–222)

Type	Status	Efficiency (min/typ./max) [%]	Cell temperature [˚C]	Pressure (min/typ./max) [bar]
Alkaline	Commercial	47/70/82	40-90	1/15/30
PEM	Early commercial	48/63/83	20-100	7/15/200+
SOE	Laboratory	69/85/100	800-1000	Unknown

Type	Operating range (min-max) [%]	Flexibility	Response time [s]	Capital cost Current [$]	Projected [$]
Alkaline	20-100+	Causes problems	$10\text{-}10^3$	1000-2000	200-300
PEM	5-100+	Good	~1	3000-4000	125-300
SOE	Unknown	Very poor	$10^4\text{-}10^5$	N/A	175-300

Proton Exchange Membrane Electrolysers

Proton exchange membrane electrolysers (PEM), also called polymer electrolyte membrane electrolysers, are commercially available but not yet a mature technology. In these electrolysis cells, a solid ion conducting membrane is featured in place of the aqueous solution in alkaline cells. The supplied electricity polarizes the cathode negatively where electrons combine with hydrogen ions that have crossed the membrane to form hydrogen gas as in Equation 5. The hydrogen ions originate at the anode by the oxidation half-reaction that also creates oxygen gas and releases electrons (Equation 6). PEM electrolysers are fundamentally PEM fuel cells operating in reverse, and require high-purity deionized water.

Cathode: $$2H^{+}_{(aq)} + 2e^{-} \rightarrow H_{2(g)} \quad (5)$$

Anode: $$H_2O_{(l)} \rightarrow \frac{1}{2}O_{2(g)} + 2H^{+}_{(aq)} + 2e^{-} \quad (6)$$

PEM electrolysers offer many benefits, but also face several challenges. Benefits include high current density (higher H_2 production density), wide operating range, flexible operation, and hydrogen gas that may not require further purifying or compression. However, as it is a relatively new technology, capital costs remain high, hydrogen production rates are low, and lifetimes are short (130,148,223).

Solid Oxide Electrolysers

Solid oxide electrolysers (SOE), or steam electrolysers, are the least developed of the three types. Fundamentally solid oxide fuel cells operating in reverse, SOE operate at high temperatures to reduce the electricity requirement (224). Unlike the other types, the gas phase of water in this process makes it challenging to maximise interfacial contact with electrodes. The steam is reduced to produce hydrogen at the cathode (Equation 7), while oxygen ions pass through the solid electrolyte (ceramic membrane) to form oxygen gas at the anode (Equation 8).

Cathode: $$H_2O_{(l)} + 2e^{-} \rightarrow H_{2(g)} + O^{2-}{}_{(aq)} \quad (7)$$

Anode: $$O^{2-}{}_{(aq)} \rightarrow \frac{1}{2}O_{2(g)} + 2e^{-} \quad (8)$$

Increasing the temperature from 25 ˚C to 1000 ˚C reduces the reversible cell voltage by 26% and theoretically allows over 40% of the required process energy to come from heat (225). As electricity is generally more costly than heat, this technology reduces the variable operating costs of electrolysis – its main advantage. SOE would be well suited for constant operation in proximity to a high temperature heat source such a nuclear power plant. The main challenges for SOE are the limited long-term stability of the cells due to electrolyte aging and electrode deactivation (225), and the limited flexibility (226). Table 2 presents a summary of advantages and disadvantages of the three electrolyser types.

Table C.6.2 Advantages and disadvantages of alkaline, PEM, and SOE electrolysers (149)

Alkaline electrolysis	PEM electrolysis	SOE electrolysis
Advantages		
Well established technology	High current densities	Efficiency up 100%; thermoneutral
Non noble catalysts	High voltage efficiency	Efficiency >100% w/hot steam
Long-term stability	Good partial load range	Non noble catalysts
Relative low cost	Rapid system response	High pressure operation
Stacks in the MW range	Compact system design	
Cost effective	High gas purity	
	Dynamic operation	
Disadvantages		
Low current densities	High cost of components	Laboratory stage
Crossover of gases (degree of purity)	Acidic corrosive environment	Bulky system design
Low partial load range	Possibly low durability	Durability (brittle ceramics)
Low dynamics	Commercialization	No dependable cost information
Low operational pressures	Stacks below MW range	
Corrosive liquid electrolyte		

BALANCING AND FLEXIBILITY

Increasing penetration of VRE create fluctuations in residual load. This has been shown to depress market prices and increase spot price variance (227,228). Some studies have explored close-coupling storage with wind farms as a means of increasing reliability and smoothing output (229–233). Storage at this small scale, particularly PtG, is not economic under current conditions. Other research suggests that with technology improvements, cost reductions, and additional economic incentives, storage may be cost effective. This chapter contains a review of research that assesses storage as a means of providing flexibility to power systems.

Isolated, small, or weak systems

A recent review of PtG projects reveals that 76% of existing installations at the time were stand-alone systems not connected to a public power grid (130). Many of these were pilot projects to study PtG as a form of energy storage on isolated systems attempting to integrate more VRE and rely less on fossil fuel generation.

One such demonstration project on the Norwegian island of Utsira was capable of 2-3 days of electricity autonomy for the 10 households on the island (131). A 600 kW of wind turbine fed a 50 kW alkaline electrolyser capable of 10 Nm^3/h hydrogen production that was compressed to 200 bar for the 2400 Nm^3 storage tank. A 55 kW engine-generator and 10 kW PEM fuel cell provided two alternatives for electricity generation from the stored hydrogen. At maximum operation, electrolyser stack efficiency was approximately 73%, while overall system efficiency of hydrogen production was 53%. The project had challenges with premature equipment failure, access to service personnel, a weak grid, and installation mistakes, and has since be decommissioned. Areas for improvement were identified as more efficient load-following electrolysers, wind forecasting, load management, more efficient and reliable fuel cells, and a more diverse VRE portfolio that reduces fluctuations in power generation.

A wind-electrolyser-fuel cell system is modelled for a chicken farm in Turkey by Genç et al. (234). The authors find that hydrogen production costs decrease by utilising lower capacity electrolysers more fully, and hydrogen production costs decrease with larger turbines.

Kaldellis and Zafirakis explore several storage technologies' abilities to integrate VRE on two Greek islands (133). Results suggest that PtG is competitive with other storage options for longer autonomy requirements (over 1 day) and when high levels of renewable-sourced electricity is desired.

Korpaas and Greiner explore the opportunities of PtG for weak grids with wind power (134). The authors find that using electrolysers as a dispatchable load decreases curtailment of wind power, particularly at high penetration levels. Generated hydrogen may be used for transportation purposes, although the necessary storage may not be economic and reliability of the hydrogen supply cannot be guaranteed. Nonetheless, this may be a viable option if transmission reinforcements are costly or controversial.

General storage

Storage of electricity is becoming increasingly important in power systems for integrating large amounts of renewables; improving flexibility and reliability; and decreasing transmission requirements. Many studies have shown that storage enables VRE integration by decreasing curtailment (112,114–116,235).

Bathurst and Strbac model the optimal dispatch of a generic storage system providing balancing service based on imbalance from wind farms' anticipated generation (112). The researchers find that storage can add value to the system from balancing and arbitrage.

The coupling of generic energy storage to a wind farm to avoid transmission constraints and permit more dynamic market participation is studied in (229). The authors present a method of sizing, scheduling and operating the hybrid plant to take advantage of the spot market. However, current storage costs and efficiencies are unlikely to result in net revenue gains from such a hybrid plant.

Lund et al. modelled a compressed air energy storage (CAES) unit participating in the Danish spot market for electricity arbitrage (236). The basic operational strategy modelled is essentially to compress air when the spot price was below a threshold and generate when the price is above a threshold. Using historical data, sufficiently volatile spot prices are shown to make such arbitrage profitable. However, market feedback from the unit's participation is not modelled so the impact of such involvement is unknown.

A similar study for CAES was conducted by Foley and Diaz Lobera using Plexos in a future power system on the island of Ireland with high VRE penetration (237). Results indicate that the storage decreases curtailment of VRE, however power system costs increase and emissions do not necessarily decrease.

Nyamdash et al. study the impacts of combining wind power and dedicated energy storage on the Irish power system (238). Based on storage reserves and the day-ahead wind forecast, a constant output (wind supported by storage discharge) is determined for the following day. Three scenarios define 6, 12, and 24 hour discharge blocks, with the remaining hours to charge the generic 75% efficient storage from wind generation. The

maximum wind capacity modelled is approximately half of the peak system demand. Depending on the length of the discharge block, baseload or mid-merit plants are displaced on the system. A 12 hour charge/discharge cycle is found to be most effective at levelling the net system load. Current conditions are shown to be insufficient to support a merchant storage facility as modelled.

The potential arbitrage value of storage on the PJM wholesale electricity market was evaluated by Sioshansi et al. (239). The authors asses different storage times and efficiencies using several historical years, and also explore the impact of uncertainty in operating a storage system. Storage is shown to have economic value, and also provide other social welfare benefits such as improve utilisation of infrastructure, reduce congestion, and defer building of new infrastructure. There may not be a sufficient economic case for a merchant operator, so the investment and ownership of such large-scale storage may require a novel strategy. Long-term, inter-day arbitrage was shown to capture 85% of the potential value with eight hours of storage.

Nuclear applications

Several studies have explored electrolysis applications with nuclear-based power systems. Nuclear power is a low-carbon source of electricity with low operating costs, but it also has very limited flexibility. The operation of PtG in these systems would likely differ from a system with high VRE penetration.

Bennoua et al. model pairing alkaline electrolysers with individual reactors in a French nuclear plant to provide a flexible load so the reactors can operate at a constant output regardless of called dispatch power (135). The authors find that the unit cost of hydrogen is very sensitive to assumptions regarding the electrolyser minimum load and lifetime, as well as the cost of storage. Salt cavern storage results in hydrogen costs (7.2 €/kg) nearly four times lower than if tube trailers are used for storage. The same study also explores using electrolysers as a downward balancing mechanism on the French system, i.e. dispatchable load as tertiary reserve. Sizing the electrolysers for the peak power requirement results in a capacity factor of less than 10%, therefore the authors

recommend lower electrolyser capacity to increase its usage and simultaneously lower hydrogen costs.

Floch et al. evaluated hydrogen production from unused capacity during off-peak hours in the French power system (136). They discovered that it was not viable to attempt to use all the energy due to the low capacity factors. The authors suggest that for such an application, low capital cost electrolysers would be necessary, even if it meant higher operating costs.

Similar studies on electrolysis in the French power system have been conducted by Mansilla et al. (137–139). Avoiding peak price times and operating at 75% utilisation factor results in the lowest costs. However, the authors warn that impact of cycling from discontinuous operation may lead to accelerated degradation and additional maintenance or replacement costs (137). A second study exploring utilisation of captured CO_2 to create methanol also finds cost reductions by discontinuous operation (138). Somewhat surprisingly, price volatility in the French system was greater than in Germany and Spain in 2010-2012, which is shown to lead to lower hydrogen production costs, although only marginally (139).

Naterer et al. explore off-peak electrolysis and thermochemical hydrogen production from nuclear energy (129). Decentralised electrolysis is found to be more cost effective below production of 10-20 tH_2/day. Hydrogen production through the copper-chlorine thermochemical cycle using heat from nuclear reactors is more economic with higher production quantities, and when situated close to hydrogen demand.

Power-to-Gas studies

Balancing services to alleviate errors in wind forecasting for a “typical European country” are assessed in research by Guandalini et al. (240). Electrolysers serve as dispatchable load while gas turbines provide generation in order to minimise discrepancy from committed wind generation volumes and therefore reduce imbalance costs. For PtG to be economic in the researchers’ modelling, some of the following conditions are required: low electricity prices, “green gas” incentives, high carbon taxes, high imbalance costs,

and/or high curtailment costs. In a scenario with a green gas incentive and carbon tax, electrolyser capacity was optimally sized at 6% of the wind capacity.

The economic viability of an electrolysis plant to provide balancing services to the French power market is assessed by Guinot et al. (241). This is similar to the Bennoua study (135), except a fast-reacting PEM electrolyser is modelled that purchases electricity in the day-ahead market to produce hydrogen, and also participates in primary (frequency) and secondary reserve markets, with the goal of minimising hydrogen production costs. Participation in the secondary market was minimal under current compensation schemes, and primary regulation participation would require much greater compensation to be economic.

A future Spanish power system is assessed for its potential to use PtG as flexible load to generate hydrogen in (242). The proposed operational strategy is constant power generation during the day in excess of the demand and dispatching electrolysers to utilise the net electricity. This is an interesting approach as it requires dispatchable generation complimentary to the VREs in order to maintain a flat generation profile.

LARGE-SCALE ELECTRICITY STORAGE

The plot in Figure C.6.1 presents energy and power characteristics of many possible forms of electricity storage. A comprehensive review of many of these technologies was conducted by Díaz-González et al. (116). In the bottom left of the plot are technologies that can provide power quality and short-term storage services. PtG ("H2") is seen in the top right with other technologies that are able to store large amounts of energy and operate at high power ratings. However, unlike CAES and pumped hydro storage (PHS), PtG is not limited to geographically-appropriate sites. "SNG", synthetic natural gas, involves further processing hydrogen with carbon dioxide to make CH_4, which is sometimes the 'gas' in power-to-gas.

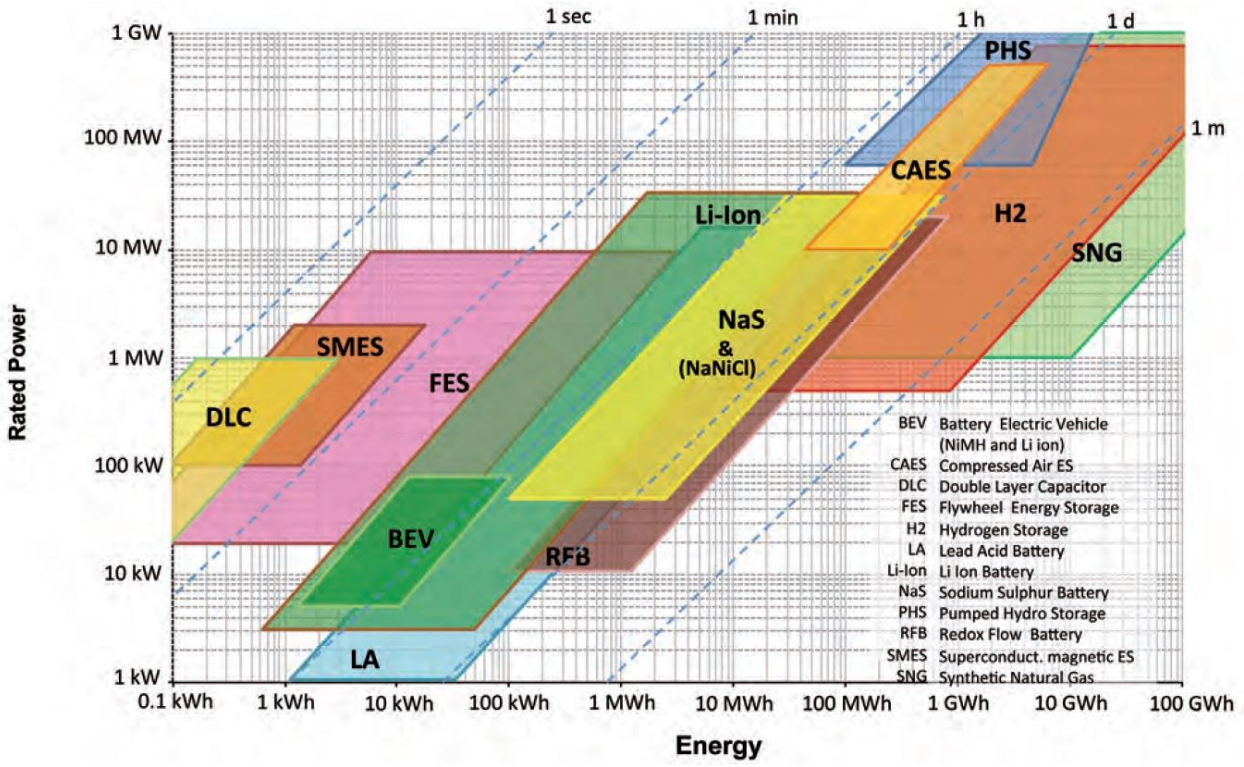

Figure C.6.1**: Power and energy ranges of electricity storage options, from** (118)**.**

A comparison of lifecycle costs for various electrical storage technologies was conducted by Steward et al. (243). All technologies are evaluated for the same arbitrage scenario: a mid-sized 300 MWh storage capacity that is charged during 18 off-peak hours each weekday and all weekend, and discharged at 50 MW during 6 peak hours on weekdays. PtG is found to be competitive with battery storage technologies, but more costly than PHS and CAES, as summarised by Figure C. 6.2.

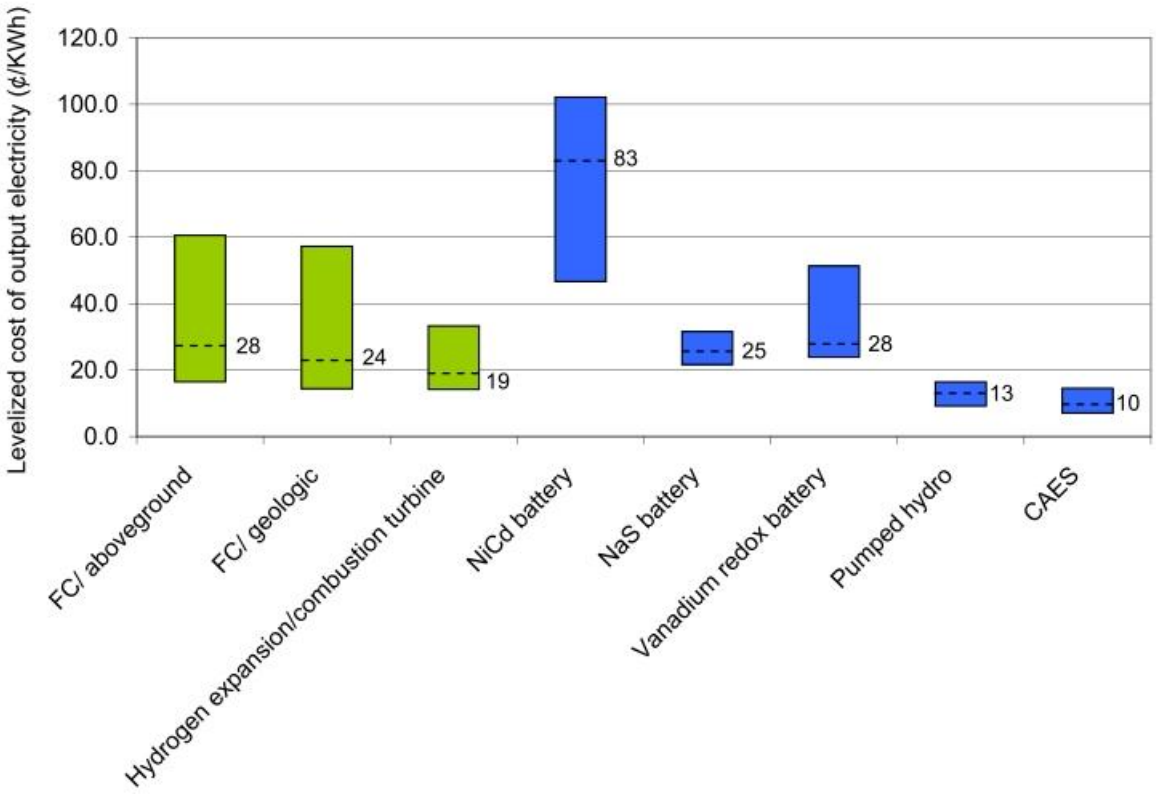

Figure C. 6.2**: Levelised cost of electricity from storage systems, from** (243)**.**

de Boer et al. compare the economic and environmental implications of CAES, PHS and PtG on a system with different penetrations of wind power (117). The scenario analysis with a unit commitment model is conducted on an inflexible (thermal) Dutch power system. Installed wind capacity is increased incrementally up to the average system demand, and storage loading power is increased up to ¼ of the average system demand. Capital costs of storage were not included, but results indicate that storage reduces operating costs of the power system by reducing fuel and startup/shutdown costs. Somewhat unexpectedly, at lower levels of wind penetration, CO_2 emissions increased because in high wind, low demand times coal plants utilise the storage to avoid startup/shutdown costs. In this study, PHS and CAES are more effective than PtG at reducing operating costs because they have higher roundtrip efficiencies.

PtG impacts on the power, gas, and CO_2 sectors in a future Belgian power system with a VRE penetration of 76% is analysed by Vandewalle et al. (141). The modelled interactions

between the three sectors are illustrated in Figure C. 6.3. In this study, hydrogen from electrolysis is processed with CO_2 captured from gas plants to make renewable (synthetic) methane that is fed into the gas grid. Optimising all three systems together for lowest cost, the researchers find that relative to the impact of VRE alone, PtG has little impact on the power system, but greater impact on the natural gas and CO_2 sectors. The case study indicates that PtG transfers capacity and flexibility issues from the power system to the gas system, and suggests these complex interactions should be kept in mind when designing systems with high VRE penetration.

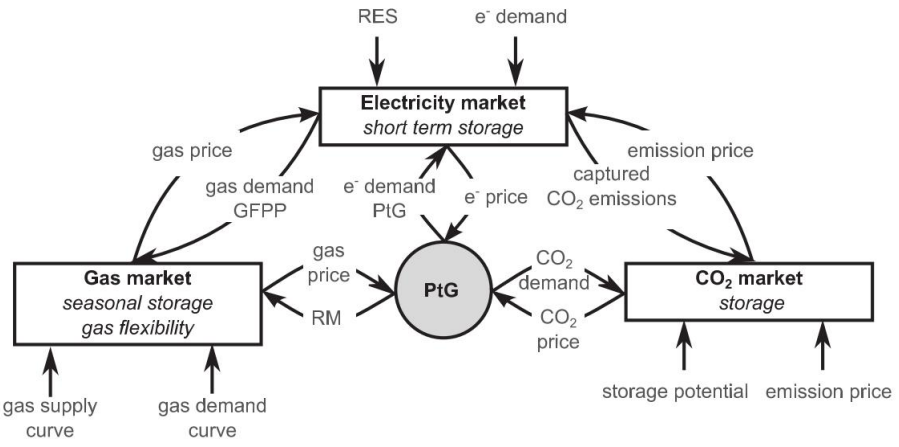

Figure C. 6.3: The interactions modelled by Vandewalle et al. (141). GFPP stands for gasfired power plant, RM for renewable methane, RES for renewable energy sources (VRE), and e- for electricity.

Qadrdan et al. use a combined gas and electricity network optimisation model to analyse PtG in Great Britain in 2020 with a wind capacity penetration of 30% (30 GW) (115). The power system is resolved into 16 nodes and the gas transmission network is simplified to a couple dozen nodes and pipelines with 20 hydrogen injection locations. A high demand day and low demand day are used as case studies to evaluate how the combined system can meet the power and gas demands at lowest cost. Great Britain currently permits a maximum of 0.1% hydrogen by volume on the gas grid which motivates the 0% reference case, but the study also models a 5% case and an unlimited case. PtG decreases

operating costs and emissions in all cases by utilising wind energy that would otherwise be curtailed, achieving greater reductions when there is no limit on hydrogen concentration. Much of the wind curtailment is due to transmission constraints, and PtG allows the wind energy in the north to meet load in the south via the natural gas grid. A non-rigorous assessment of the economics indicates a 10-14 year payback for the PtG infrastructure.

A high-level study of meeting 100% of Europe's electricity demands with wind, solar, storage, and additional transmission is conducted by Bussar et al. (244). The model determined that 2500 GW of wind and solar is required to meet the demand that varies between 300 - 670 GW. The inter-country transmission system has a total capacity of 375,000 GW·km, with capacities as high as 41 GW. PtG makes up most of the 530 GW, 250 000 GWh storage system, serving seasonal storage tasks while pumped hydro and batteries perform short- and medium-term duties.

Jentsch et al. use a high-level model to find PtG capacities and locations to facilitate 85% VRE penetration in Germany (145). The combined installed capacity of wind (90 GW) and solar (80 GW) is 260% of the average load. All the hydrogen electrolysed undergoes methanation so it can be injected to the natural gas grid without issue; however the source of cost of CO_2 is not assessed. Electrolysers are primarily sited in the North, where most wind power, including significant offshore capacity, is located. Increasing PtG capacity is found to decrease variable system costs and emissions. The economic optimal capacity of electrolysers is found to be 9 - 18% of the average system load.

Heide et al. modelled the optimal mix of wind and solar power to provide up to 100% of European electricity (146). If 100% penetration is the target, 55% wind and 45% solar power generation is the optimal mix, requiring half the storage capacity of a system using only one of the technologies. For penetration levels less than 100%, the optimal fraction of wind power increases because of its higher correlation with seasonal demand.

Varone and Ferrari model the Germany power system in 2050 with two cases that provide 79 and 94% of electricity from renewables, primarily wind and solar (123). The

system generates significant excess electricity that is used by solid oxide electrolysers to produce methane and methanol that can satisfy much of the country's heating and transportation needs. An economic analysis shows sensitivity to electricity prices and capacity factors of the fuel cells. A system that captures, distributes, and recycles CO_2 for this future scenario would require significant investment and face many challenges.

Karlsson and Meibom use the linear optimisation model Balmorel to discover a future Nordic system that can provide most electricity, district heating, and transportation fuel demands from renewables (4). Balmorel uses a one-year optimisation horizon using the cost and performance parameters for that year. The power system configuration is determined by running the optimisation once every 5-years to 2050. The resulting system has an installed wind capacity approximately equal to the average power demand (80 GW), as well as significant biomass, hydro, and nuclear capacity. Electrolysis is the preferred method of hydrogen generation (72%) and is supplemented by SRM. Hydrogen is used for heat and transportation demands, and is not stored for power generation at a later time because of efficiency losses. However, when run at hourly resolution, it is revealed that there are some significant power system capacity deficits that would require additional flexible generation.

Meibom and Karlsson expanded their Balmorel model to include heat, process energy, and Germany, and assume all primary energy must come from renewables (14). Much of the hydrogen from electrolysis was used to meet transportation demands, and investment in storage capacity for hydrogen corresponds to up to 4% of the annual wind generation. Variable wind power was also accommodated by flexible hydro and CHP, interties, and thermal storage. The largest source of electricity is biomass, then wind, hydro, and nuclear, with the authors noting that hydrogen is being produced by electrolysis from biomass-fired electricity. A scenario with plug-in cars still requires hydrogen storage because the storage potential of the cars is relatively low and is not sufficient for storage periods lasting several weeks.

CLEAN HYDROGEN PRODUCTION

The vast majority of current hydrogen production comes from fossil fuels. With electricity sourced from low-carbon or renewables, electrolysis provides a clean source of hydrogen. However, several advancements in technology and process are required for PtG to become competitive and increase its share of hydrogen production. A comparison of delivered hydrogen costs in Figure C. 6.4 reveals the low-costs of steam methane reforming (SMR).

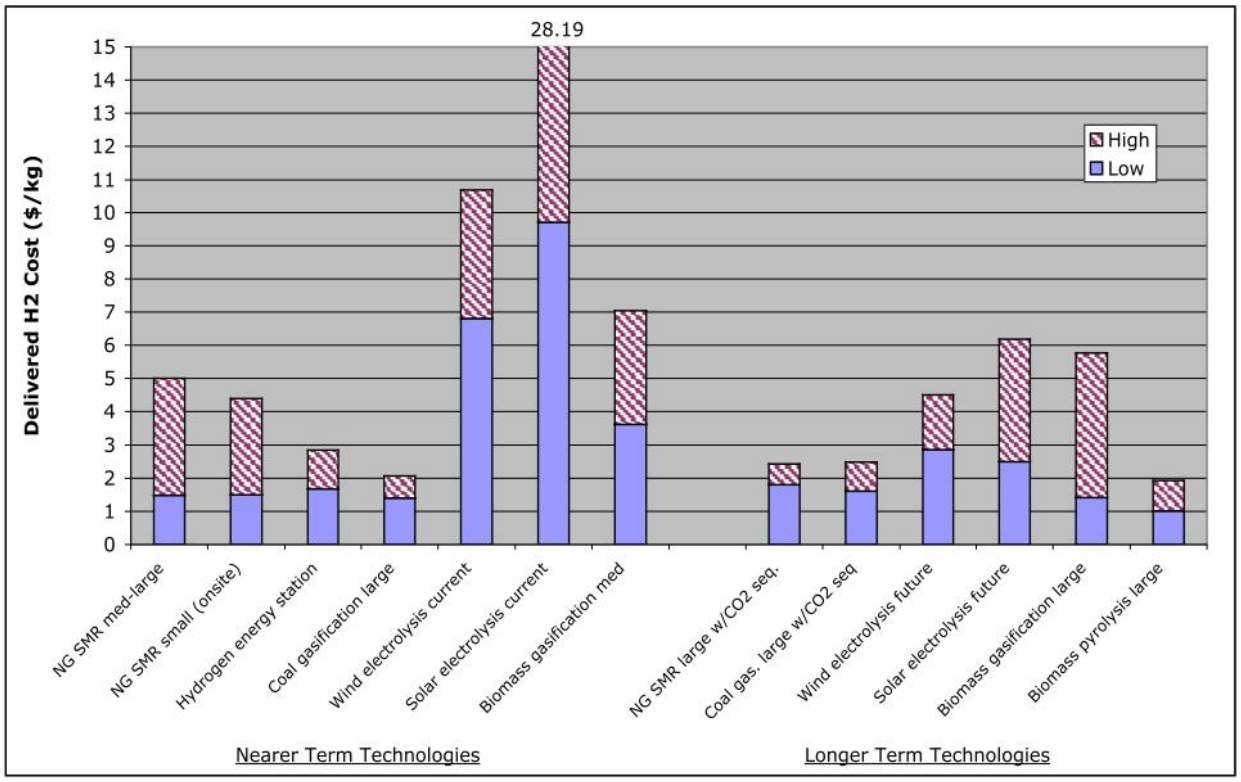

Figure C. 6.4: Delivered hydrogen cost estimates for various processes, from (212).

The US Department of Energy is targeting a delivered and dispensed clean hydrogen cost of US$2-4/kg (245). '$/kg' is commonly used as the cost metric because one kilogram of hydrogen has approximately the same amount of energy as a gallon of gasoline, also referred to as a gallon of gasoline equivalent (GGE). Therefore, $/kg$H_2$ for fuel cell

vehicles can be compared to $/gallon for conventional internal combustion vehicles for mileage purposes, assuming the efficiencies of the vehicles are the same.

Hydrogen production costs are dominated by the cost of electricity and the electrolyser capital cost. Figure C. 6.5 demonstrates the contribution of electricity costs to hydrogen production. Electricity costs can make up ½ to two-thirds of total costs, while capital costs contribute ¼ to ½ (233,246). In certain applications, such as a refuelling station, compression, storage, and dispensing can greatly increase costs.

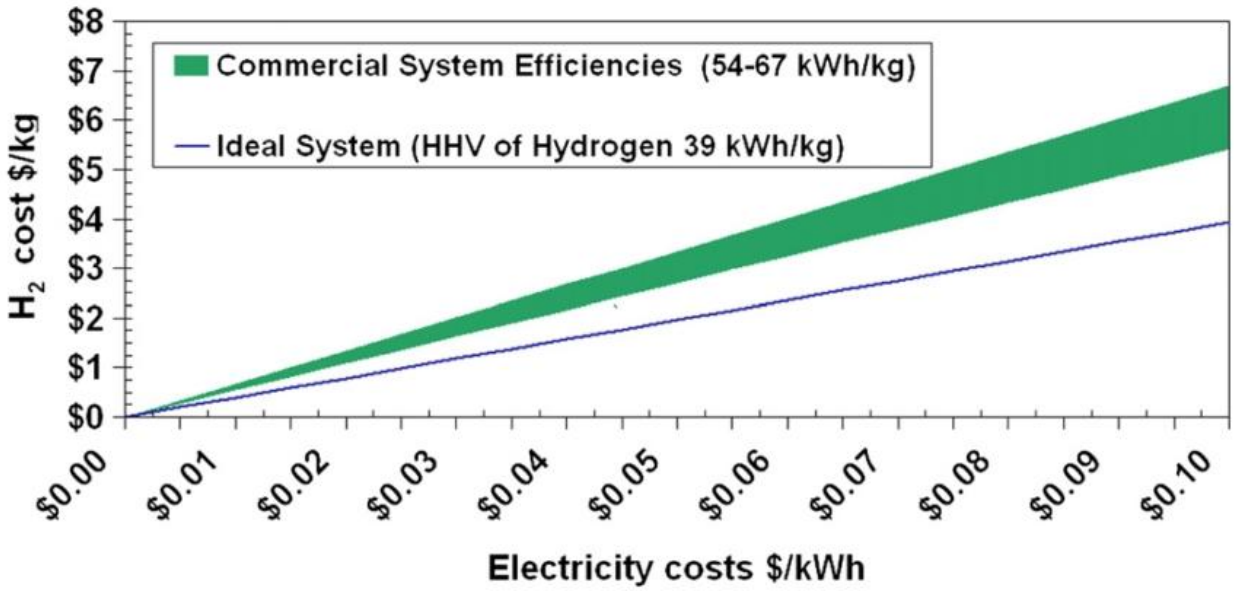

Figure C. 6.5: Electricity cost component for hydrogen production (no capital, operating, maintenance costs included). Taken from (246).

As demonstrated in the studies by Floch et al. (136) and Jørgensen and Ropenus (247), the power market dictates the operational strategy of the electrolyser and the resulting cost components per kilogram. In general, higher capacity factors reduce hydrogen costs by lowering the capital cost component per kilogram. However, as demonstrated in (129), if electricity is purchased from a deregulated market, there is an electricity purchase price threshold above which operation of the electrolyser is no longer cost effective because of the significant variable cost to produce additional hydrogen. A fossil

fuel-based market system with wind will typically have greater price volatility than, say, a nuclear-based system, and fewer operating hours may result in lower production costs (136). In either case, optimising for lower hydrogen production costs will result in different operational strategy than using electrolysis for peak shaving, balancing, or energy storage purposes (247,248).

Studies on the costs of hydrogen production via electrolysis depend greatly on assumptions for electricity and capital costs. Current, low-end estimates of costs are typically in the 6 to 8 $/kg range, with some estimates as high as 32 $/kg (126,127,135,247). Studies that consider future cost reductions for electrolysers and cheap electricity that may arise from high VRE penetration report production costs of 2.90 to 4 $/kg (4,243,249), suggesting that the DOE cost targets may be achievable. On the other hand, policy such as a carbon tax or "green gas" credit is likely necessary for electrolysis to be cost competitive with conventional SMR.

CHALLENGES

The extent to which PtG will provide flexibility, storage, and clean hydrogen depends on how much progress is made on certain challenges. Electrolysers need to achieve major cost reductions, as well as improvements on flexibility, durability, and size. A review of existing PtG plants reveals several problems, such as lower performance and durability than claimed by the manufacturer, as well as safety concerns over the corrosive alkaline electrolyte (130).

One of the major benefits of PtG for energy storage is the possibility of leveraging natural gas infrastructure. However, there is concern and debate over how much hydrogen the natural gas grid can safely accommodate, with estimates in the 2-20% range (159–161). Injecting hydrogen into the natural gas grid may also raise non-trivial regulatory issues.

Oxygen gas, the by-product of electrolysis, is typically vented to the atmosphere, and most studies assume this operation. The scale of electrolysis for some of the applications

discussed could result in excessive oxygen generation that cannot be simply vented. The oxygen could be captured and potentially sold as a merchant gas, but this would entail additional infrastructure and costs.

Appendix C: DAC STUDY ASSUMPTIONS

Resource costs in 2060. Presented in 2016USD.

	Capital $/kW	VOM $/MWh	FOM $/kW-yr
Nuclear	5,880	0.0023	100
Coal-Existing	-	0.0047	40
Coal-CCS	5,562	0.0095	81
CCGT	1,094	0.0020	10
CCGT-CCS	2,153	0.0071	33
OCGT	672	0.0106	7
RICE	1,342	0.0059	7
Biomass	3,790	0.0055	110
Cogen	1,357	0.0020	10
Hydro	2,442	0.0027	15
Geothermal	12,294	-	173
Wind-N	1,582	-	47
Wind-SW	1,518	-	47
Wind-SC	1,731	-	47
Wind-SE	1,718	-	47
Solar	747	-	22
DAC	1,869	-	62

Time slice durations

Box plot of time slice durations for years 2060 through 2065.